phil 56
10/19/67

AEROSPACE NUCLEAR SAFETY

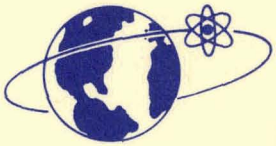

SC-CR-67-2656
June 1967

STUDY OF THE CHEMICAL INTEGRITY OF RADIOISOTOPE CONTAINMENT MATERIALS IN LAUNCH ABORT ENVIRONMENTS SUMMARY TECHNICAL REPORT PHASE III—TASK I—THE BEHAVIOR OF CONTAINMENT MATERIALS IN HYDROGEN-FLUORINE FLAME ENVIRONMENTS

MASTER

Prepared by

W. Gregson, Jr.
J. R. Ogren
R. C. Ham

TRW Systems Group
Redondo Beach, California

SANDIA LABORATORIES

OPERATED FOR THE U. S. ATOMIC ENERGY COMMISSION BY SANDIA CORPORATION | ALBUQUERQUE, NEW MEXICO; LIVERMORE, CALIFORNIA

DISTRIBUTION OF THIS DOCUMENT IS UNLIMITED

DISCLAIMER

This report was prepared as an account of work sponsored by an agency of the United States Government. Neither the United States Government nor any agency Thereof, nor any of their employees, makes any warranty, express or implied, or assumes any legal liability or responsibility for the accuracy, completeness, or usefulness of any information, apparatus, product, or process disclosed, or represents that its use would not infringe privately owned rights. Reference herein to any specific commercial product, process, or service by trade name, trademark, manufacturer, or otherwise does not necessarily constitute or imply its endorsement, recommendation, or favoring by the United States Government or any agency thereof. The views and opinions of authors expressed herein do not necessarily state or reflect those of the United States Government or any agency thereof.

DISCLAIMER

Portions of this document may be illegible in electronic image products. Images are produced from the best available original document.

Issued by Sandia Corporation,
a prime contractor to the
United States Atomic Energy Commission

LEGAL NOTICE

This report was prepared as an account of Government sponsored work. Neither the United States, nor the Commission, nor any person acting on behalf of the Commission:

A. Makes any warranty or representation, expressed or implied, with respect to the accuracy, completeness, or usefulness of the information contained in this report, or that the use of any information, apparatus, method, or process disclosed in this report may not infringe privately owned rights; or

B. Assumes any liabilities with respect to the use of, or for damages resulting from the use of any information, apparatus, method, or process disclosed in this report.

As used in the above, "person acting on behalf of the Commission" includes any employee or contractor of the Commission, or employee of such contractor, to the extent that such employee or contractor of the Commission, or employee of such contractor prepares, disseminates, or provides access to, any information pursuant to his employment or contract with the Commission, or his employment with such contractor.

Printed in the United States of America
Available from
Clearinghouse for Federal Scientific and Technical Information
National Bureau of Standards, U. S. Department of Commerce
Springfield, Virginia 22151
Price: Printed Copy $3.00; Microfiche $0.65

LEGAL NOTICE

This report was prepared as an account of Government sponsored work. Neither the United States, nor the Commission, nor any person acting on behalf of the Commission:

A. Makes any warranty or representation, expressed or implied, with respect to the accuracy, completeness, or usefulness of the information contained in this report, or that the use of any information, apparatus, method, or process disclosed in this report may not infringe privately owned rights; or

B. Assumes any liabilities with respect to the use of, or for damages resulting from the use of any information, apparatus, method, or process disclosed in this report.

As used in the above, "person acting on behalf of the Commission" includes any employee or contractor of the Commission, or employee of such contractor, to the extent that such employee or contractor of the Commission, or employee of such contractor prepares, disseminates, or provides access to, any information pursuant to his employment or contract with the Commission, or his employment with such contractor.

SC-CR-67-2656

STUDY OF THE CHEMICAL INTEGRITY OF RADIOISOTOPE CONTAINMENT MATERIALS IN LAUNCH ABORT ENVIRONMENTS

Summary Technical Report
Phase III—Task I—The Behavior of Containment Materials in Hydrogen-Fluorine Flame Environments

Prepared by

W. Gregson, Jr.
J. R. Ogren
R. C. Ham

for

Sandia Corporation

under

Contract No. 48-4912

ABSTRACT

Task I investigated the behavior of four nuclear containment materials (Type 316 stainless steel, Hastelloy C, Haynes alloy 25, and tantalum) in simulated abort fires containing large concentrations of fluorine and hydrogen fluoride. Samples were exposed to hydrogen-fluoride flames of two mixture ratios over a wide range of steady state sample temperatures. Metallographic analysis of some samples were performed to determine the degree of internal interaction for both fluorine and hydrogen rich flame environments. Electron microprobe and x-ray diffraction techniques were used to identify reaction products in the microstructure of certain samples.

June 1967

DISTRIBUTION OF THIS DOCUMENT IS UNLIMITED

SUMMARY

This report is the Summary Technical Report describing the work performed by TRW Systems for the Sandia Corporation under Task I of Phase III of Contract Number 48-4912.

The program objective is to investigate the chemical integrity of radioisotope containment materials when subjected to a booster vehicle abort environment.

The Task I investigation was concerned with the behavior of four nuclear containment materials (Type 316 stainless steel, Hastelloy C, Haynes alloy 25, and tantalum) in simulated abort fires containing large concentrations of fluorine and hydrogen fluoride.

Samples of each of the four materials were exposed to hydrogen-fluoride flames of two mixture ratios (F_2/H_2 = 1.166 and 0.689) over a wide range of steady state sample temperatures. Selected samples were then subjected to metallographic analysis to determine the degree of internal interaction for both fluorine and hydrogen rich flame environments. Electron microprobe and x-ray diffraction techniques were used to identify reaction products in the microstructure of certain samples.

Based on the experimental investigation, the following conclusions were drawn:

1. Reaction rates for Type 316 stainless steel in the H_2-F_2 flame environment at both low and moderate fluorine concentrations are fairly low and are not considered to be of major concern from launch abort radioisotope containment safety considerations up to temperatures of 2000°F. Above 2000°F and up to the melting range reaction rates are rapid and the possibility exists for catastrophic failure through self heating or ignition of the stainless steel in the H_2-F_2 environment.

2. Hastelloy C does not react rapidly in an H_2-F_2 environment rich in fluorine at temperatures below 1800°F. However, in a flame environment containing large concentrations of fluorine, hydrogen-fluoride and atmospheric air, Hastelloy C is subject in a period of a few minutes to severe interior grain boundary attack to a considerable depth in the temperature range above 1800°F. The modifications to the microstructure of Hastelloy C due to the combined influences of the hydrogen-fluorine flame and atmospheric air can be expected to produce significant changes in the mechanical properties of this alloy.

3. In the fluorine and hydrogen fluoride rich flame environment, Haynes 25 does not undergo catastrophic interaction at sample temperatures below 2200°F. Radioisotope containment safety considerations should not be compromised by chemical reactions with F_2 or HF below 2200°F for periods of many minutes. Above the 2200°F temperature range and up to the alloy's melting range, flame interaction could be catastrophic.

4. Tantalum reaction rates in flame environments containing fluorine and hydrogen fluoride are slow relative to a period of minutes time scale below about 2000°F. At temperatures above 2000°F the tantalum tends to react rapidly and exothermically with the H_2-F_2 environment.

CONTENTS

LIST OF ILLUSTRATIONS

TABLES

1. INTRODUCTION

This is the summary technical report describing the work performed by TRW Systems for the Sandia Corporation under Task 1 of Phase III of contract number 48-4912. The primary objective of this program is to investigate the chemical integrity of radioisotope containment materials when subjected to a booster vehicle abort environment.

Task 1 concerns itself with the investigation of the behavior of selected nuclear containment materials in simulated launch abort fires containing fluorine and hydrogen fluoride. Since rocket systems are under development which will utilize fluorine propellants and since it certainly will be desirable from a mission standpoint to "fly" radioisotope heat sources on these rocket systems, the behavior of radioisotope containment materials in launch pad abort fires containing fluorine and hydrogen fluoride becomes a key aerospace nuclear safety question. The Task 1 effort was aimed, therefore, at determining as a function of temperature and time the extent of chemical interaction between typical radioisotope containment materials and thermochemically defined hydrogen-fluorine flame environments.

Samples of four radioisotope containment materials (Type 316 stainless steel, Hastelloy C, Haynes alloy 25 and tantalum) were exposed to hydrogen-fluorine flame environments over a range of flame compositions, exposure times and sample temperatures. Selected containment material samples were then subjected to metallographic and chemical analyses to determine the type and extent of flame interaction.

The experimental facility, procedures, and results are discussed and presented in the following sections and conclusions are drawn.

2. EXPERIMENTAL EQUIPMENT AND PROCEDURES

2.1 HYDROGEN-FLUORINE FLAME FACILITY

Hydrogen-fluorine flame interaction studies are conducted in a facility designed for this type of hazardous interaction work. The toxic and corrosive nature of gaseous fluorine and fluorine-oxygen (FLOX) oxidizers requires special precautions and handling procedures which are not suited to the flame facilities used in other phases of the (launch abort) program.

The H_2-F_2 interaction facility is housed in a concrete block test cell at the TRW Systems Inglewood Test Site. The cell is provided with an exhaust system to remove the toxic fluorine combustion species during and after testing.

The fluorine gas supply cylinder is housed within a barricade in the test cell. All fluorine valves and plumbing are confined to this structure. Flow metering and control functions for this facility are accomplished by "reach rods" operated from outside the confines of the cell or, where possible, by remotely operated solenoid valves. Two observation windows, located at the center of adjacent walls, are provided for visual test monitoring. The torch system is controlled from one observation window. The second window, located within an adjacent structure, is used for optical pyrometry, photography and instrument recording functions.

The hydrogen-fluorine flame system is represented schematically in Figure 1. The system consists of an external mixing co-axial torch supplied by metered flows of hydrogen and fluorine. The mixing of the hypergolic gases results in an inherently stable flame over a wide range of flow and mixture ratio conditions. Provisions are made to purge all lines with nitrogen at the conclusion of each test series. The solenoid valves (Figure 1), just upstream from the torch assembly, are closed to maintain a positive nitrogen pressure in all lines, during the time the system is inoperative.

The torch assembly and containment material sample handling device used in this investigation are represented in Figure 2. The test apparatus is positioned in the center of the test cell in line with both observation windows. Observer to sample distance is less than five feet.

Test specimens are supported on the rotary table (Figure 2) and exposed in sequence to the stabilized hydrogen-fluorine flame environment. By this method, all samples of a set are subjected to the same flame temperature and composition within narrow limits. The test program is expedited, since safety considerations require a 20-30 minute delay before personnel are permitted to enter the test cell to change samples.

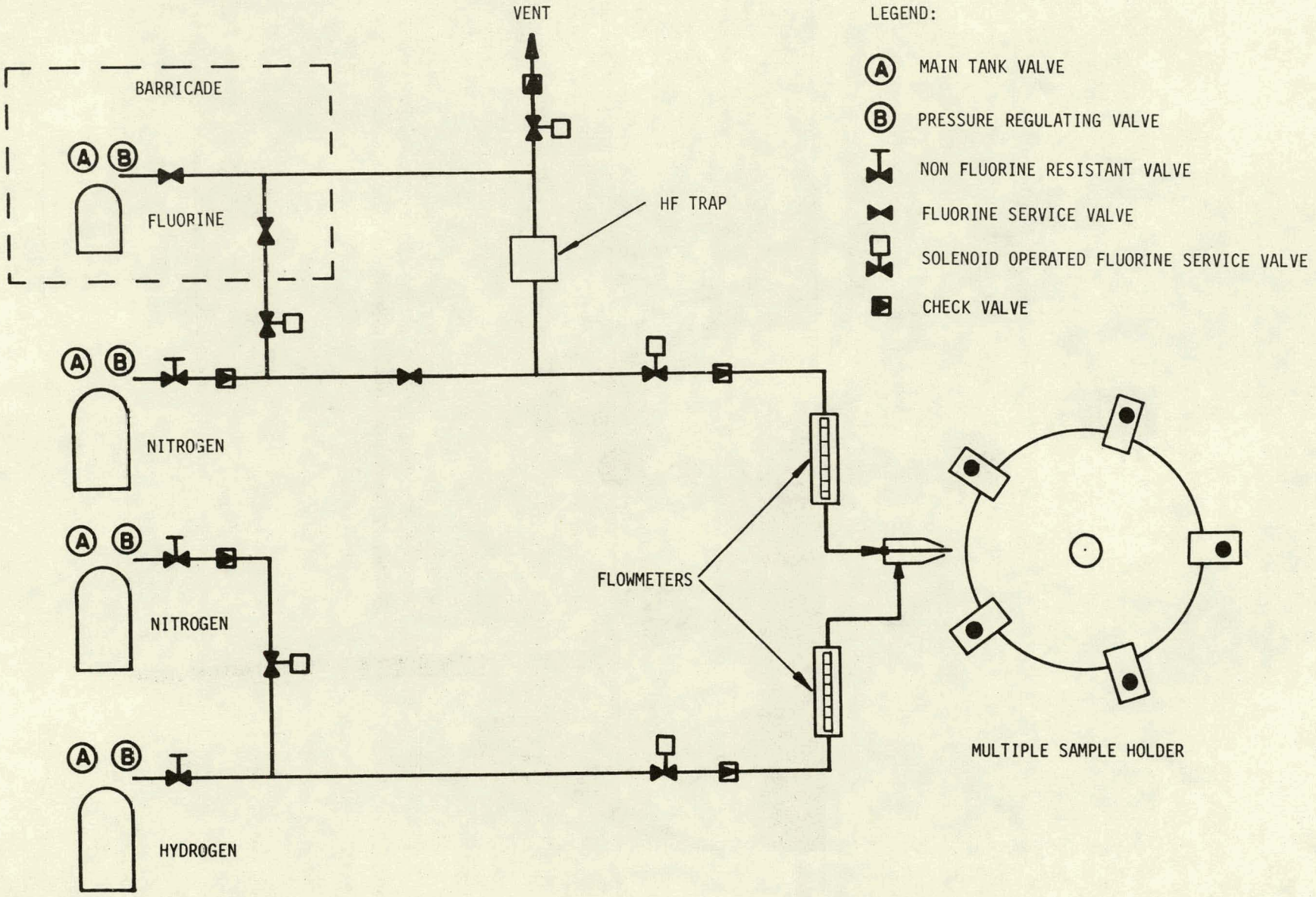

Figure 1. Schematic Diagram of the H_2-F_2 Flame Facility

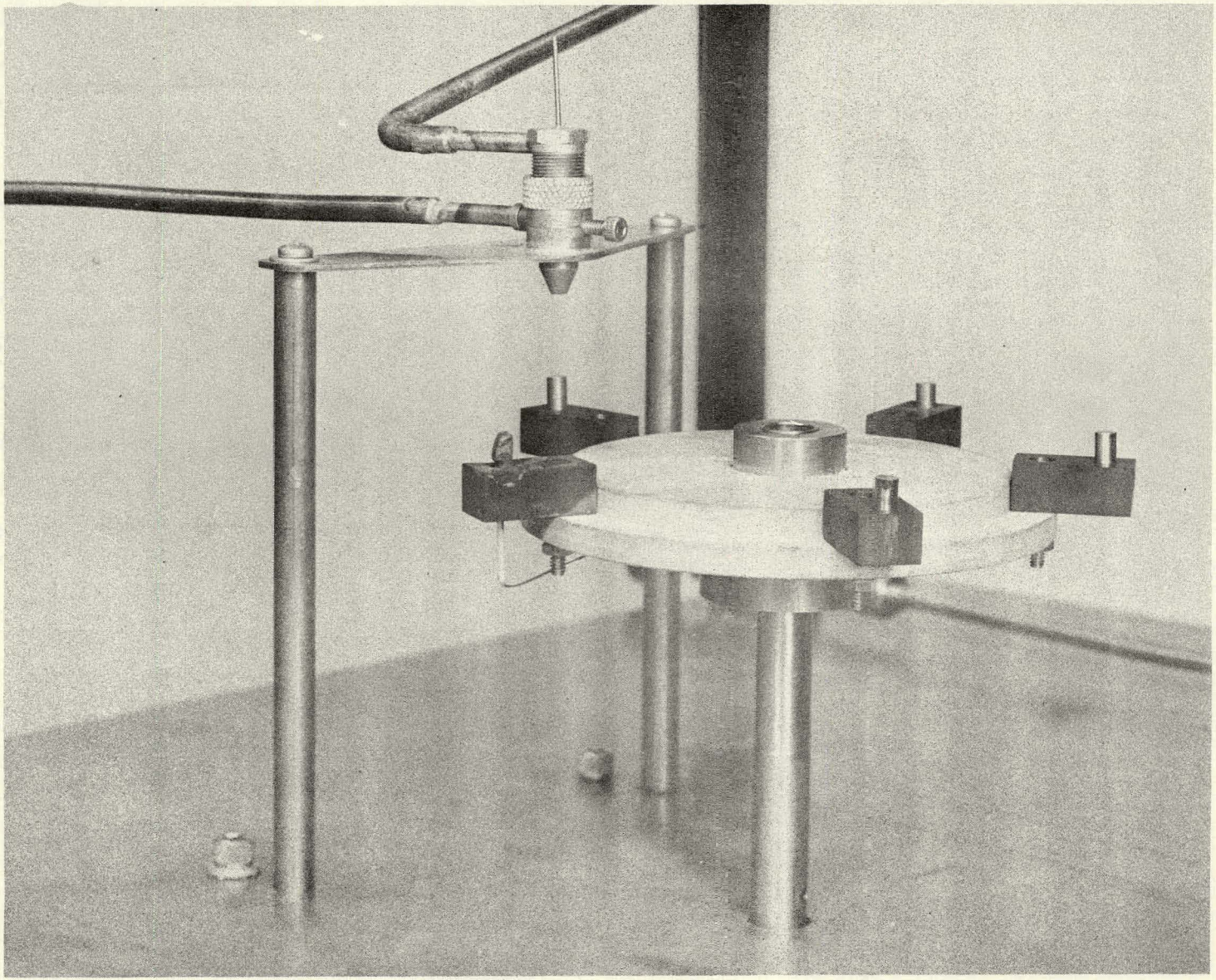

Figure 2. H_2-F_2 Torch and Multiple Sample Holder

The transite sample holders used in the hydrogen-oxygen flame interaction studies could not be adapted to the hydrogen-fluorine interaction system. Transite, an asbestos composite, was found to react violently with the hydrogen-fluorine flame environment. Sample holders were, therefore, fabricated from a high density graphite. The 3/16" diameter x 1/2" long samples were embedded in the graphite block which was then attached to a transite disc (Figure 2). This configuration was adopted in an attempt to minimize the heat capacity of the sample holding system.

Safety considerations limit the test facility fluorine capacity to approximately 150 standard liters. For the test series reported herein, fluorine flowrates varied from a minimum of 1.0 to approximately 2.0 liters per minute. Only 75% of the capacity of the fluorine cylinder is usable and a portion of this is expended in establishing the correct flame conditions for each test series. Total sample exposure time for any one test sequence is limited, therefore, to approximately sixty minutes.

The hydrogen-fluorine flame facility is capable of exposing interaction samples up to approximately 1/4" diameter in a totally engulfing hydrogen-fluorine flame. Other sample geometries are possible, however, where total exposure of the sample to the flame is not essential. The 3/16" diameter x 1/2" long domed sample geometry used in the Task 1 investigation proved to be an ideal configuration.

2.2 INSTRUMENTATION AND TEST PROCEDURE

Each 3/16" diameter x 1/2" long containment material sample tested was equipped with a No. 28 A.W.G. chromel-alumel thermocouple embedded in a longitudinal hole drilled to a depth 1/10" below the top surface of the sample. The thermocouple leads were insulated from the containment material and the graphite support by a 1/16" diameter alumina sheath. The surface temperatures of exposed samples were measured by means of a recording two-color pyrometer or micro-optical brightness pyrometer sighting on portions of the sample, through the test cell observation window. Continuous records of thermocouple and two-color pyrometer outputs were made on two single-channel millivolt chart recorders (Figure 3).

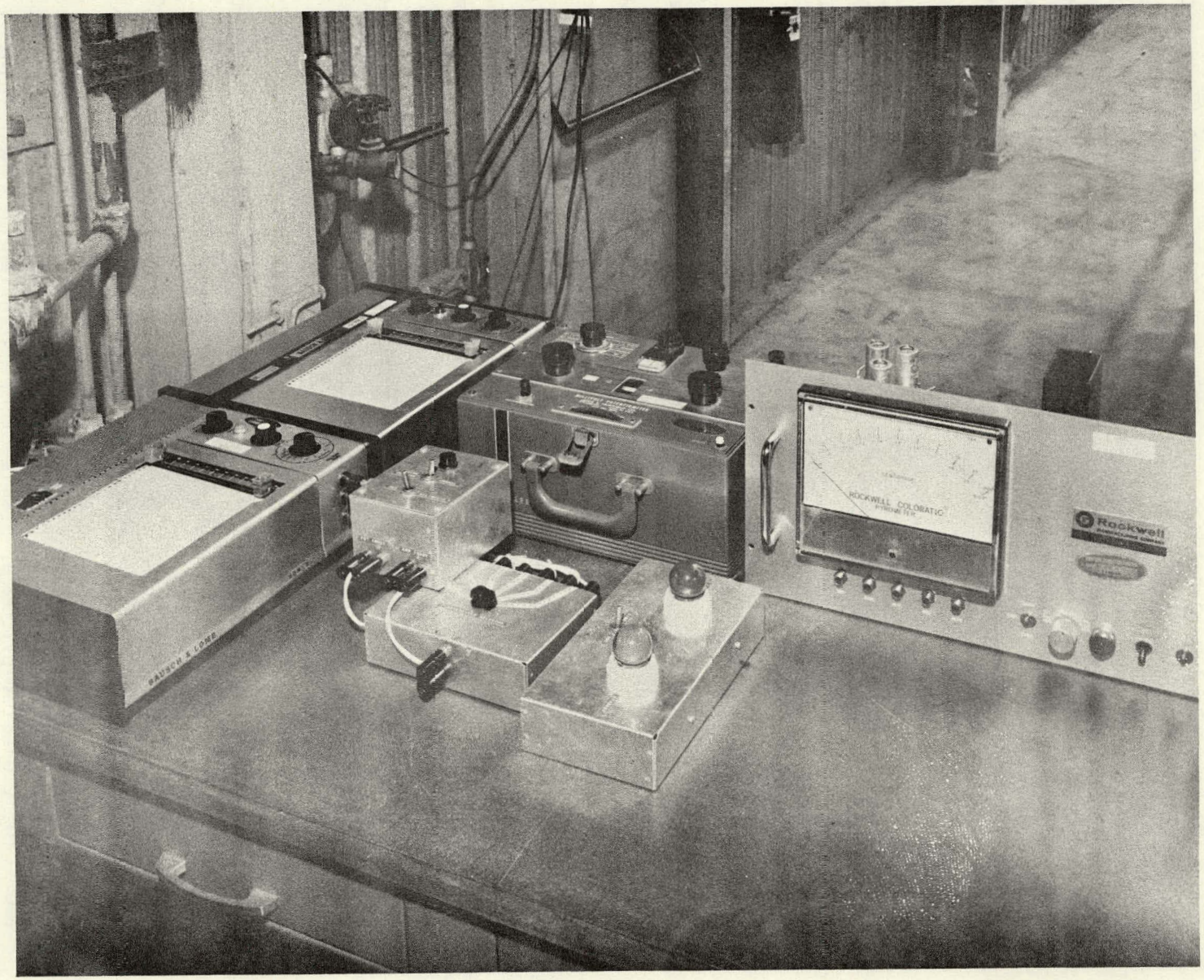

Figure 3. Test Instrumentation

A fixed sample to torch spacing was maintained for all experiments. Flame to sample heat transfer rates were raised by increasing the volumetric flows of fluorine and hydrogen to the torch at a constant mixture ratio. Samples of each of the four containment materials (Type 316 stainless steel, Hastelloy C, Haynes alloy 25, and tantalum) were exposed in sequence to a carefully controlled, stable hydrogen-fluorine flame. In general, each experiment was limited to a duration of from two to three minutes. The timing of the experiment was determined by either the time required for the sample to reach a pseudo thermal-equilibrium (thermocouple recording) or by the severity of the reaction between the containment material sample and the flame. The graphite sample support represents a significant heat sink due to its relatively large mass in comparison to that of the containment material sample. The resulting thermal response of this system is relatively slow, and thermal equilibrium was not attained in the 2-3 minute duration of the experiment. Actual temperature versus time records were obtained for all experiments, however, from individual thermocouple traces.

A copper "calorimeter" having the same shape, size, and physical configuration as the test specimens was exposed to each new flame condition as a calibration experiment to determine an initial heat flux value.

3. DISCUSSION OF RESULTS

Each sample of the four containment materials (Type 316 stainless steel, Hastelloy C, Haynes 25 and tantalum) exposed to the hydrogen-fluorine flame was photographed for the record. These macro-photographs together with the temperature history of each exposed sample are included in order of accomplishment in Appendix A.

Selected containment material samples were mounted and sectioned in preparation for metallographic analysis. After polishing and etching, macro and micro-photographs of the sample cross-sections were prepared. These photographic data summaries are presented in the body of this report.

A concise data summary of all hydrogen-fluorine interaction experiments is included as Table 1. Initial heat flux data for each experiment are included in the summary. Steady state temperatures calculated from initial heat flux data were compared with the temperature versus time (thermocouple) traces (Table 1). The comparison in most cases tends to substantiate the thesis that true thermal equilibrium was not attained in the majority of the hydrogen-fluorine interaction experiments because of the relatively large mass of the graphite sample holder configuration. A comparison of two-color pyrometer surface temperature data and calculated steady state sample temperatures (Table 1) indicates the occurrence of severe sample-flame exothermic interactions in some experiments.

The results of the initial hydrogen-fluorine interaction experiments (experiment Nos. 1 through 8) are also presented in Table 1. These samples were 3/16" diameter x 1/2" long cylinders. No metallographic analyses were conducted on these specimens which were characterized by severe top erosion. In order to present a better profile to the hydrogen-fluorine flame, the remaining 3/16" diameter x 1/2" long cylindrical samples were prepared with hemispherical (domed) tops. The domed sample configuration, with no sharply defined edges, resulted in more uniform heat distribution. The results of these domed sample experiments are felt to be more significant than those of the earlier cylindrical configuration.

3.1 METALLOGRAPHIC ANALYSIS

The results of metallographic analyses of the four radioisotope containment material samples (Type 316 stainless steel, Hastelloy C, Haynes 25, and tantalum) are presented by material types below:

3.1.1 Type 316 Stainless Steel

Four type 316 stainless steel samples, previously exposed to a fluorine rich flame environment (F_2/H_2 = 1.166) for 2-3 minutes, were subjected to metallographic analysis. A very thin surface-reaction coating is apparent from a study of the 50X photomicrographs of sample Nos. 13 and 40 (Figures 4 and 5) after exposures at maximum temperatures of 1400°F and 1700°F, respectively. Sample No. 21 (Figure 6) exposed to the same fluorine rich flame environment at a maximum bulk sample temperature of 1830°F underwent a slight interaction along its upper surface to a depth of approximately

TABLE 1

HYDROGEN-FLUORINE INTERACTION DATA SUMMARY

Exp. No.	Material	Configuration	F_2 Flow lpm	H_2 Flow lpm	F_2/H_2*	Initial Heat Flux BTU/Ft^2-sec	Calculated Steady State Temp.-°F	Cr-Al Thermocouple Temp.-°F	Peak Surface Temp.-°F	Total Exposure Time-Sec
1	316 S.S.	Cylindrical	1.32	1.13	1.166/1	39.0	2370	2230	3630	75
2	Tantalum	Cylindrical	1.32	1.13	1.166/1	39.0	>2600	2360	3050	150
3	Hastelloy C	Cylindrical	1.32	1.13	1.166/1	39.0	2330	2120	2910	165
4	Haynes 25	Cylindrical	1.32	1.13	1.166/1	39.0	2440	2300	2100	185
5	316 S.S.	Cylindrical	2.08	1.79	1.166/1	52.1	2550	>2500	3450	78
6	Tantalum	Cylindrical	2.08	1.79	1.166/1	52.1	>2600	>2500	3810	60
7	Hastelloy C	Cylindrical	2.08	1.79	1.166/1	52.1	2510	>2500	3360	234
8	Haynes 25	Cylindrical	2.08	1.79	1.166/1	52.1	2600	>2500	3180	138
9	316 S.S.	Domed	1.32	1.13	1.166/1	32.6	2260	2120	2800	112
10	Tantalum	Domed	1.32	1.13	1.166/1	32.6	2580	2420	2520	119
11	Hastelloy C	Domed	1.32	1.13	1.166/1	32.6	2220	2350	2420	123
12	Haynes 25	Domed	1.32	1.13	1.166/1	32.6	2330	2280	<2300	128
13	316 S.S.	Domed	0.90	0.77	1.166/1	14.7	1820	1400	<2300	195
14	Tantalum	Domed	0.90	0.77	1.166/1	14.7	2110	1560	<2300	147
15	Hastelloy C	Domed	0.90	0.77	1.166/1	14.7	1790	1570	<2300	147
16	Haynes 25	Domed	0.90	0.77	1.166/1	14.7	1880	1630	<2300	131
17	Haynes 25	Domed	1.71	1.46	1.166/1	21.0	2070	2460	2890	200
18	Tantalum	Domed	1.71	1.46	1.166/1	21.0	2320	2360	3240	303
19	Tantalum	Domed	2.08	1.79	1.166/1	46.0	>2600	2490	3540	120
20	Tantalum	Domed	2.43	2.09	1.166/1	52.5	>2600	2530	3470	174
21	316 S.S.	Domed	1.10	0.95	1.166/1	19.8	1980	1830	<2300	328
22	Haynes 25	Domed	1.10	0.95	1.166/1	19.8	2040	1840	<2300	153
23	316 S.S.	Domed	1.32	1.92	0.689/1	37.6	2330	2120	<2300	172

TABLE 1 (CONTINUED)

HYDROGEN-FLUORINE INTERACTION DATA SUMMARY

Exp. No.	Material	Configuration	F_2 Flow lpm	H_2 Flow lpm	F_2/H_2 **	Initial Heat Flux BTU/ft^2-sec	Calculated Steady State Temp -°F	Cr-Al Thermocouple Temp.-°F	Peak Surface Temp.-°F	Total Exposure Time-Sec
24	Tantalum	Domed	1.32	1.92	0.689/1	37.6	2630	2150	<2300	160
25	Hastelloy C	Domed	1.32	1.92	0.689/1	37.6	2290	2110	<2300	141
26	Haynes 25	Domed	1.32	1.92	0.689/1	37.6	2400	2250	<2300	145
27	316 S.S.	Domed	1.71	2.48	0.689/1	51.7	2510	2400	3160	148
28	Tantalum	Domed	1.71	2.48	0.689/1	51.7	>2600	2380	3300	198
29	Hastelloy C	Domed	1.71	2.48	0.689/1	51.7	2480	2400	2890	142
30	316 S.S.	Domed	2.08	3.02	0.689/1	47.4	2460	2440	2950	173
31	Tantalum	Domed	2.08	3.02	0.689/1	47.4	>2600	2360	3250	180
32	Hastelloy C	Domed	2.08	3.02	0.689/1	47.4	2430	>2500	2970	128
33	Haynes 25	Domed	2.08	3.02	0.689/1	47.4	2530	>2500	2970	124
34	316 S.S.	Domed	2.08	3.02	0.689/1	47.4	2460	2373	3380	108
35	Hastelloy C	Domed	1.51	2.20	0.689/1	35.4	2250	2200	2426	185
36	Haynes 25	Domed	1.71	2.48	0.689/1	34.0	2340	2270	--**	196
37	Hastelloy C	Domed	1.10	0.95	1.166/1	22.0	2000	1750	--	202
38	Hastelloy C	Domed	1.42	2.06	0.689/1	30.0	2150	2100	--	185
39	Haynes 25	Domed	1.21	1.04	1.166/1	21.0	2070	1950	--	277
40	316 S.S.	Domed	1.21	1.04	1.166/1	21.0	2010	1700	2000***	120
41	316 S.S.	Domed	1.21	1.04	1.166/1	21.0	2010	2010	2180***	900
42	Hastelloy C	---	--	--	---	--	--	--	--	--****
43	Tantalum	Domed	1.21	1.04	1.166/1	21.0	2320	2000	2080***	900
44	Haynes 25	Domed	1.21	1.04	1.166/1	21.0	2070	2280	2560***	900
45	Hastelloy C	Domed	1.10	0.95	1.166/1	22.0	2000	2250	2280***	895
46	Tantalum	Domed	1.32	1.13	1.166	39.0	>2600	2350	2900***	900

*Equilibrium Flame Composition and Temperature

Mole Ratio F_2/H_2	Adiabatic Flame Temp.-°F	Composition-Mole Fraction F	F_2	H	H_2	HF
1.166	6745	.275	10^{-6}	.138	.007	.580
0.689	6426	.066	10^{-7}	.266	.053	.615

**No data available.

***Micro-optical pyrometer data.

****Sample accidentally destroyed.

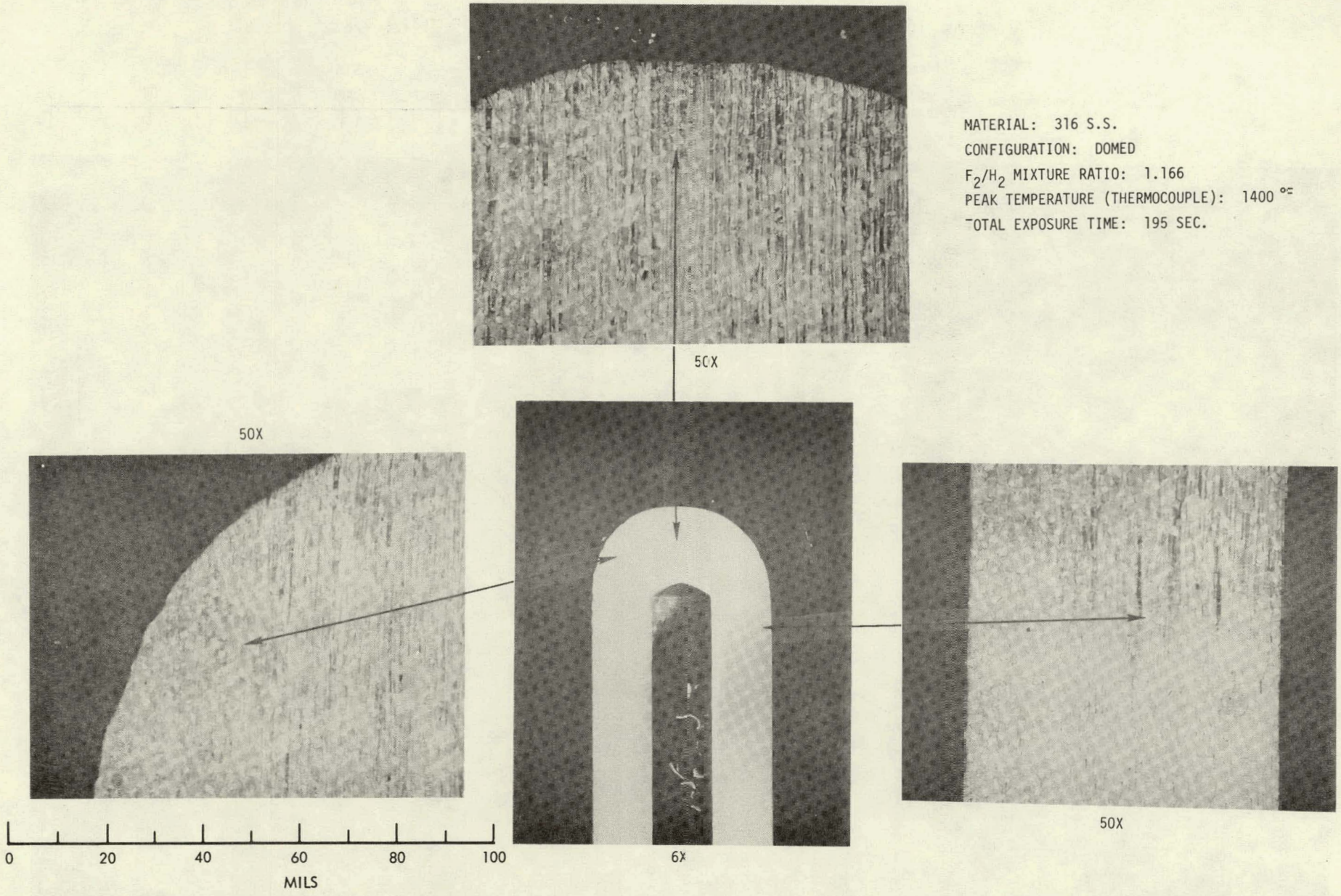

Figure 4. Hydrogen-Fluorine Experiment No. 13

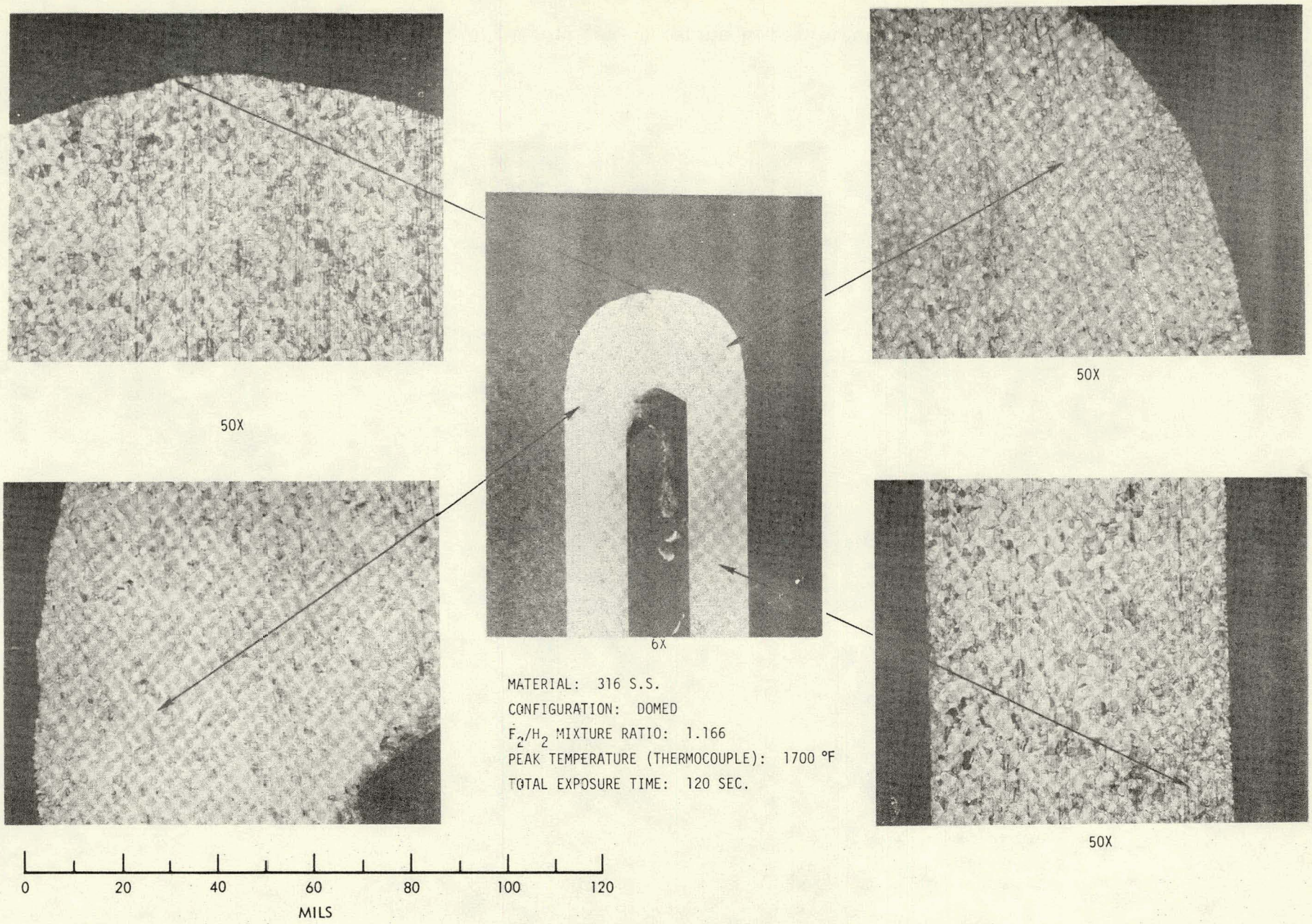

Figure 5. Hydrogen-Fluorine Experiment No. 40

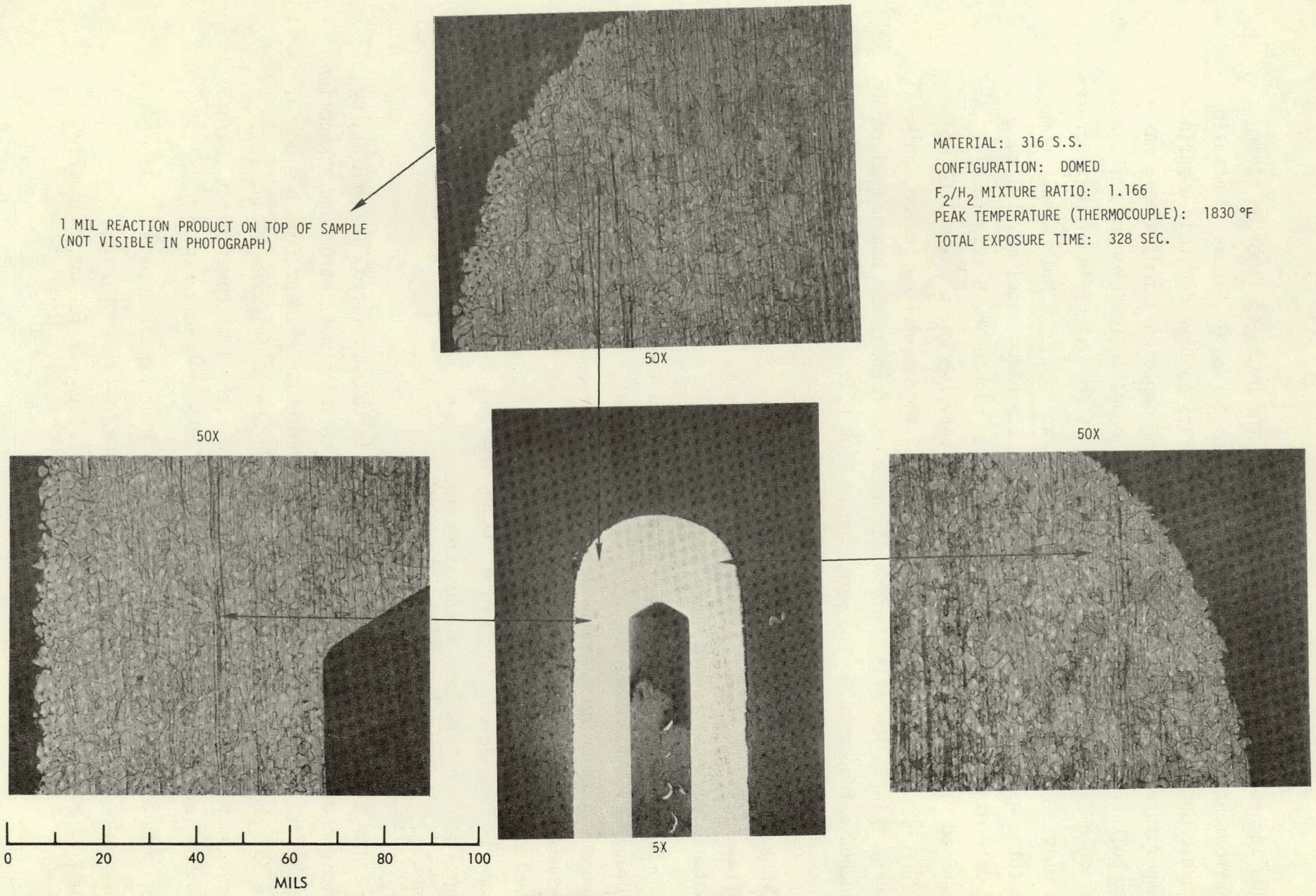

Figure 6. Hydrogen-Fluorine Experiment No. 21

.005 inches. A moderate interaction with the hydrogen-fluorine flame environment is apparent from a study of sample No. 9 (Figure 7) metallographic data. The top of this sample appears to have ignited; a surface temperature of 2800°F was measured. Thermocouple data indicates a maximum bulk sample temperature of 2130°F. The 50X photomicrographs (Figure 7) are of special interest, since a study of this sample's microstructure reveals a molten region at the hemispherical top. The bulk sample temperature was some 300°F below the Type 316 stainless steel melting range as determined by thermocouple measurement. Sample No. 9 (Figure 7) remained virtually intact except for the very top which was melted and eroded by the hydrogen-fluorine flame. In the non-melted region, only a very thin (a few mils) corrosion layer was formed; the non-melted region reached a temperature of approximately 2100°F.

A fifteen minute duration exposure to the fluorine rich flame (F_2/H_2 = 1.166) at a bulk temperature of 2010°F (Figure 8) reveals no significant surface reaction. Only a thin corrosion layer is evident in the 50X photomicrographs (Figure 8).

Sample No. 23 (Figure 9) was exposed to a thermochemically defined hydrogen rich flame environment (F_2/H_2 = 0.689). This sample appears to have suffered no appreciable interaction by exposure at 2120°F for 172 seconds. The presence of air in the vicinity of the flame and sample preclude the existence of free hydrogen in the flame. The F_2/H_2 = 0.689 flame is considered, in general, to be the less severe of the two environments used in this Task 1 investigation.

3.1.2 Hastelloy C

The Hastelloy C metallographic data is characterized, in general, by severe chemical interaction within the material's microstructure. Reaction in the grain boundaries to considerable depths is evident from a study of the 50X photomicrographs of sample Nos. 38 and 25 (Figures 10 and 11). These samples were exposed to the hydrogen rich flame environment (F_2/H_2 = 0.689) at temperatures of 2100°F and 2120°F, respectively.

Sample No. 37 (Figure 12) appears to have experienced only slight grain boundary interaction near the surface after exposure to the fluorine rich flame at a peak temperature of 1750°F for approximately

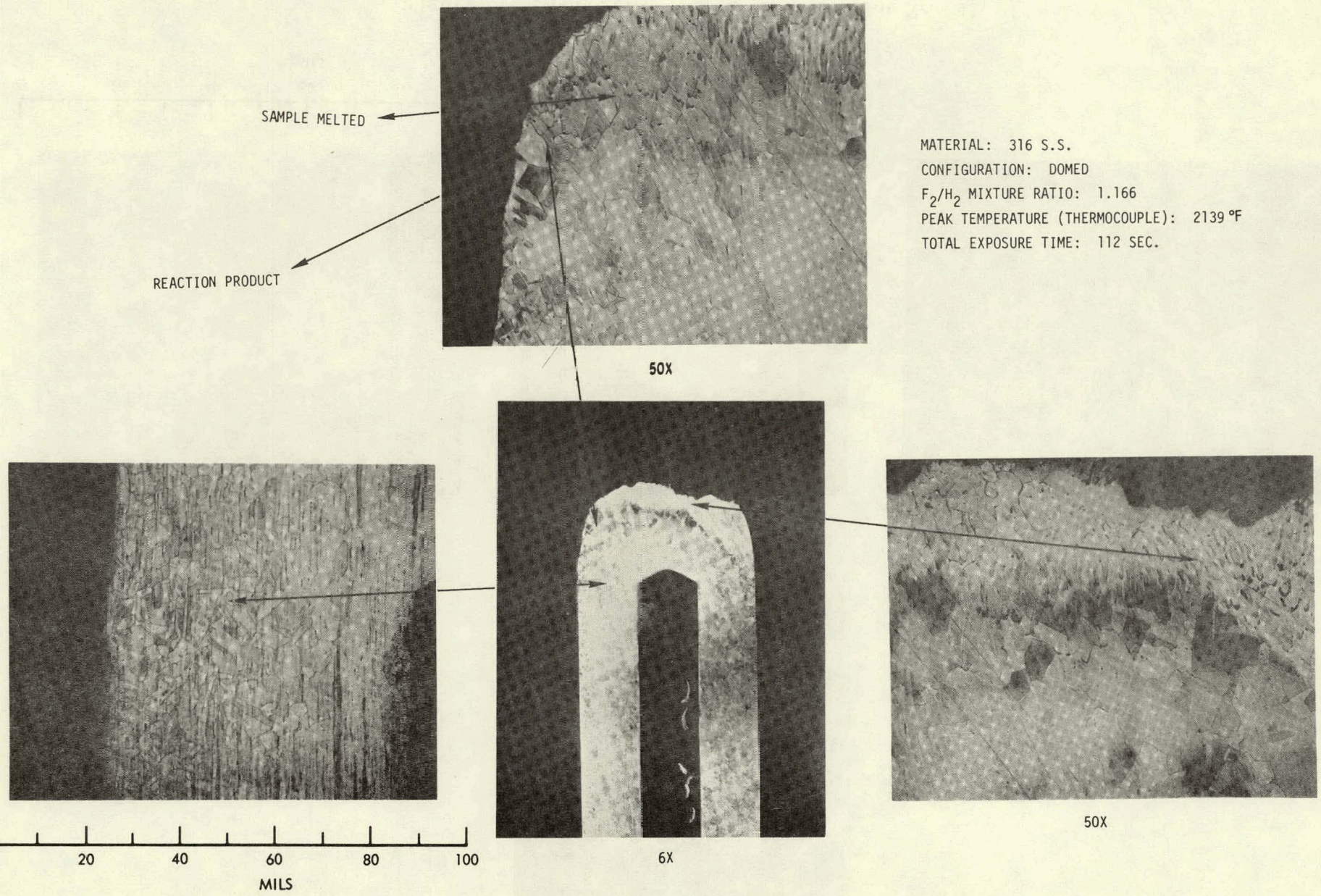

Figure 7. Hydrogen-Fluorine Experiment No. 9

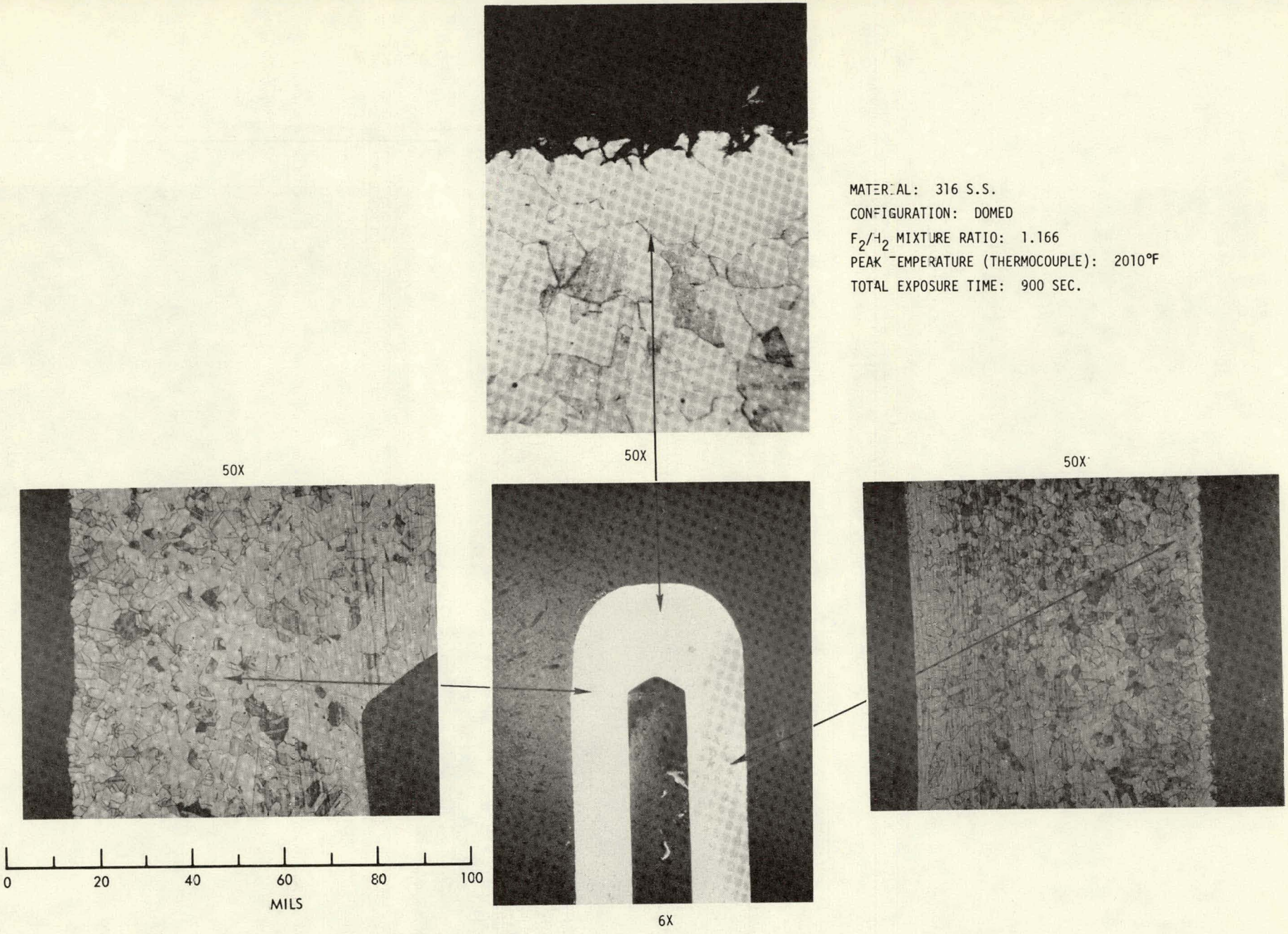

Figure 8. Hydrogen-Fluorine Experiment No. 41

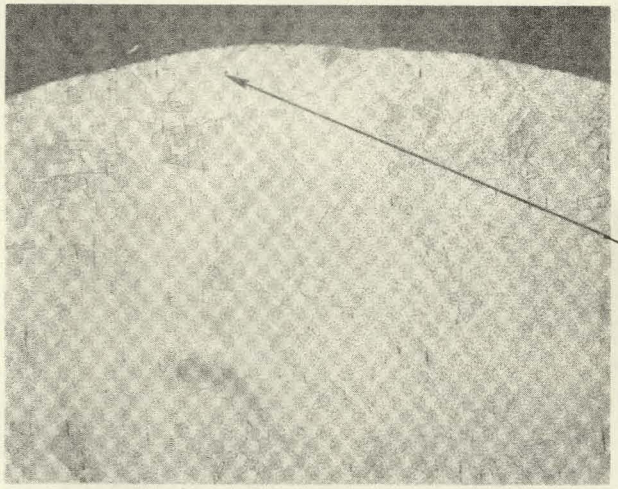

50X

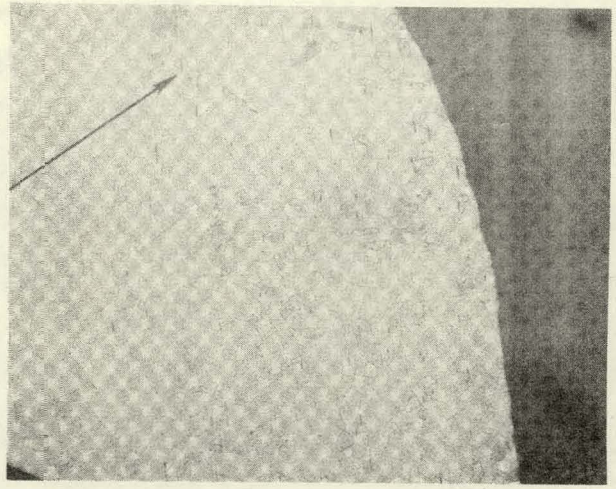

50X

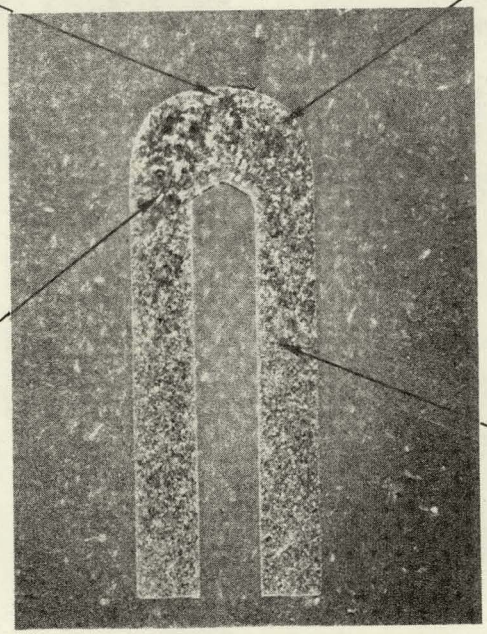

6X

MATERIAL: 316 S.S.
CONFIGURATION: DOMED
F_2/H_2 MIXTURE RATIO: .689
PEAK TEMPERATURE (THERMOCOUPLE): 2160°F
TOTAL EXPOSURE TIME: 172 SEC.

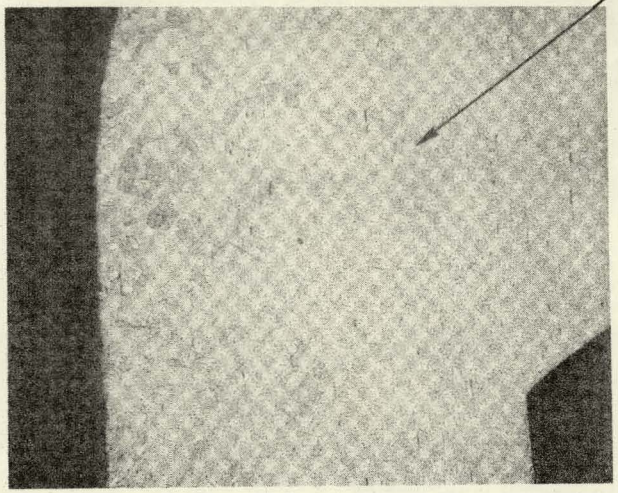

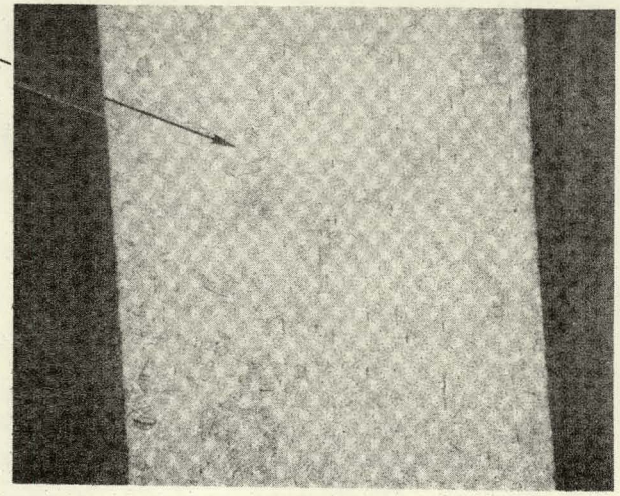

50X

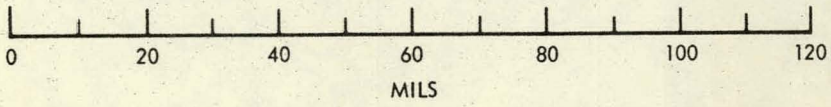

Figure 9. Hydrogen-Fluorine Experiment No 23

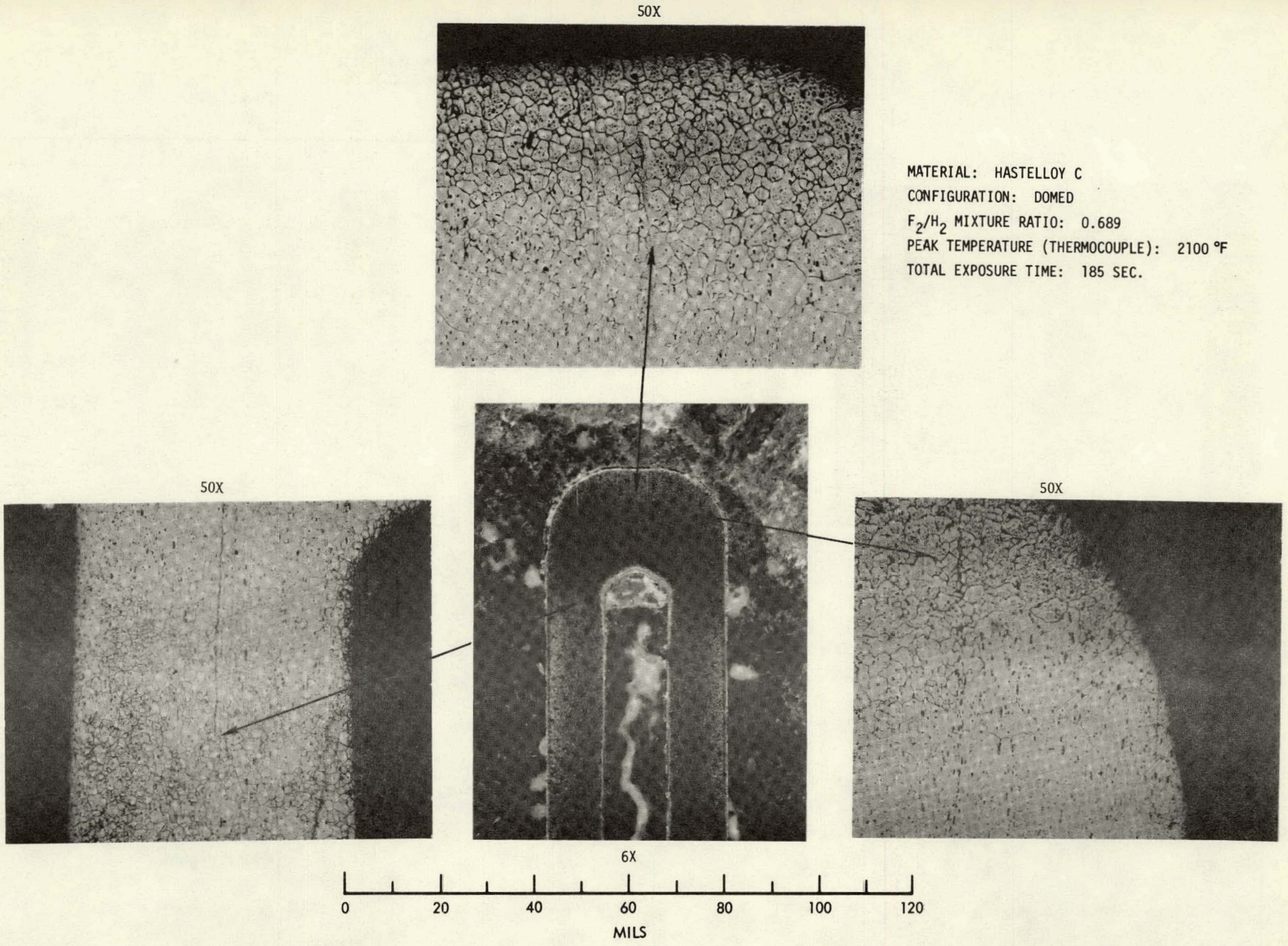

Figure 10. Hydrogen-Fluorine Experiment No. 38

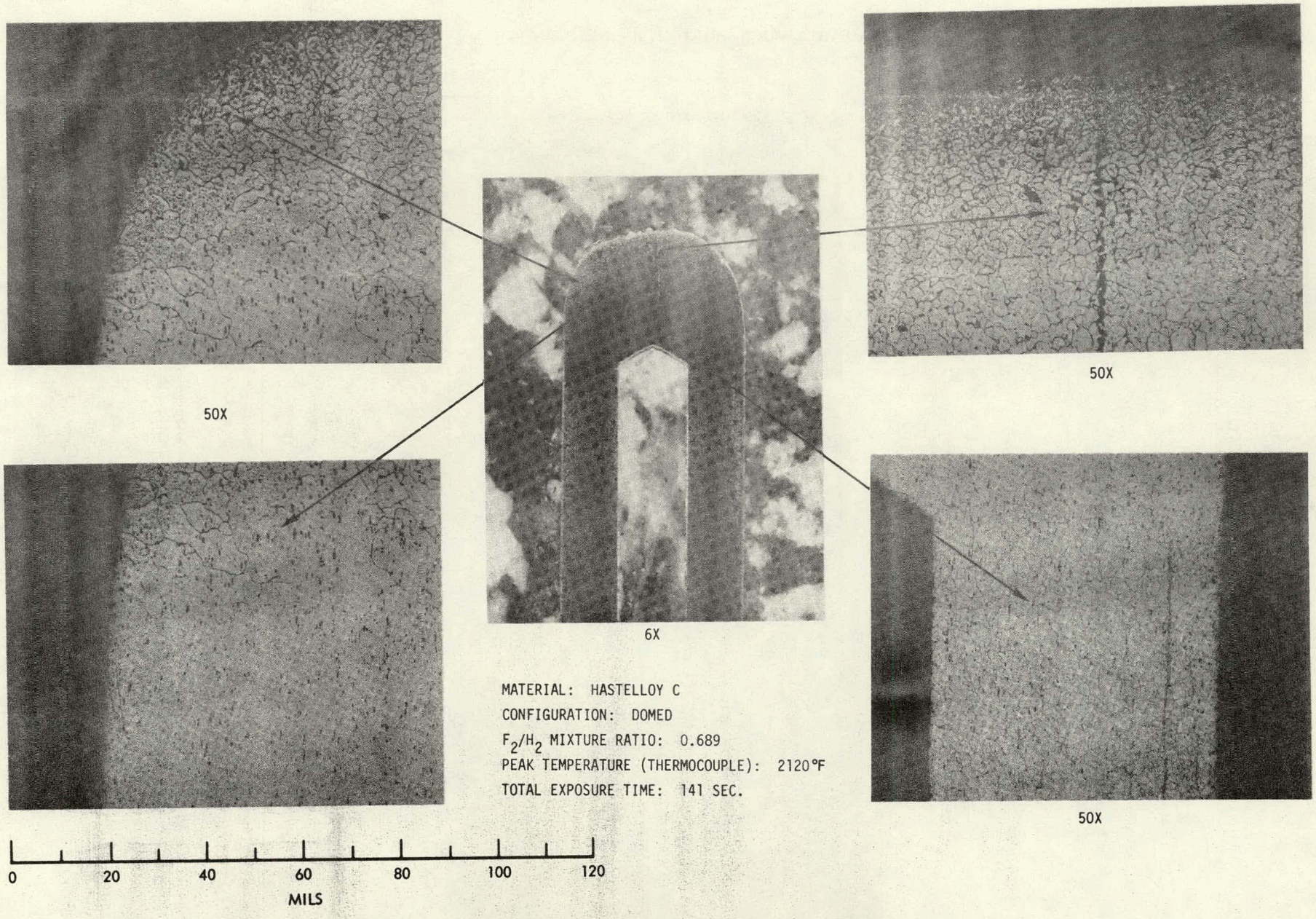

Figure 11. Hydrogen-Fluorine Experiment No. 25

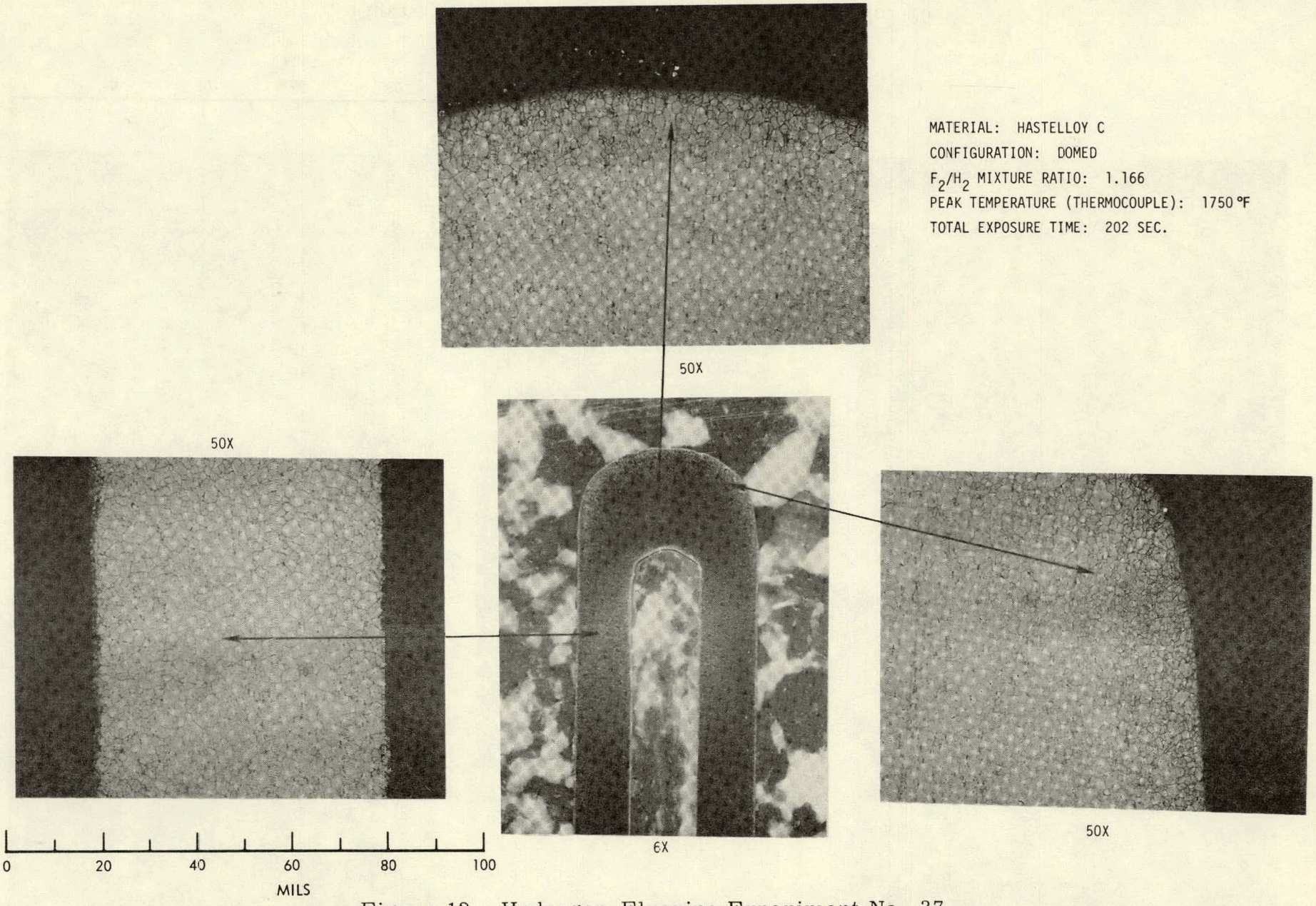

Figure 12. Hydrogen-Fluorine Experiment No. 37

three minutes. After a fifteen minute exposure to a similar flame* (F_2/H_2 = 1.166), sample No. 45 (Figure 13) exhibited severe grain boundary attack to a considerable depth. A thin corrosion layer a few mils thick is also evident in the 50X photomicrographs (Figure 13). Two-color pyrometer surface temperature data (Table 1) for sample No. 11 (Figure 14) indicates a surface temperature of 2420°F which is close to the Hastelloy C melting range. The sample did indeed melt, but with no evidence of any severe exothermic reaction with the flame environment.

Electron microprobe analysis of Sample No. 45 (Figure 13) was also conducted in an attempt to identify the Hastelloy C grain boundary reaction products. The results of this analysis are discussed in section 3.2.

3.1.3 Haynes 25

Figure 15 is the metallographic data summary of hydrogen-fluorine interaction sample No. 39. This sample attained a temperature of 1950°F during a 277 second exposure to the fluorine rich flame (F_2/H_2 = 1.166). Sample geometry remained intact and only a thin surface reaction layer is evident from a study of the 50X photomicrographs (Figure 15). The apparent flat dome of this sample was caused by machining, not by any flame interaction process.

The eroded sample depicted in Figure 16 (sample No. 12) was subjected to a heat flux severe enough to cause melting. The thermocouple data for this experiment, however, indicates a maximum sample temperature of only 2280°F. A large thermal gradient existed down the axis of the sample. The low temperature reading was caused by a mislocation of the thermocouple in the drilled passage. This is an isolated occurrence, since great care was taken to insure contact of the thermocouple with the sample throughout this study. The 50X photomicrographs of Figure 16 clearly show the Haynes 25 melting mechanism but fail to yield any evidence of surface flame interaction.

Sample No. 17 (Figure 17) was subjected to a much lower initial heat flux (Table 1) than the previous sample (Figure 16). The sample's microstructure (Figure 17) differs from that of the previous sample (Figure 16) due to the different thermal environments to which they were each subjected.

*Although the flame conditions were the same in experiments 37 and 45, the peak sample temperature ultimately reached 2280°F in the fifteen minute experiment 45.

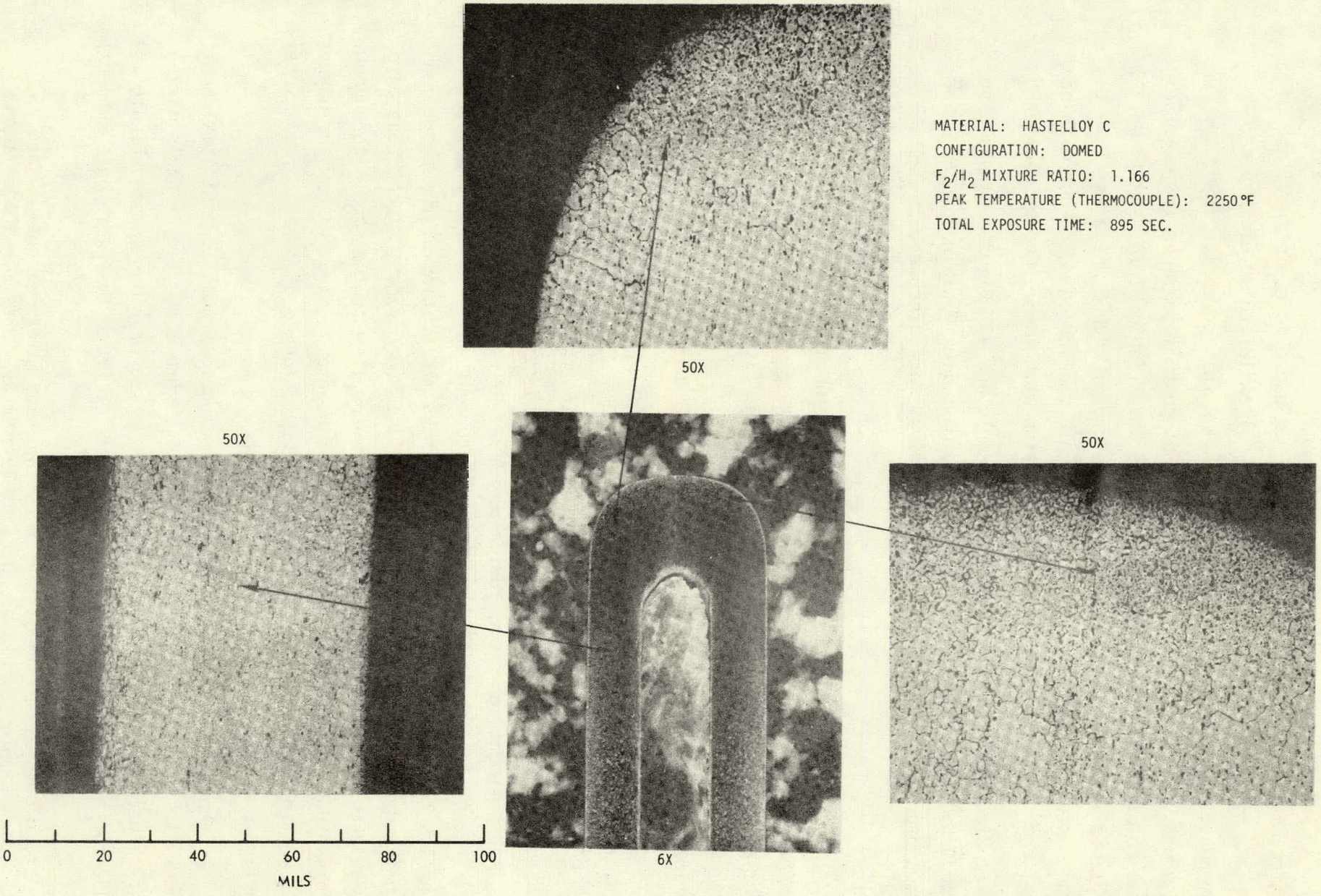

Figure 13. Hydrogen-Fluorine Experiment No. 45

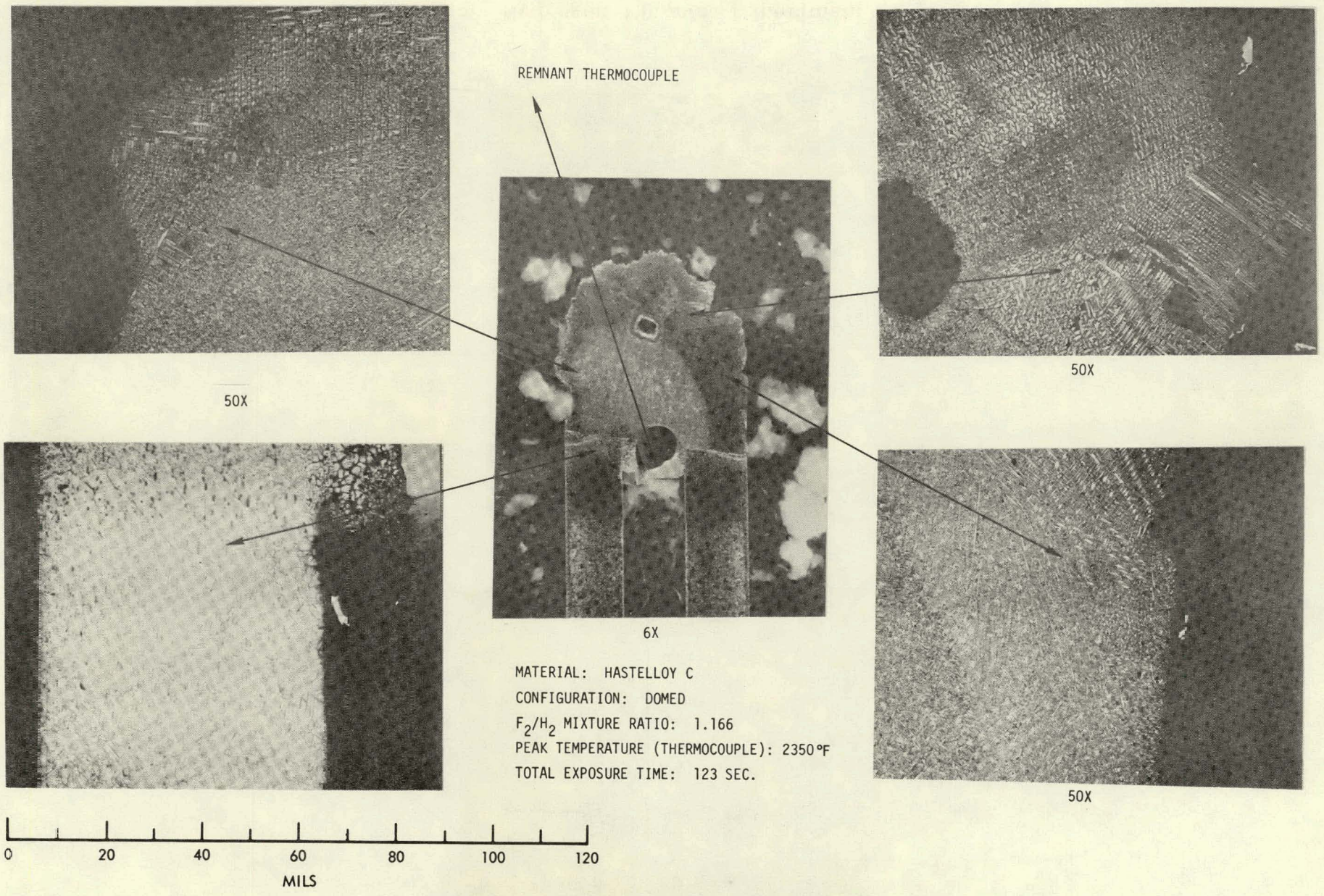

Figure 14. Hydrogen-Fluorine Experiment No. 11

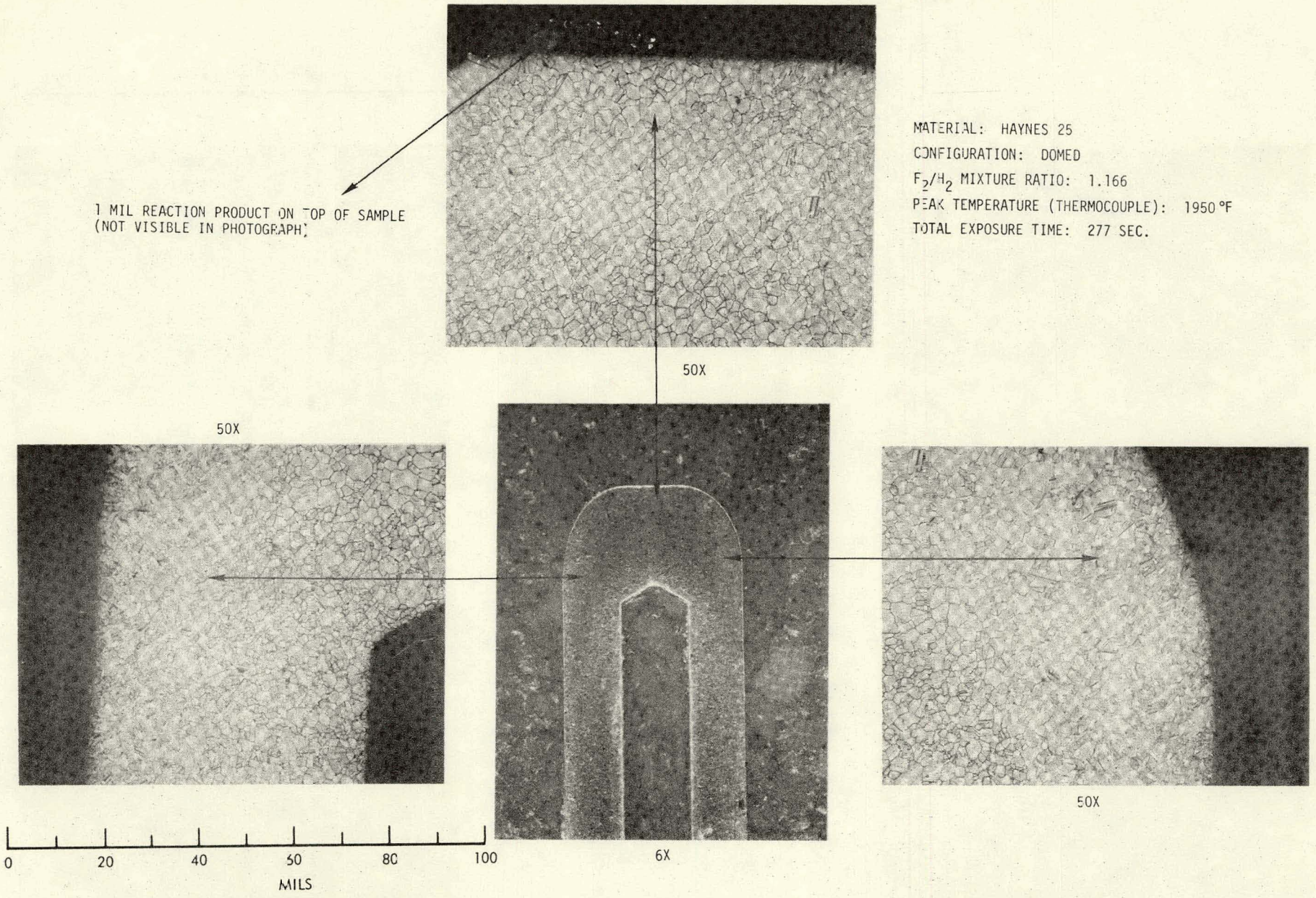

Figure 15. Hydrogen-Fluorine Experiment Nc. 39

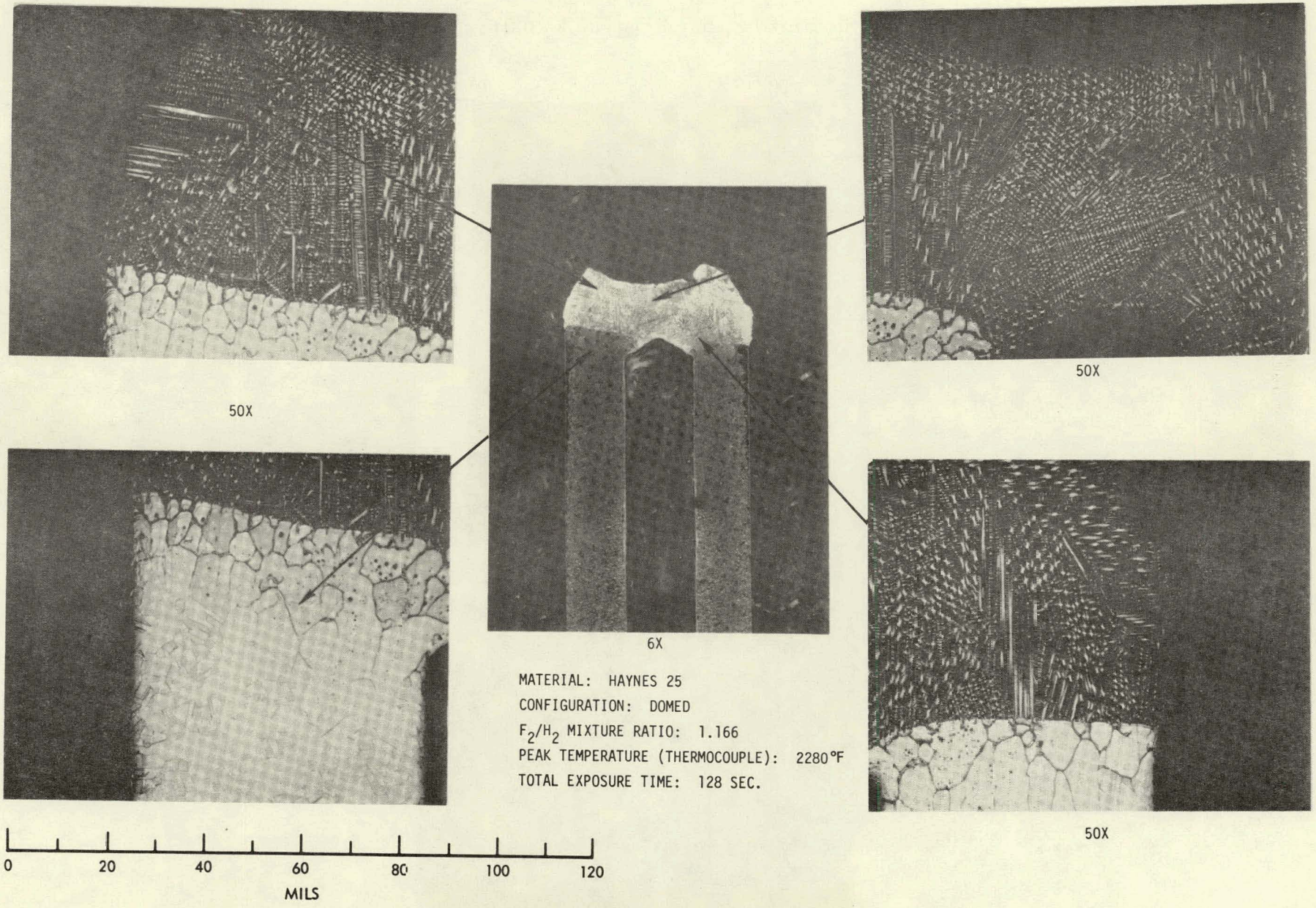

Figure 16. Hydrogen-Fluorine Experiment No. 12

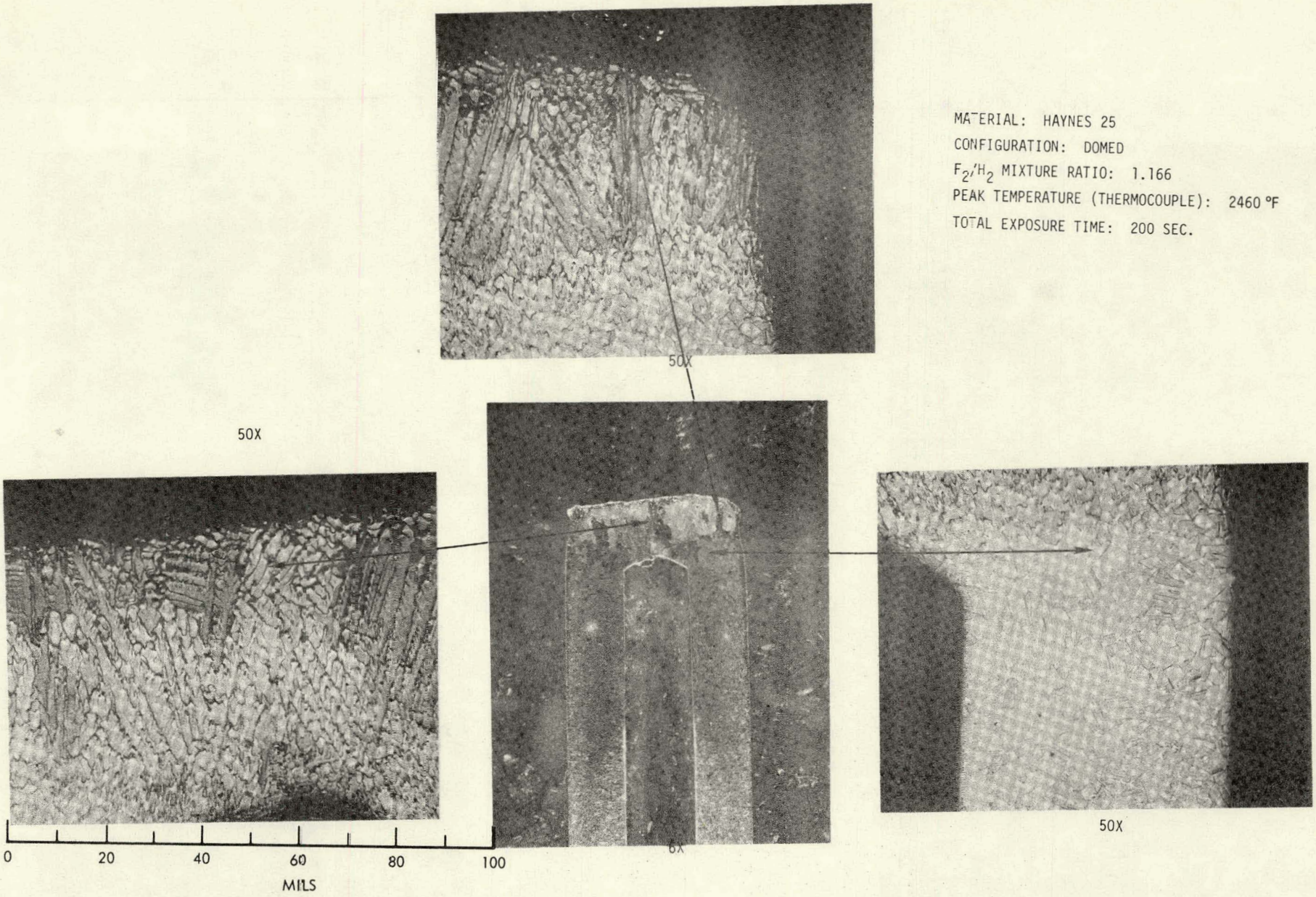

Figure 17. Hydrogen-Fluorine Experiment No. 17

Sample No. 44 (Figure 18) was exposed to the fluorine rich flame (F_2/H_2 = 1.166) environment for fifteen minutes up to a maximum measured bulk temperature of 2280°F. The top of the sample was just beginning to melt as the test was concluded. This portion of the sample can, therefore, be assumed to have reached a temperature of about 2500°F. The sample geometry remained intact and no appreciable interaction, other than a thin surface coating, is apparent from the photomicrographs (Figure 18) at temperatures approaching the Haynes 25 melting range. Limited grain boundary attack is in evidence at the very top of the sample, the hottest spot. This sample was subjected to electron microprobe analysis. The results of this analysis are discussed in section 3.2 of this report.

Figure 19 is the photographic data summary for Sample No. 36, a sample exposed to the hydrogen rich (F_2/H_2 = 0.689) flame at a maximum temperature of 2270°F. There is no evidence of gross reaction with this particular flame environment, other than the thin surface reaction coating and a very limited grain boundary attack at the hottest portion of the sample.

3.1.4 Tantalum

All tantalum samples subjected to metallographic analyses and reported herein showed considerable interaction and corrosion with both the fluorine and hydrogen rich flame environments (F_2/H_2 = 1.166 and 0.689) for temperatures above 2350°F. Two-color pyrometer surface temperature data of the order of 1000°F higher than calculated steady state values (Table 1) indicate rapid exothermic interaction at the flame-sample interface. Figures 20, 21, 22, and 23 are the metallographic data summaries for those tantalum samples which were exposed to these flame environments at temperatures of 2350°F and above. The typical 50X photomicrographs (Figures 20, 21, 22, 23) indicate reaction zones of .010 to .020 inch thick with oxidation figures, at the tantalum reaction zone interface, .002 to .005 inch in depth. Severe erosion of the upper sample surface is evident from the appearance of the 6X photomicrographs of Figures 20 and 22.

Sample No. 43 (Figure 24) was exposed to the fluorine rich (F_2/H_2 = 1.166) flame environment for fifteen minutes attaining a maximum temperature of 2000°F during this exposure. The only evidence of interaction was

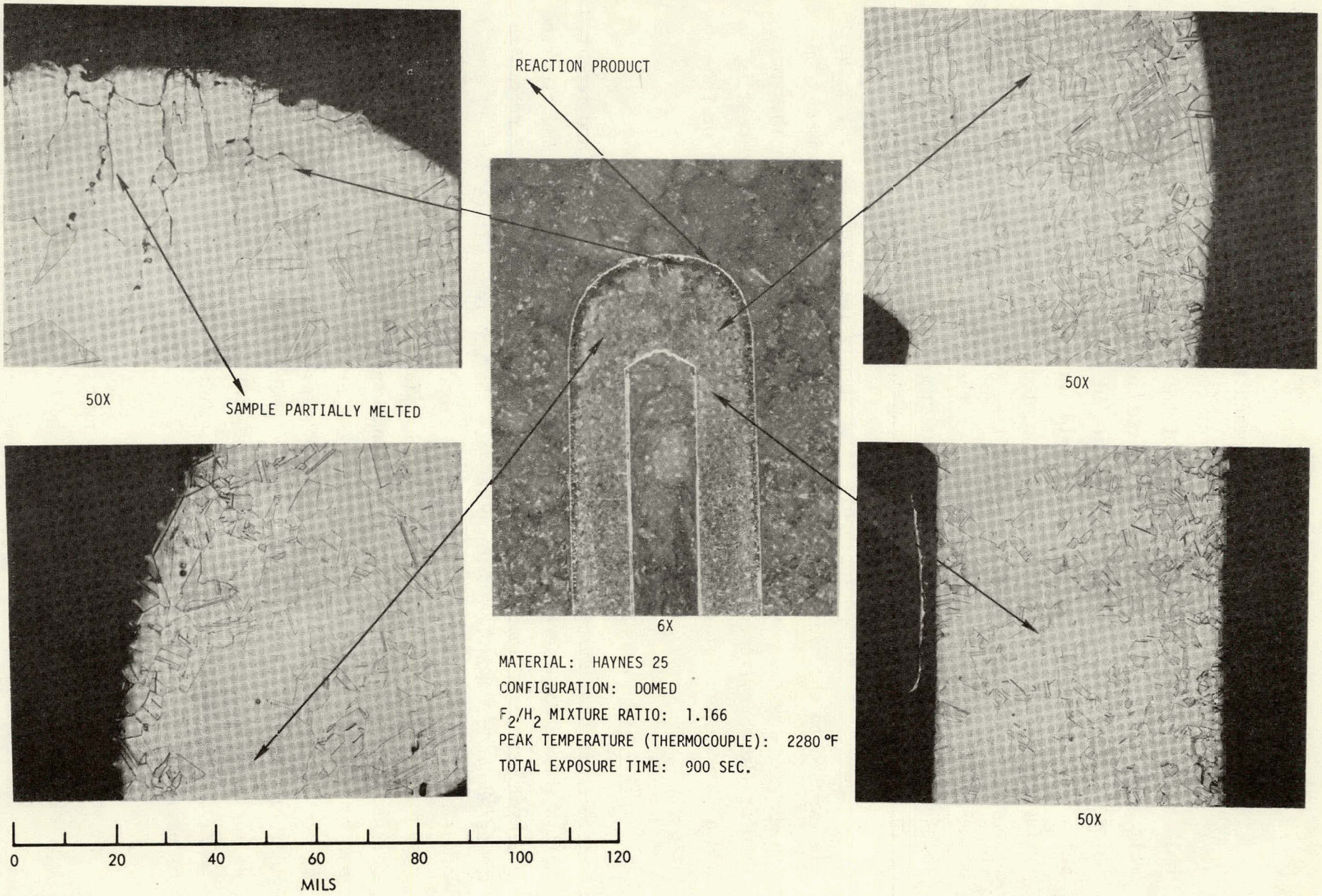

Figure 18. Hydrogen-Fluorine Experiment No. 44

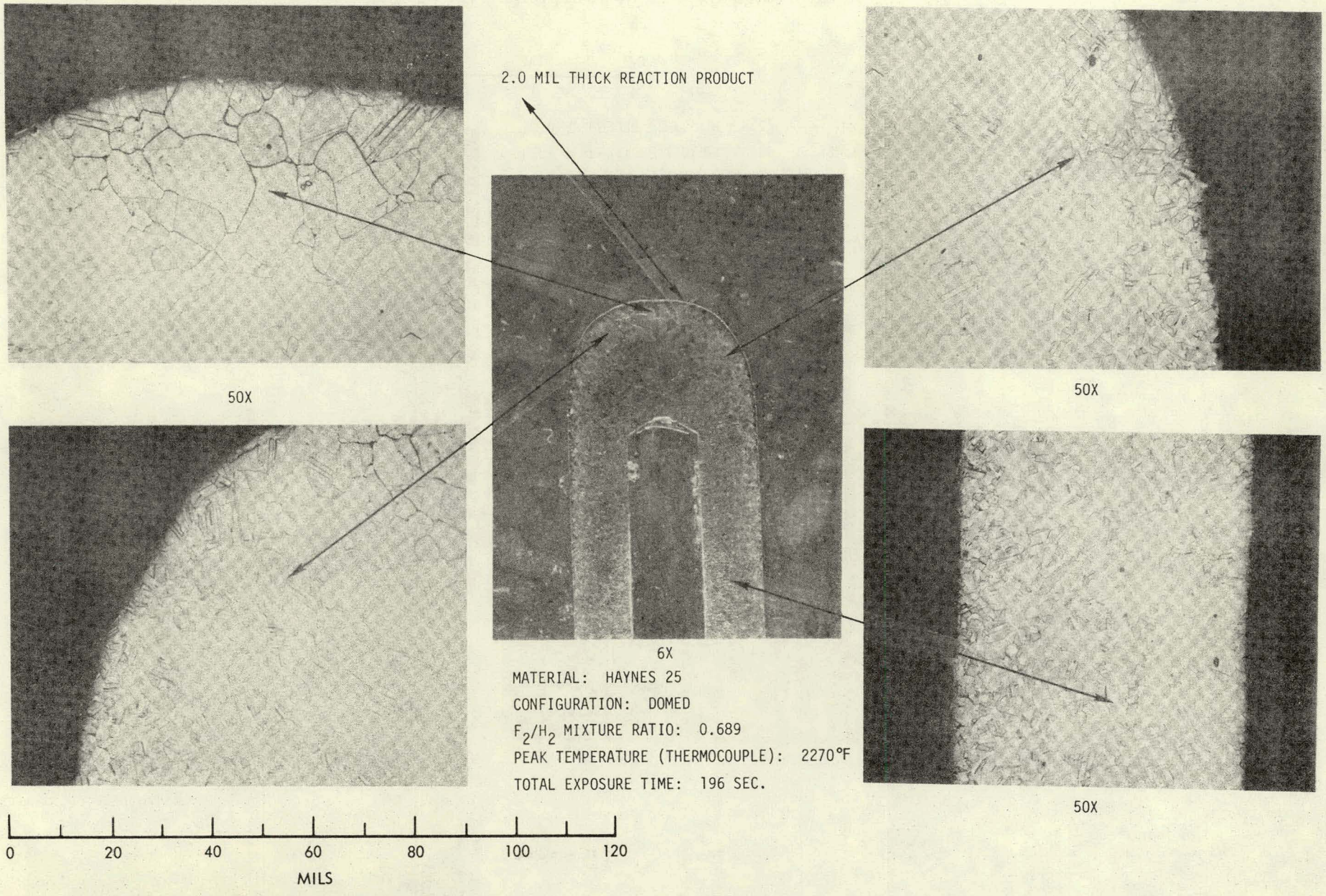

Figure 19. Hydrogen-Fluorine Experiment No. 36

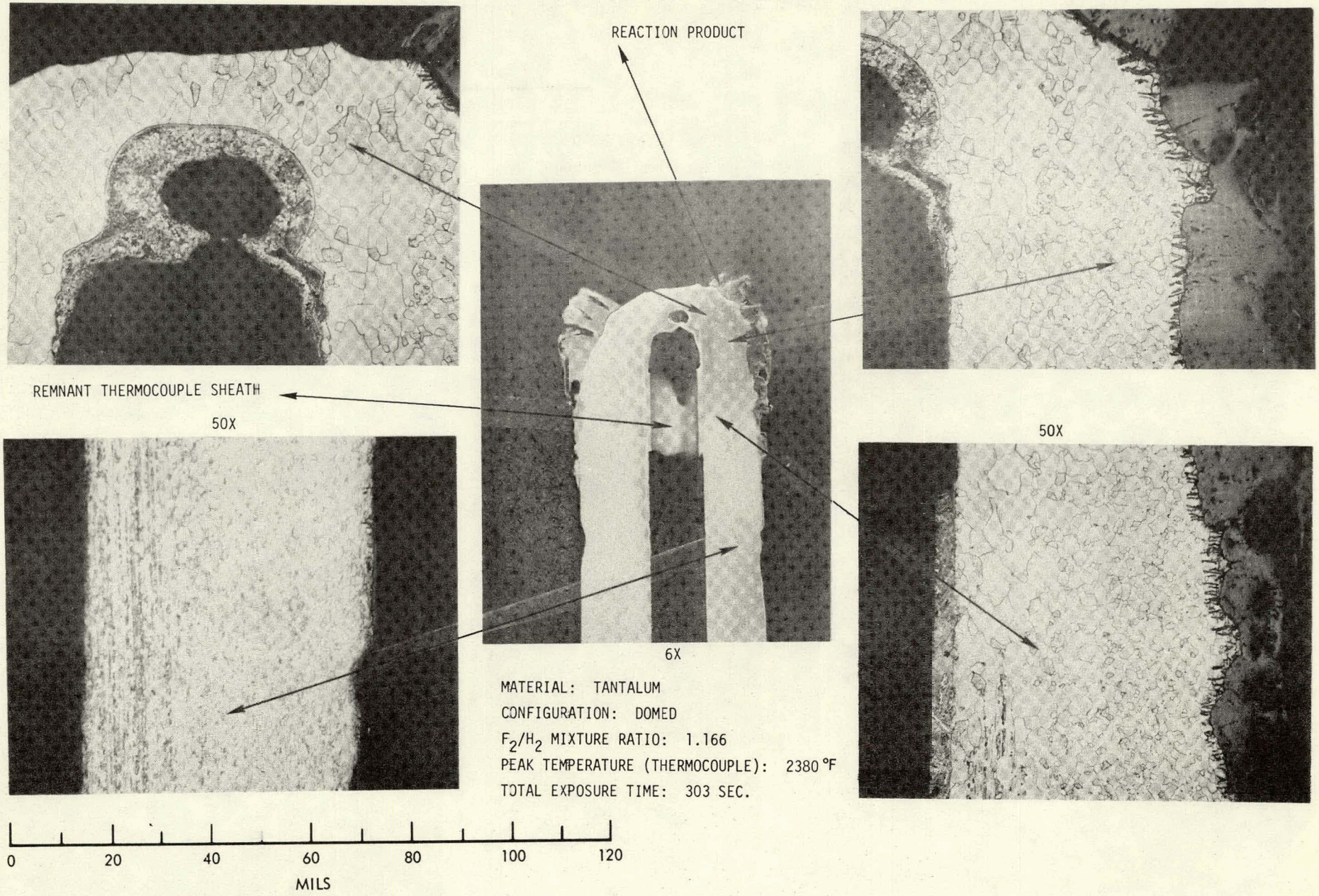

Figure 20. Hydrogen-Fluorine Experiment No. 18

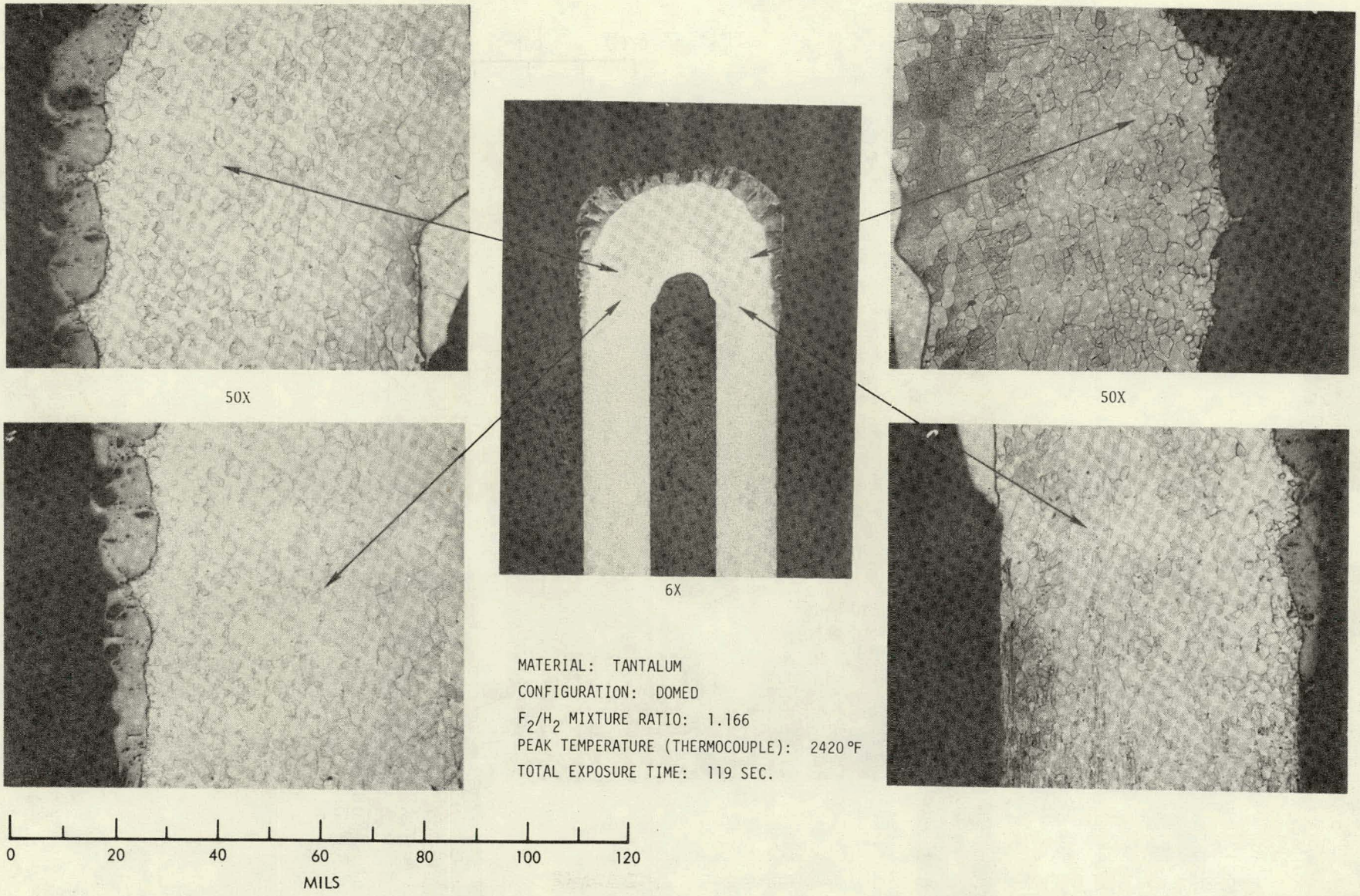

Figure 21. Hydrogen-Fluorine Experiment No. 10

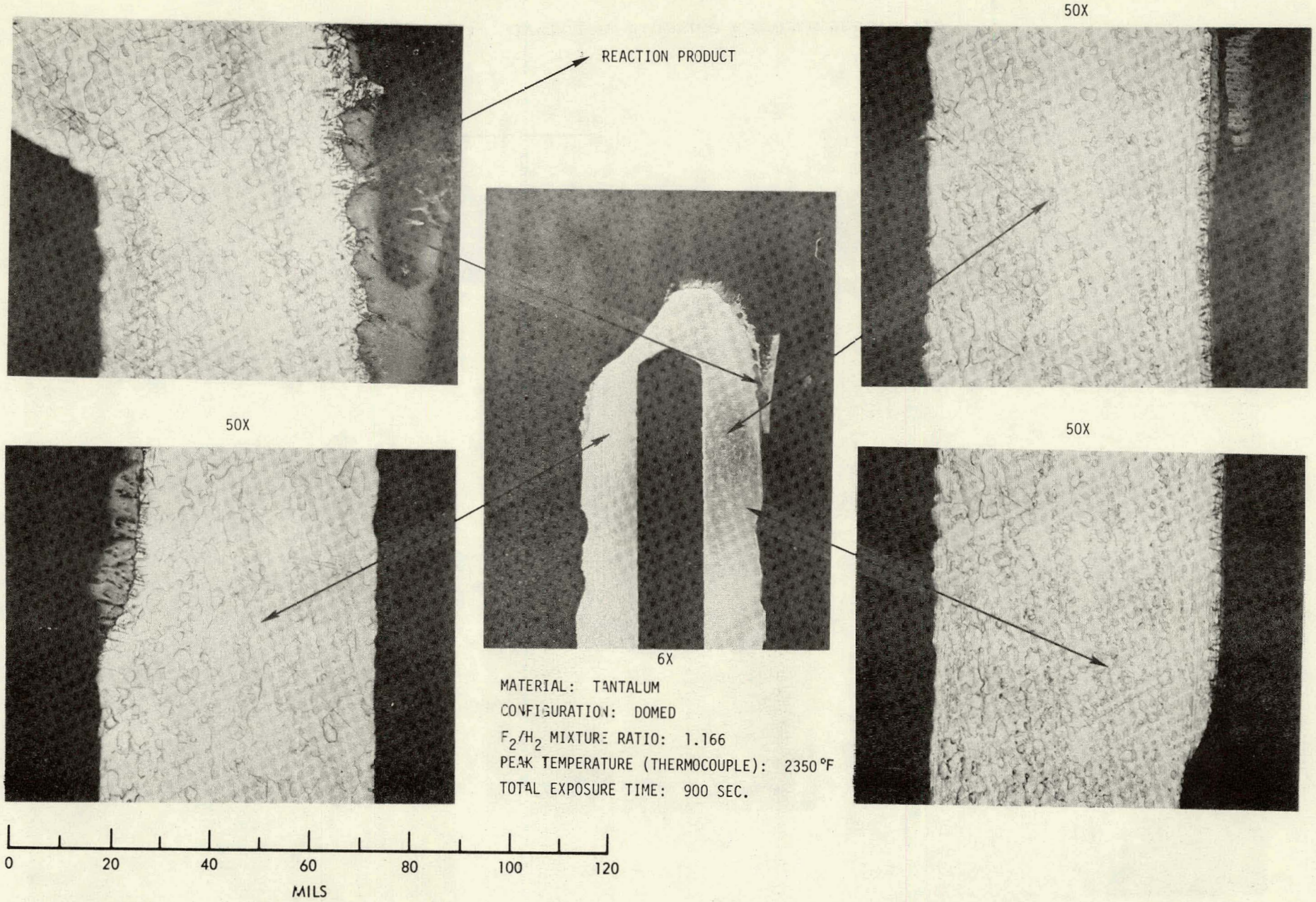

Figure 22. Hydrogen-Fluorine Experiment No. 46

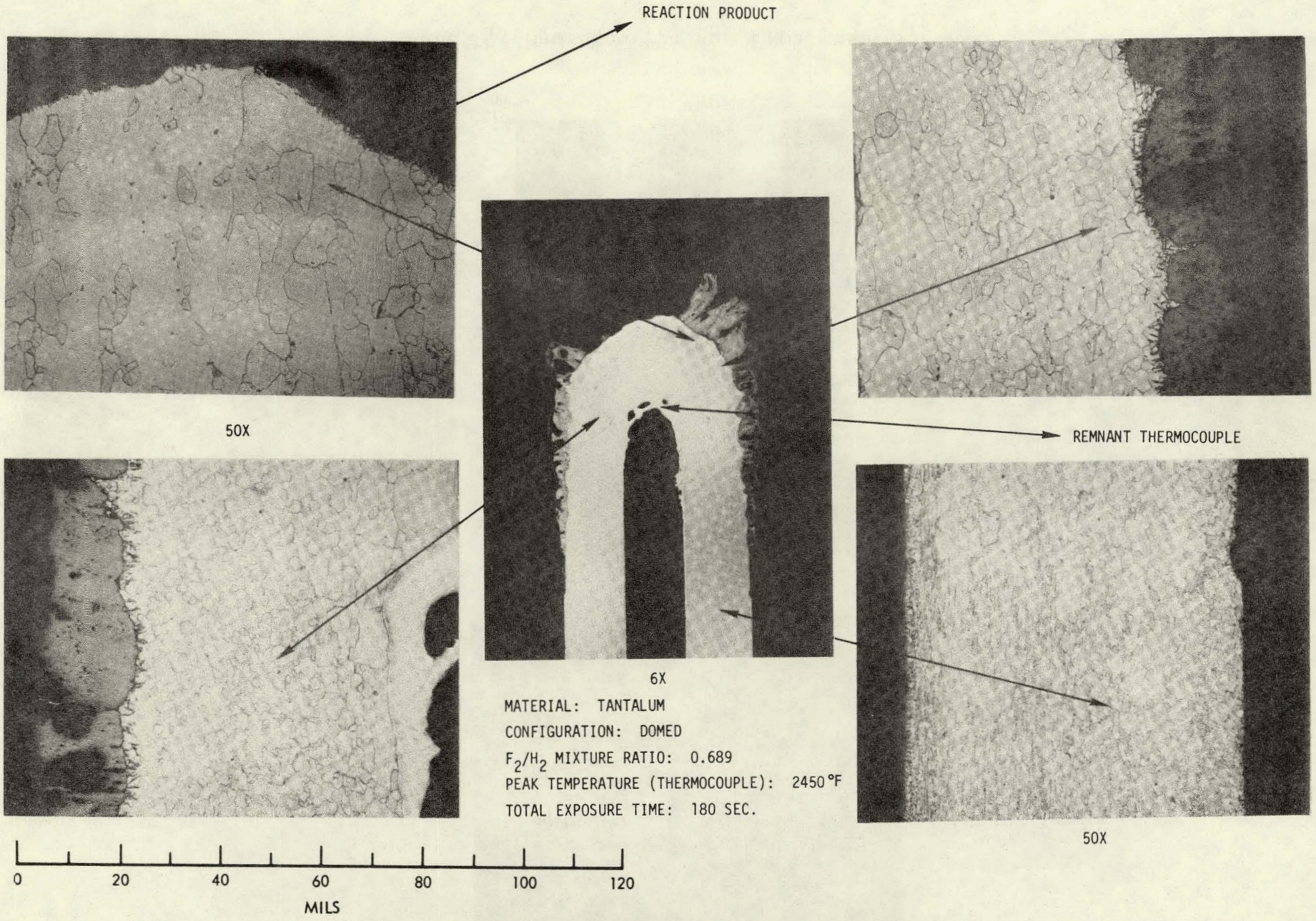

Figure 23. Hydrogen-Fluorine Experiment No. 31

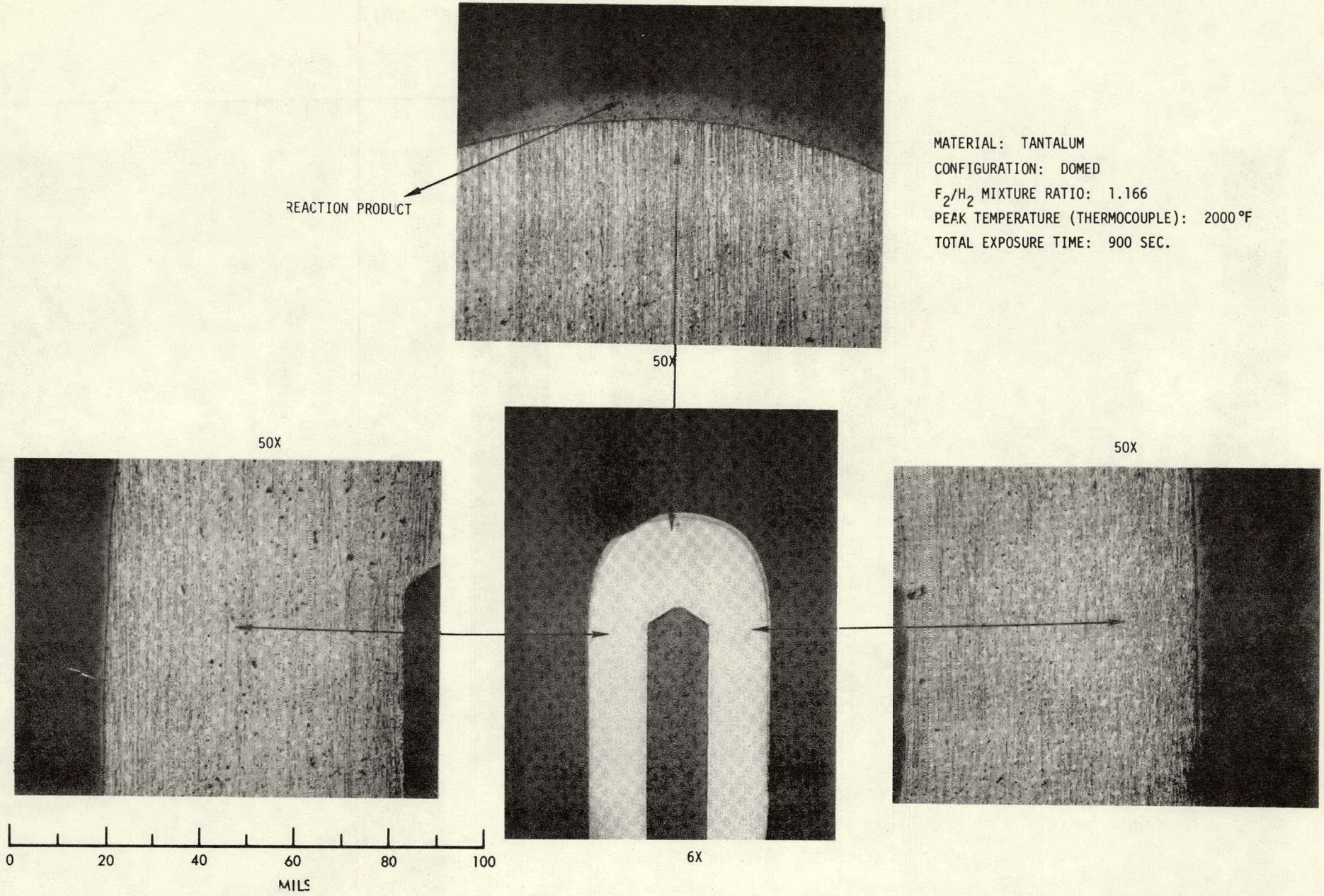

Figure 24. Hydrogen-Fluorine Experiment No. 43

a thin surface corrosion layer with no visible interaction in the sample microstructure immediately below this surface.

The white crystalline reaction product, present on all tantalum samples exposed to the hydrogen-fluorine flame environments, has been identified by x-ray diffraction techniques as tantalum oxide. All hydrogen-fluorine interaction studies were performed in a surrounding ambient air atmosphere. This tends to simulate true launch abort conditions. Tantalum fluoride (TaF_5) most probably was formed but, because of its low boiling point (229.5°C), its presence in the exposed sample was not detected.

Sample No. 43 (Figure 24) was subjected to electron microprobe analysis in a further attempt to determine the reaction products in the exposed sample. The results of this analysis are presented in the following section.

3.2 ELECTRON MICROPROBE ANALYSES

3.2.1 Experimental

Electron microprobe analyses (EMA) were conducted on three radioisotope containment materials for the purpose of determining the nature of the interactions that took place in the H_2-F_2 flame environment. The materials analyzed were Hastelloy C (experiment 45), Haynes 25 (experiment 44), and tantalum (experiment 43). Photomicrographs of the flame-exposed samples prior to EMA are shown in Figures 13, 18, and 24. As can be seen in the figures, the top portions of each sample had appeared to interact with the H_2-F_2 flame. Accordingly, the interacted portions were subjected to the following analyses:

1. Beam scanning for detection of metallic constituents. * The areas scanned by this technique are shown as squares in Figures 25, 26, and 27.
2. Step scanning elemental profiles. These analyses were conducted to determine what elements were present in the corrosion products and grain boundaries of the exposed samples. These analyses show up as lines in Figures 25, 26, and 27.

*The squares and lines in the figures are contamination traces due to electron impingement and are always present in EMA tested specimens.

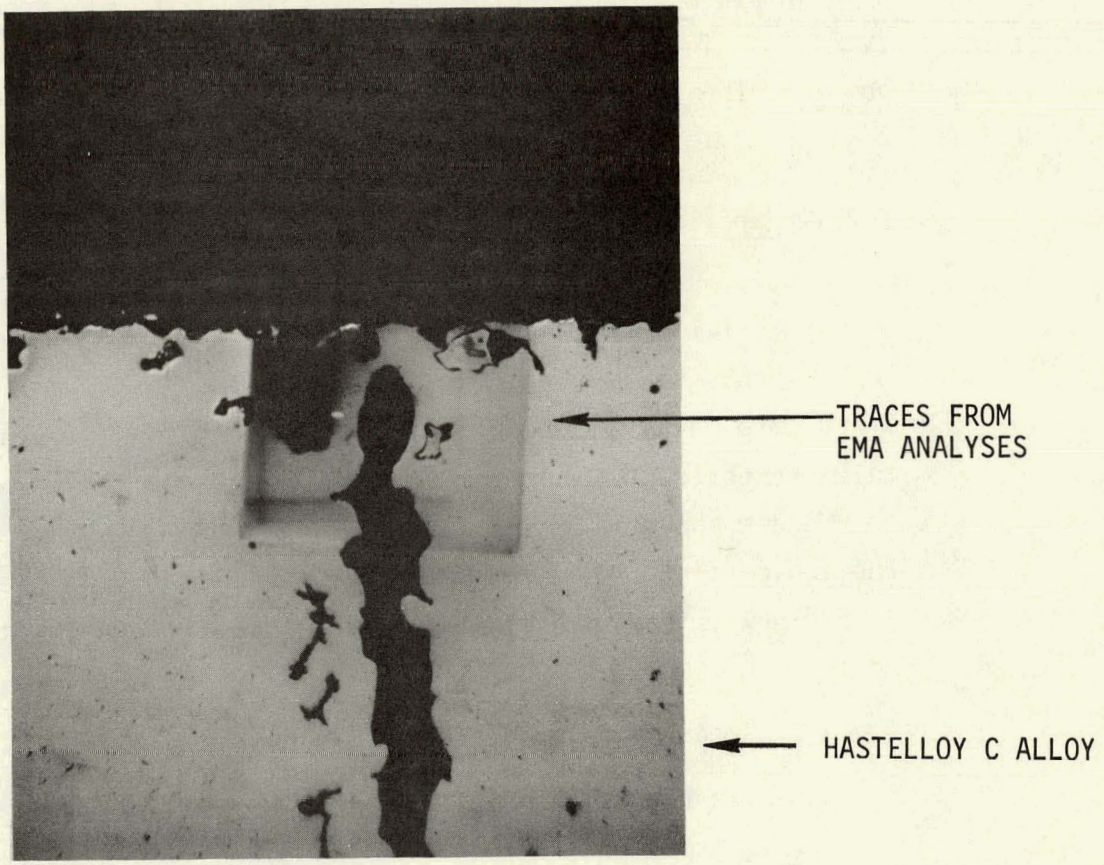

Figure 25. Hastelloy C from Experiment 45 Showing Area Examined by EMA.

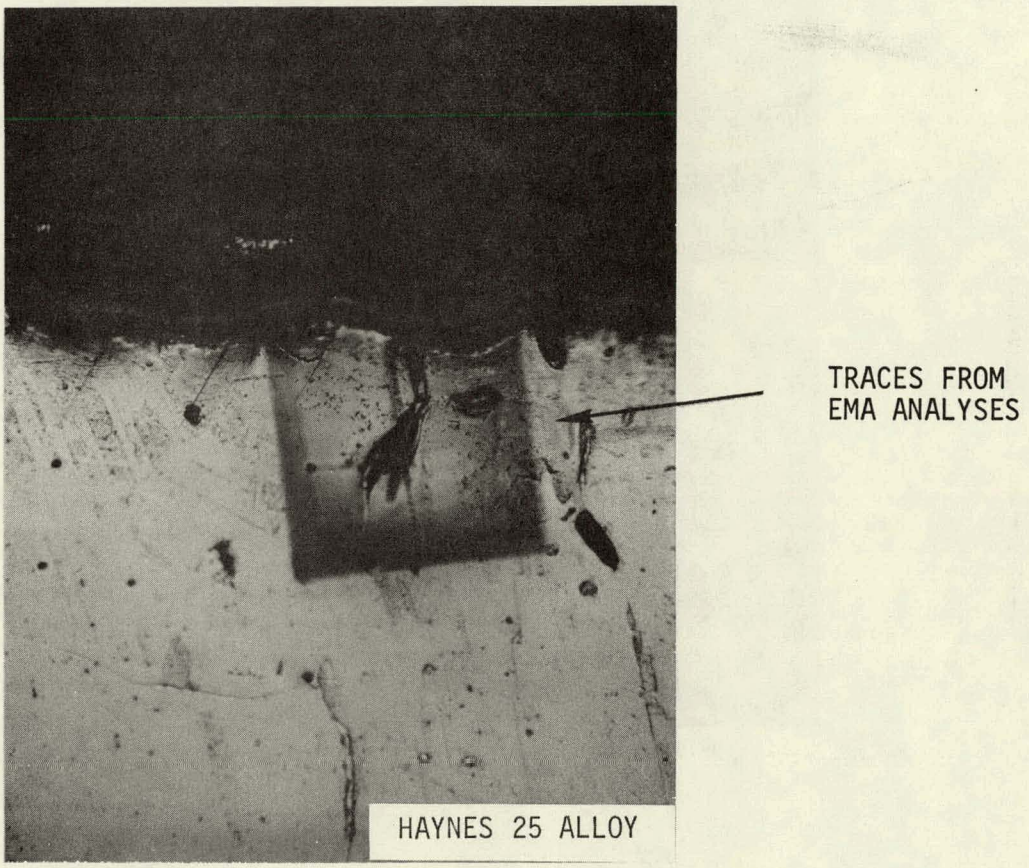

Figure 26. Haynes 25 Sample from Experiment 44 Showing Area Examined by EMA

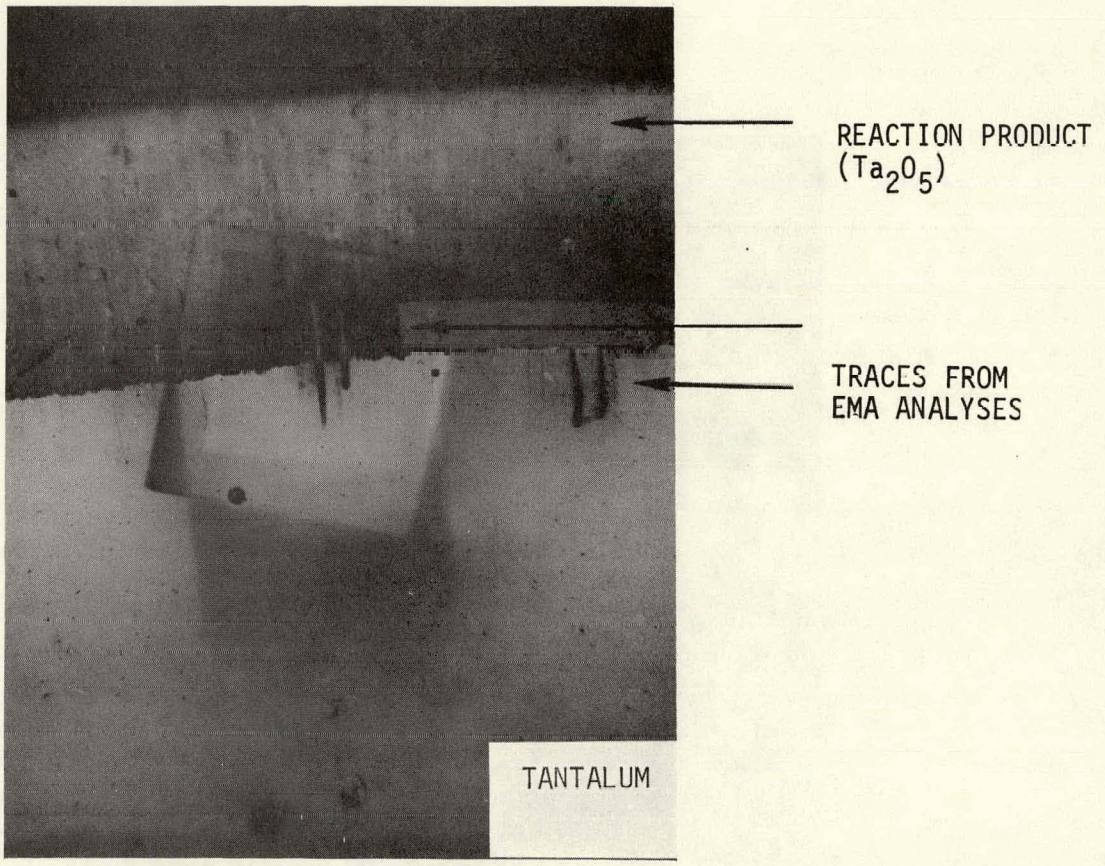

Figure 27. Tantalum Sample from Experiment 43 Showing Areas Examined by EMA

3. Peak to background ratios. These analyses employed a stationary electron beam and were used to determine a limit for the detection of oxygen, fluorine, and nitrogen in the containment materials.

All of the EMA analyses were conducted on unetched metallurgically mounted samples polished through 0.05 micron diamond. An Applied Research Laboratories Model EMX was operated at either 15 or 20 kilovolts with a 0.1 microampere beam current (on brass standard) for the peak to background determinations and 0.02 microamperes for the beam-scanning mode of operation.

3.2.2 Results of the Analysis

In the following paragraphs are presented the EMA results for Hastelloy C, Haynes 25, and tantalum.

3.2.2.1 Hastelloy C

The flame-exposed sample of Hastelloy C was characterized by the presence of extensive grain-boundary attack. Three photographs* of a single grain boundary are shown in Figure 28 for back-scattered electrons (BSE), chromium-K_α x-radiation and oxygen-K_α x-radiation. The BSE photograph clearly differentiates between the metallic (white) portion and the non-metallic (dark) portion. The second picture which was taken using chromium K_α radiation shows that the grain boundary does contain some chromium but certainly at a lower concentration than the parent material. The third photograph** shows that oxygen is concentrated within the grain boundary.

Fluorine and nitrogen determinations which were made of the Hastelloy C sample are summarized in Table 2. The data in the table indicate that fluorine is virtually non-existent in the reacted sample and that nitrogen, if present at all, is certainly no more than 1% in the grain boundary. These data, when viewed in the light of the oxygen picture shown in Figure 28 imply that the primary corrosion product in this Hastelloy C sample was

---

*It should be mentioned that the photographs from EMA are mirror images of those taken on a metallurgical metallograph. Thus, the photographs in Figure 28 show the mirror image of the photomicrograph in Figure 13.

**The third photograph required a 1-hour exposure time in order to obtain a usable film.

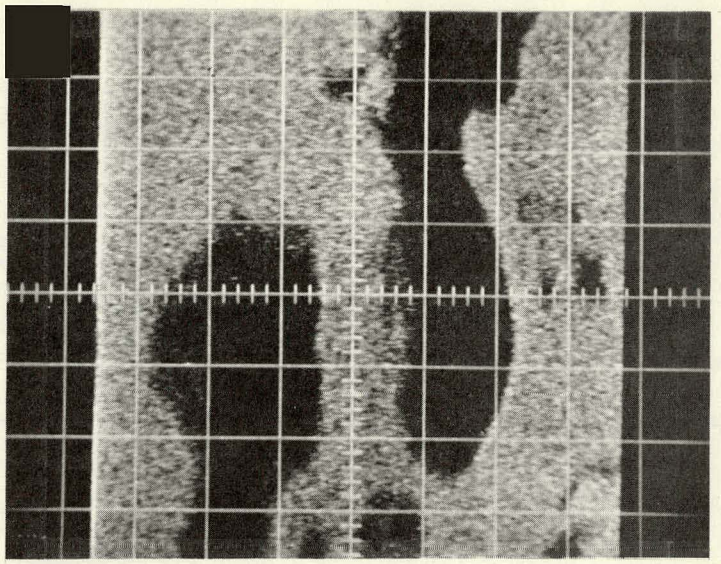

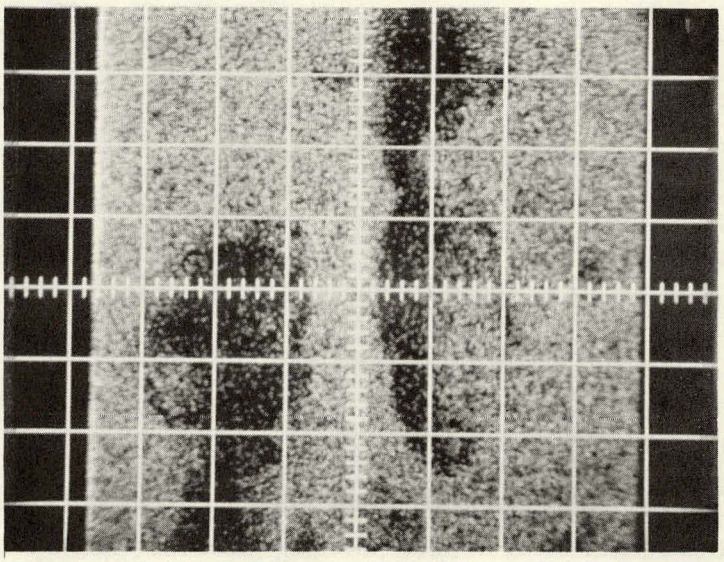

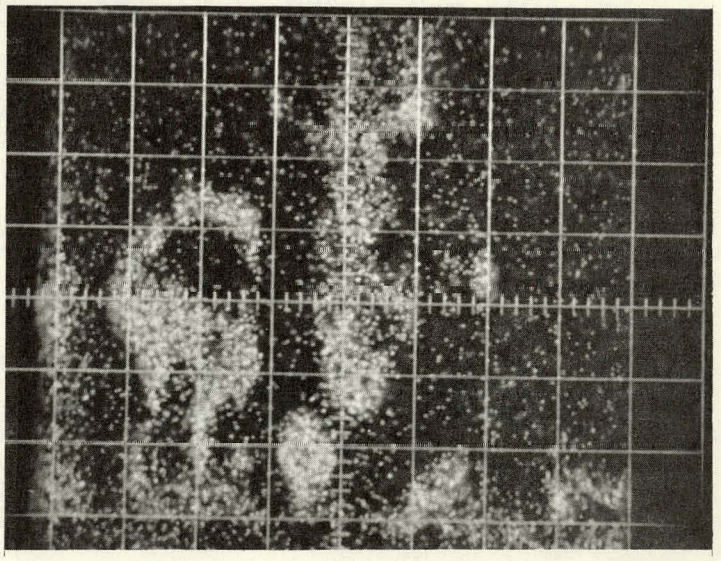

Figure 28. Hastelloy C Sample from Experiment 45

TABLE 2

SUMMARY OF FLUORINE AND NITROGEN DETERMINATIONS IN H_2-F_2 FLAME EXPOSED HASTELLOY C AND VARIOUS STANDARD SAMPLES

Element	Location	Counts per Second	
		Peak	Background
Fluorine	Hastelloy C: Standard Sample	1.4	nil
Fluorine	Hastelloy C: Exposed Sample-metallic portion	1.5	nil
Fluorine	Hastelloy C: Exposed Sample-non-metallic portion	1.1	1.1
Fluorine	Hastelloy C: Edge of Exposed Sample	0.8	0.8
Fluorine	Sodium Fluoride: Standard	631.1	2.6
Nitrogen	Hastelloy C: Standard Sample	43.1	42.6
Nitrogen	Hastelloy C: Exposed Sample-metallic portion	43.1	42.6
Nitrogen	Hastelloy C: Exposed Sample-non-metallic portion	35.7	31.6
Nitrogen	Hastelloy C: Edge of Exposed Sample	25.6	17.0
Nitrogen	Boron Nitride: Standard	357.5	13.4

oxygen. This result would indicate that the H_2-F_2 flame did not react extensively with the bulk Hastelloy C sample per se under the conditions of this experiment (2280°F peak temp.) but that the corrosion product was due to the exposure to high temperature in an atmosphere that included air.

3.2.2.2 Haynes 25 Alloy

The flame-exposed specimen of Haynes 25 was characterized by the presence of grain-boundary attack at the surface of the sample in closest proximity to the H_2-F_2 flame. Three photographs were taken of a single interaction area using back-scattered electrons, tungsten L_α x-radiation, and oxygen K_α x-radiation. The photographs are shown in Figure 29*. In the top photograph the surface corrosion area is clearly seen as the dark area in the upper right hand corner. In addition, the localized darker areas within the picture correspond to the general shape of the grain boundary shown in Figure 26. In the second picture, it is seen that the tungsten concentration is noticeably lower in the corrosion product than in the parent material. In the third picture, oxygen is indicated to be concentrated only in the corrosion product area and even there, at a low concentration (~1%).

The results of fluorine and nitrogen determinations are presented in Table 3. The data in the table indicate that the fluorine concentration in the exposed Haynes 25 sample is virtually zero. The data for nitrogen are open to some variety of interpretation due to the presence of the cobalt radiation line which overlapped the nitrogen line. However, the most reasonable approach is to assume that the unexposed sample of Haynes 25 was free of nitrogen. It then follows that the nitrogen concentration in the exposed sample is no more than the following value (based on 56% N in BN):

$$\%N = \frac{(129.4 - 46.8) - (123.9 - 47.7)}{357.5 - 13.4} \times 56\% = 1\%$$

Thus, it appears as if the principle nonvolatile corrosion product formed in experiment 44 was primarily a complex oxide-nitride rather than a fluorine-containing solid product.

*The area shown in the photographs is a mirror image of that shown in Figure 26.

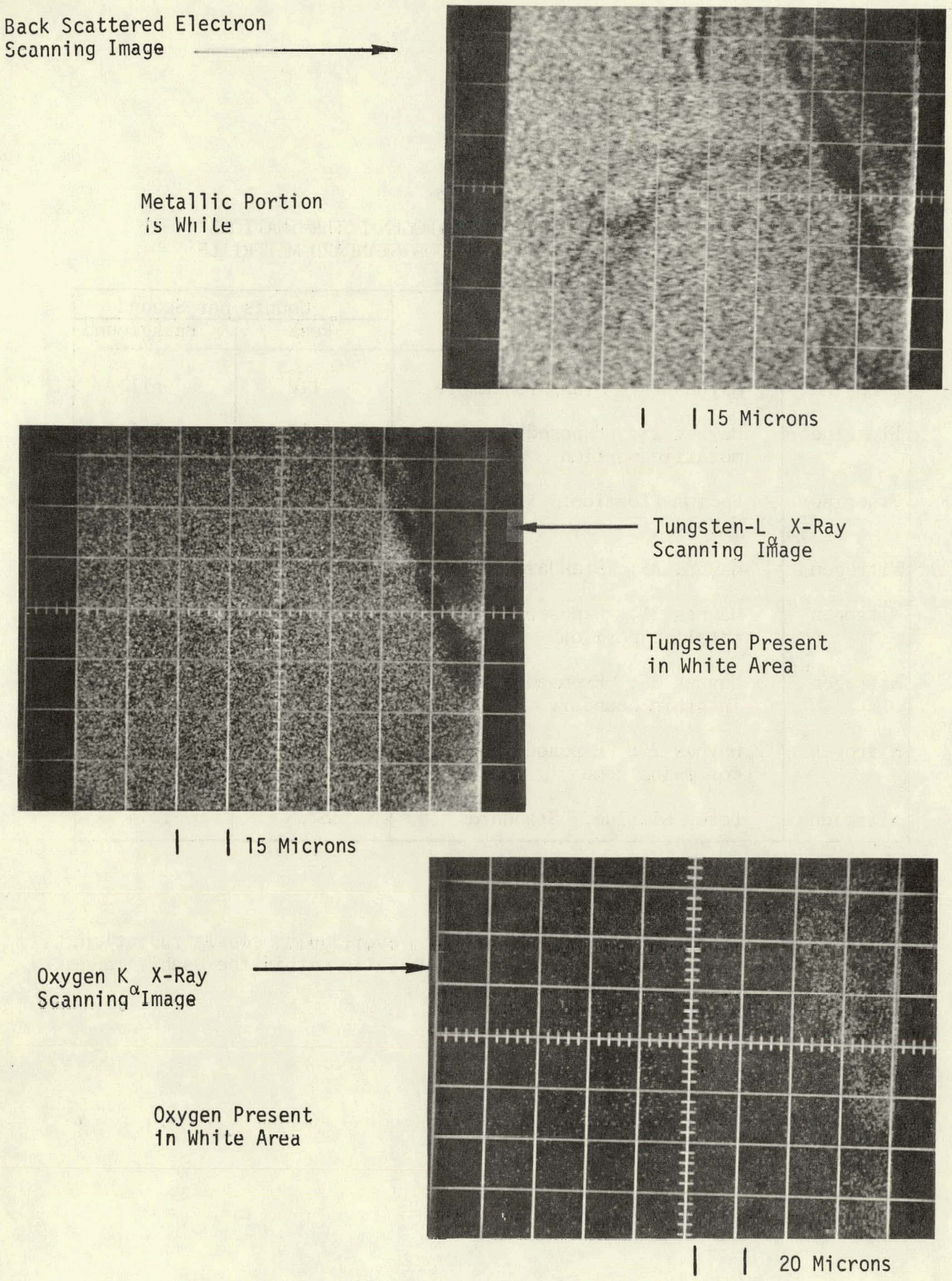

Figure 29. Haynes 25 Sample from Experiment 44

TABLE 3

SUMMARY OF FLUORINE AND NITROGEN DETERMINATIONS
IN HAYNES 25 ALLOY ON VARIOUS STANDARD MATERIALS

Element	Location	Counts per Second	
		Peak	Background
Fluorine	Haynes 25: Standard Sample	1.0	nil
Fluorine	Haynes 25: Exposed Sample; metallic portion	1.4	1.1
Fluorine	Sodium Fluoride: Standard Sample	631.1	2.6
Nitrogen*	Haynes 25: Standard Sample	123.9	47.7
Nitrogen*	Haynes 25: Exposed Sample; metallic portion	129.4	46.8
Nitrogen*	Haynes 25: Exposed Sample; in grain boundary	97.0	41.3
Nitrogen*	Haynes 25: Exposed Sample; corrosion zone	8.9	9.2
Nitrogen	Boron Nitride: Standard	357.5	13.4

*Nitrogen values include contributions from overlapping cobalt radiation. Since only one nitrogen x-ray line (the K_α) falls within the usable range of EMA, the overlap could not be avoided.

3.2.2.3 Tantalum

The flame-exposed specimen of tantalum was characterized by the presence of a thick white corrosion product on the surface of the sample. The interface between the corrosion product and the parent metal was examined by means of back-scattered electrons, tantalum L_α x-rays and oxygen K_α x-rays and the data are presented in Figure 30. The top photograph clearly shows that the corrosion product is non-metallic (due to absence of back-scattered electrons) and the second photograph shows that the product contains tantalum. The third photograph indicates that the corrosion product contains oxygen.

The results from fluorine and nitrogen determinations (by step-scanning and stationary beam techniques) are given in Table 4.

TABLE 4

SUMMARY OF FLUORINE AND NITROGEN DETERMINATIONS IN H_2-F_2 FLAME EXPOSED TANTALUM

Element	Location	Counts per Second	
		Peak	Background
Fluorine	Tantalum: Exposed sample in metallic portion and in corrosion zone.	An alternative approach was used which employed spectral line analyses. No lines due to fluorine were found.	
Nitrogen	Tantalum: Exposed sample in the metallic portion.	70.8	70.6
Nitrogen	Tantalum: Exposed sample in the corrosion zone.	56.2	56.8
Tantalum	Tantalum standard	88.0	4
Tantalum	Tantalum: Exposed sample in the corrosion zone	71	5

The data in the table indicate that fluorine and nitrogen were absent from the exposed tantalum sample. The data also provide a basis for a quantitative determination of the tantalum content in the corrosion product if a linear relation is assumed between the net Ta-intensity and the weight

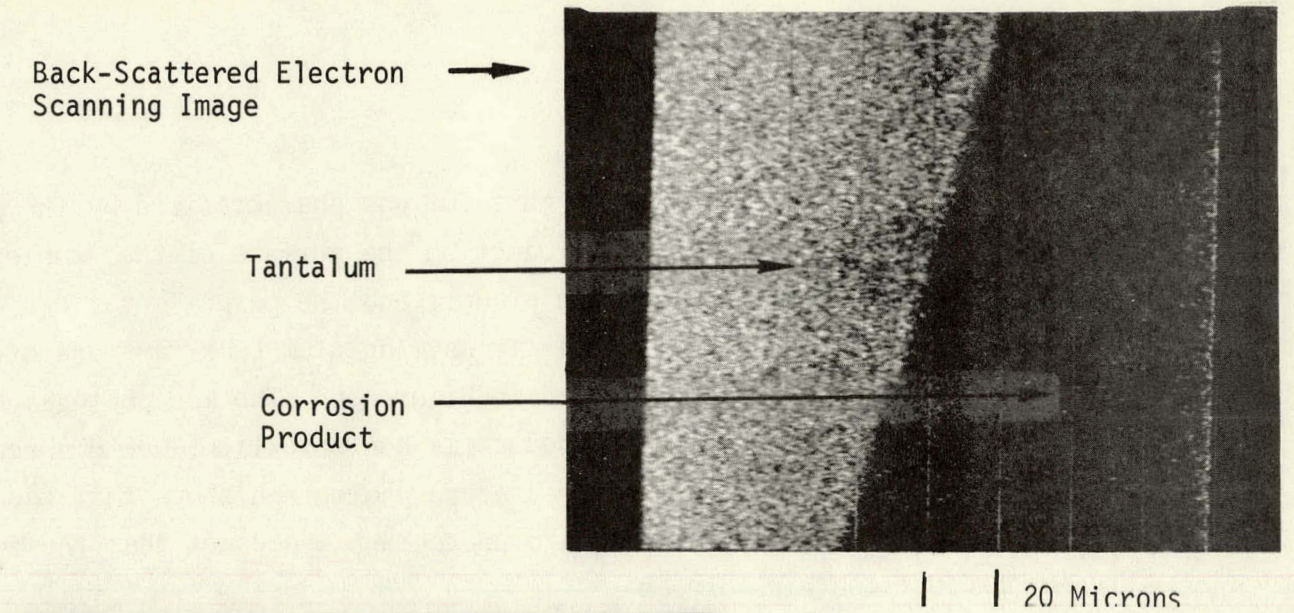

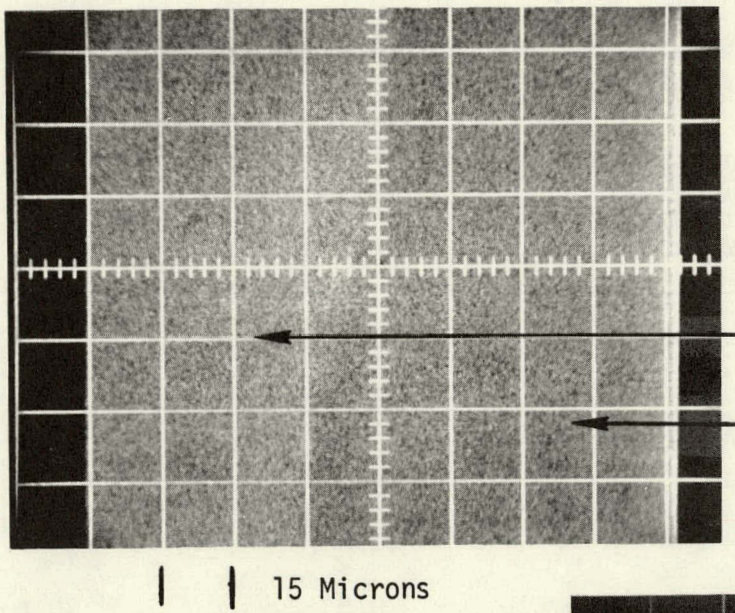

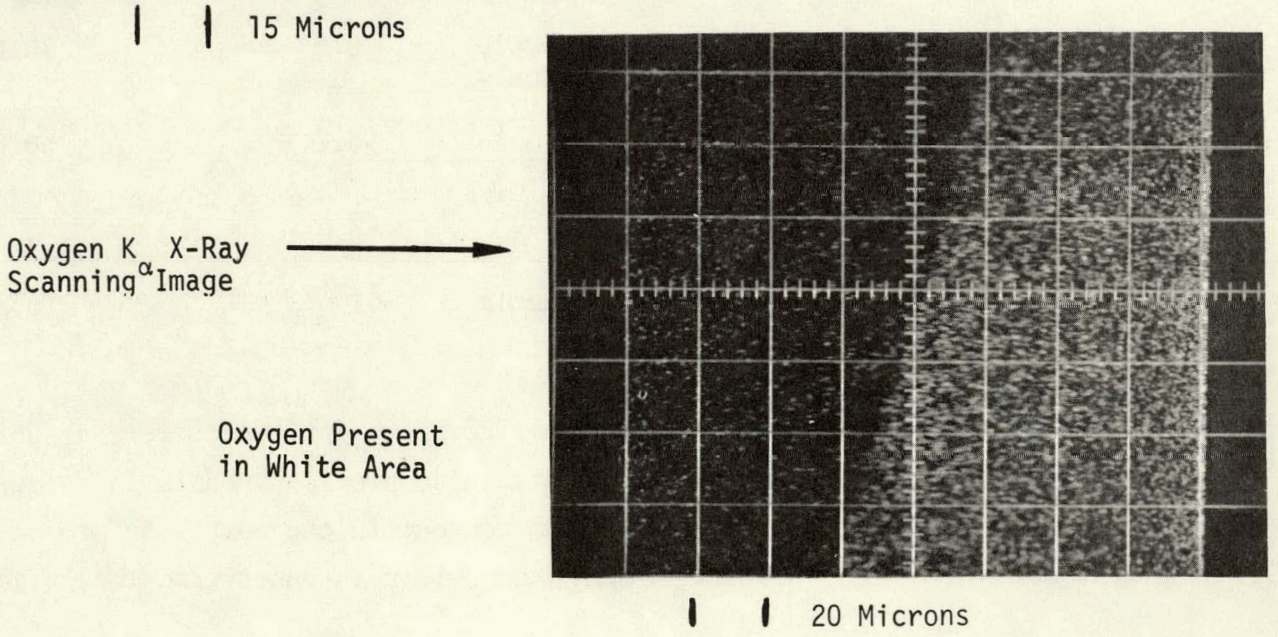

Figure 30. Tantalum Specimen from Experiment 43

percent tantalum*. The result is

$$\% \text{ TA} = \frac{(71 - 5)}{88 - 4} \times 100\% = 79\%$$

In view of the fact that Ta_2O_5 contains 82% Ta, it seems safe to state that the nonvolatile corrosion product is primarily Ta_2O_5.

The general conclusion that can be drawn from the EMA studies is that fluorine** was not found in the interior of any of the three samples that were investigated by EMA techniques. The absence of fluorine may be attributed to the high volatility of any fluorides that would have been found. However, due to the fact that the examined samples did not undergo catastrophic physical change during exposure (with the possible exception of Hastelloy C) it seems unlikely that any great amount of fluoride formation took place.

4. CONCLUSIONS

The following conclusions are based on a careful study of all available data and analyses:

1. Reaction rates for Type 316 stainless steel in the H_2-F_2 flame environment at both low and moderate fluorine concentrations are fairly low and are not considered to be of major concern from launch abort radioisotope containment safety considerations up to temperatures of 2000°F. Above 2000°F and up to the melting range, reaction rates are rapid and the possibility exists for catastrophic failure through self heating or ignition of the stainless steel in the H_2-F_2 environment.
2. Hastelloy C does not react rapidly in an H_2-F_2 environment rich in fluorine at temperatures below 1800°F. However, in a flame environment containing large concentrations of fluorine, hydrogen-fluoride and atmospheric air Hastelloy C is subject in a period of a few minutes to severe interior grain boundary attack to a considerable depth in the temperature range above 1800°F. The modifications to the microstructure of Hastelloy C due to the combined influences of the hydrogen-fluorine flame and atmospheric air can be expected to produce significant changes in the mechanical properties of this alloy.

---

*The assumption is good to ± 5 units of weight percent.

**Hydrogen cannot be detected by EMA techniques.

3. In the fluorine and hydrogen fluoride rich flame environment, Haynes 25 does not undergo catastrophic interaction at sample temperatures below 2200°F. Radioisotope containment safety considerations should not be compromised by chemical reactions with F_2 or HF below 2200°F for periods of many minutes. Above the 2200°F temperature range and up to the alloy's melting range, flame interaction could be catastrophic.

4. Tantalum reaction rates in flame environments containing fluorine and hydrogen fluoride are slow relative to a period of minutes time scale below about 2000°F. At temperatures above 2000°F, the tantalum tends to react rapidly and exothermically with the H_2-F_2 environment.

APPENDIX A

Macro-photographs for all exposed hydrogen-fluorine interaction samples are included in Appendix A. These photographs allow qualitative estimates to be made of the degree of interaction for each sample-material and flame condition investigated. The macro-photographs for the first eight experiments (cylindrical sample configuration) are included as Figures A-1 and A-2.

Temperature versus time plots for all reportable interaction experiments utilizing the "domed" sample configuration are presented together with the corresponding sample's macro-photograph. These experiments were numbered 9 through 46 inclusive and are presented as Figures A-3 through A-39 (experiment No. 42 was a blank and is not included).

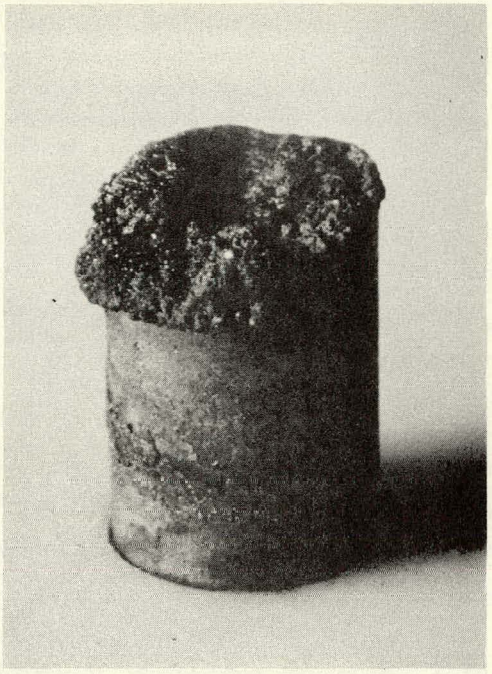

Experiment No. 1
Type 316 Stainless Steel
Temp. (T.C.) 2230°F

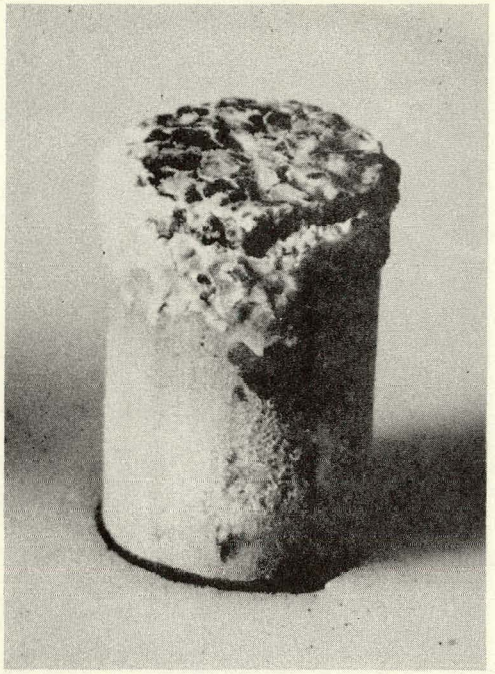

Experiment No. 2
Tantalum
Temp. (T.C.) 2360°F

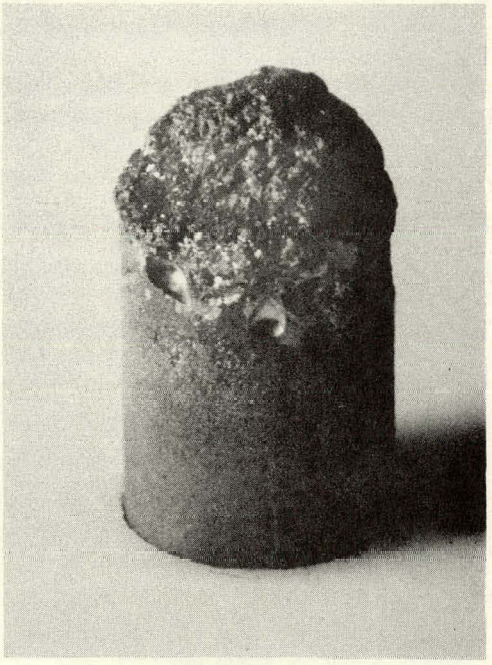

Experiment No. 3
Hastelloy C
Temp. (T.C.) 2120°F

Experiment No. 4
Haynes 25
Temp. (T.C.) 2300°F

($q = 39.0$ BTU/Ft^2-sec)

Figure A-1. Exposed Cylindrical Sample Configuration

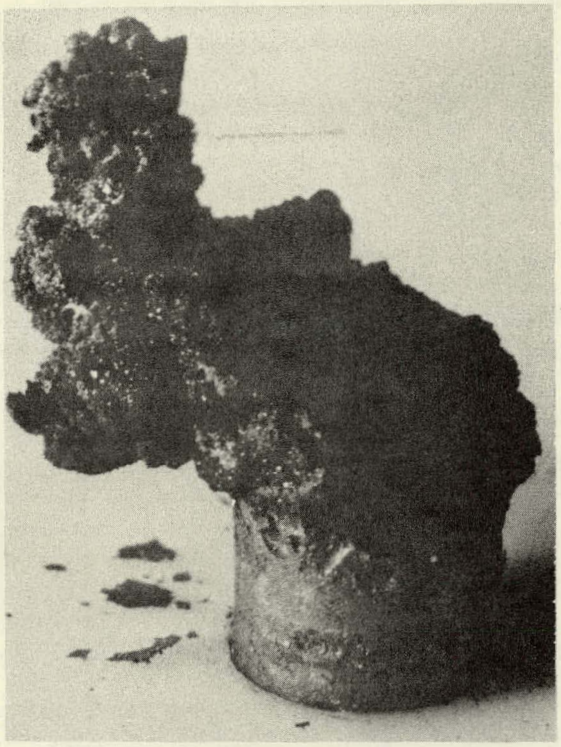

Experiment No. 5
Type 316 Stainless Steel
Temp. (T.C.) >2500°F

Experiment No. 6
Tantalum
Temp. (T.C.) >2500°F

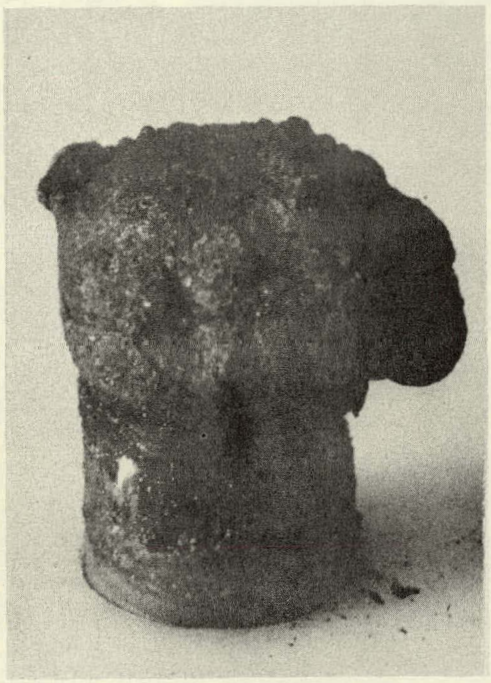

Experiment No. 7
Hastelloy C
Temp. (T.C.) >2500°F

Experiment No. 8
Haynes 25
Temp. (T.C.) >2500°F

(q = 52.1 BTU/Ft^2-sec)

Figure A-2. Exposed Cylindrical Sample Configuration

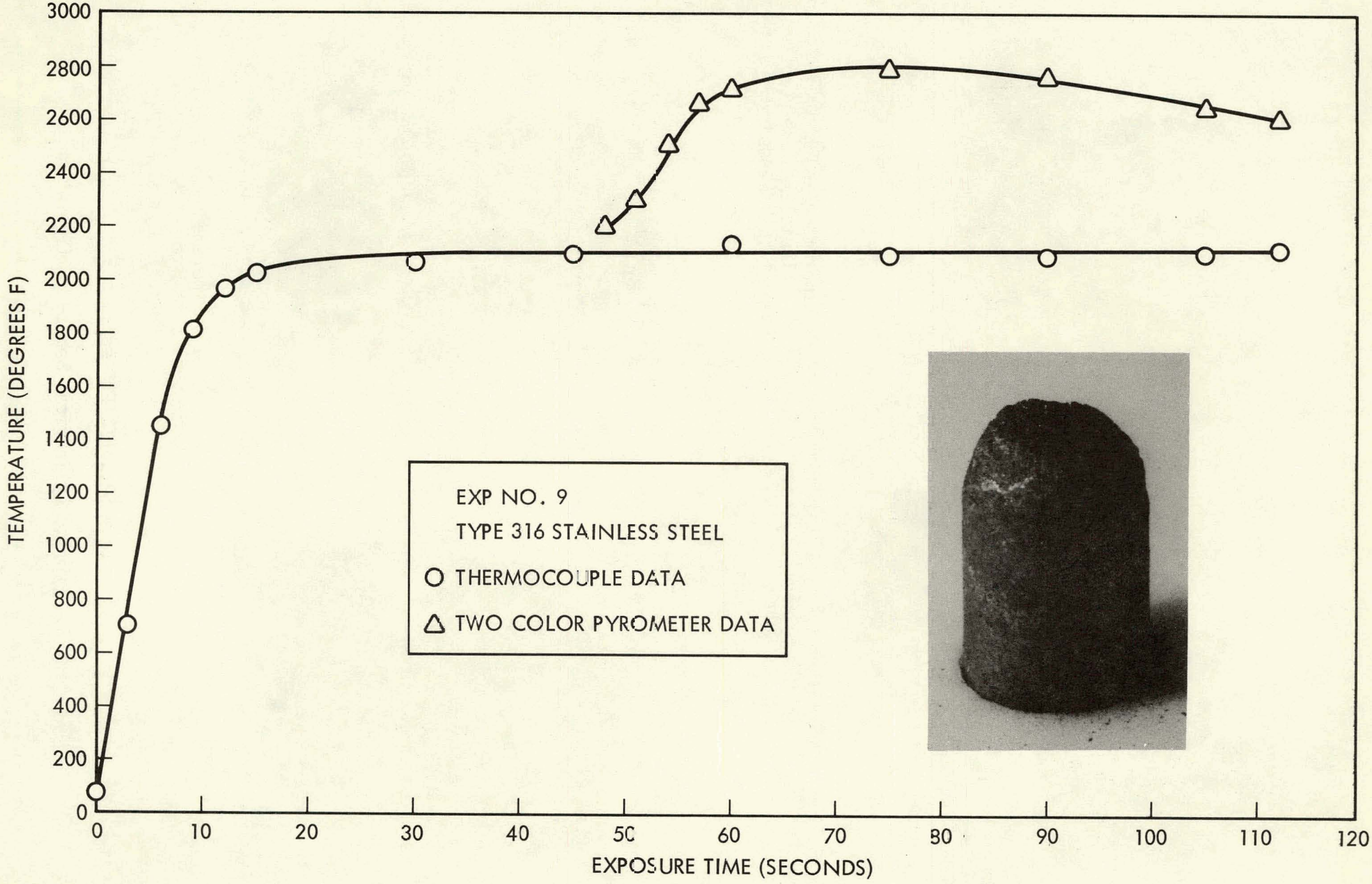

Figure A-3. Temperature vs. Time Data for Experiment No. 9

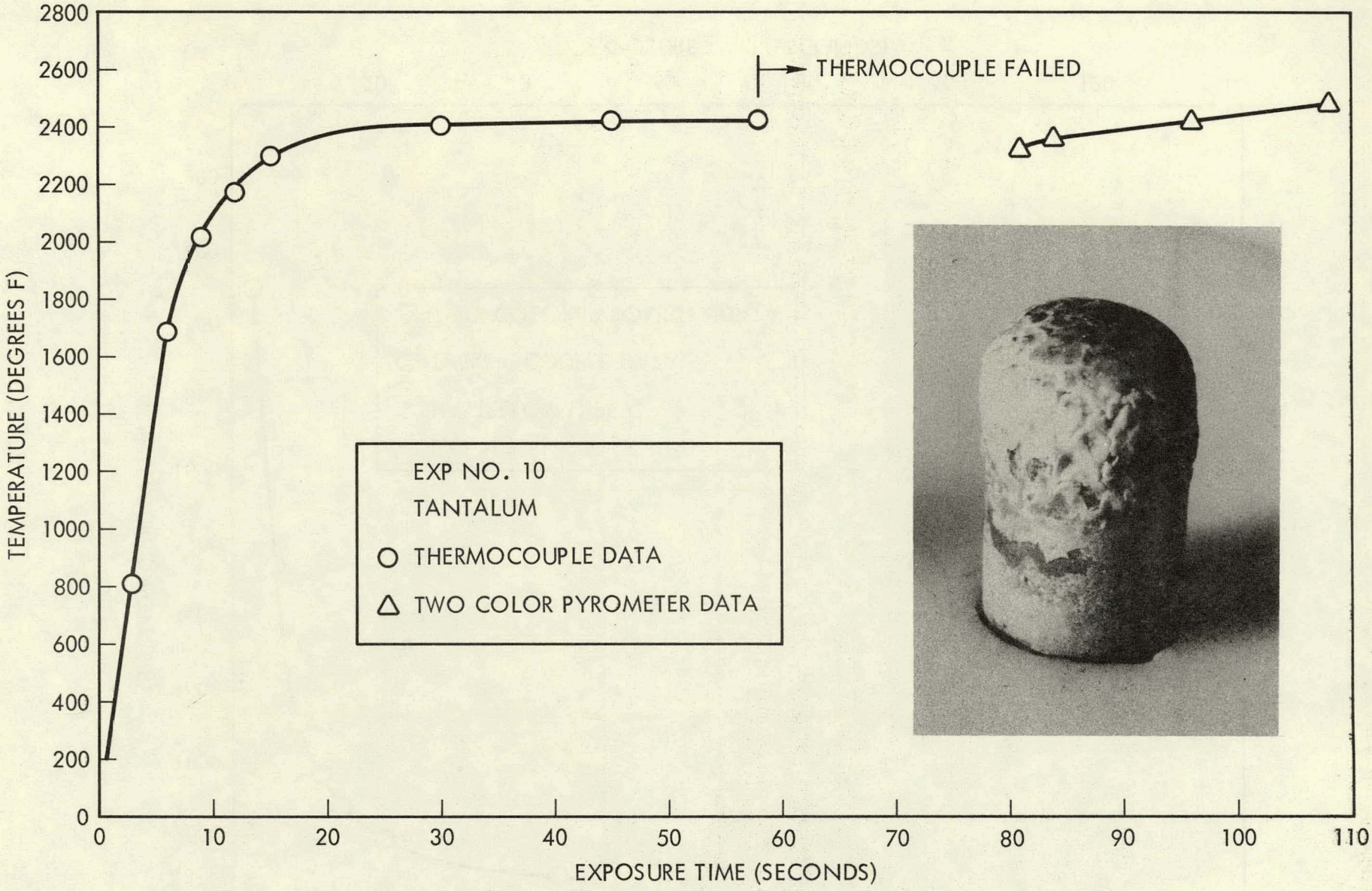

Figure A-4. Temperature vs. Time Data for Experiment No. 10

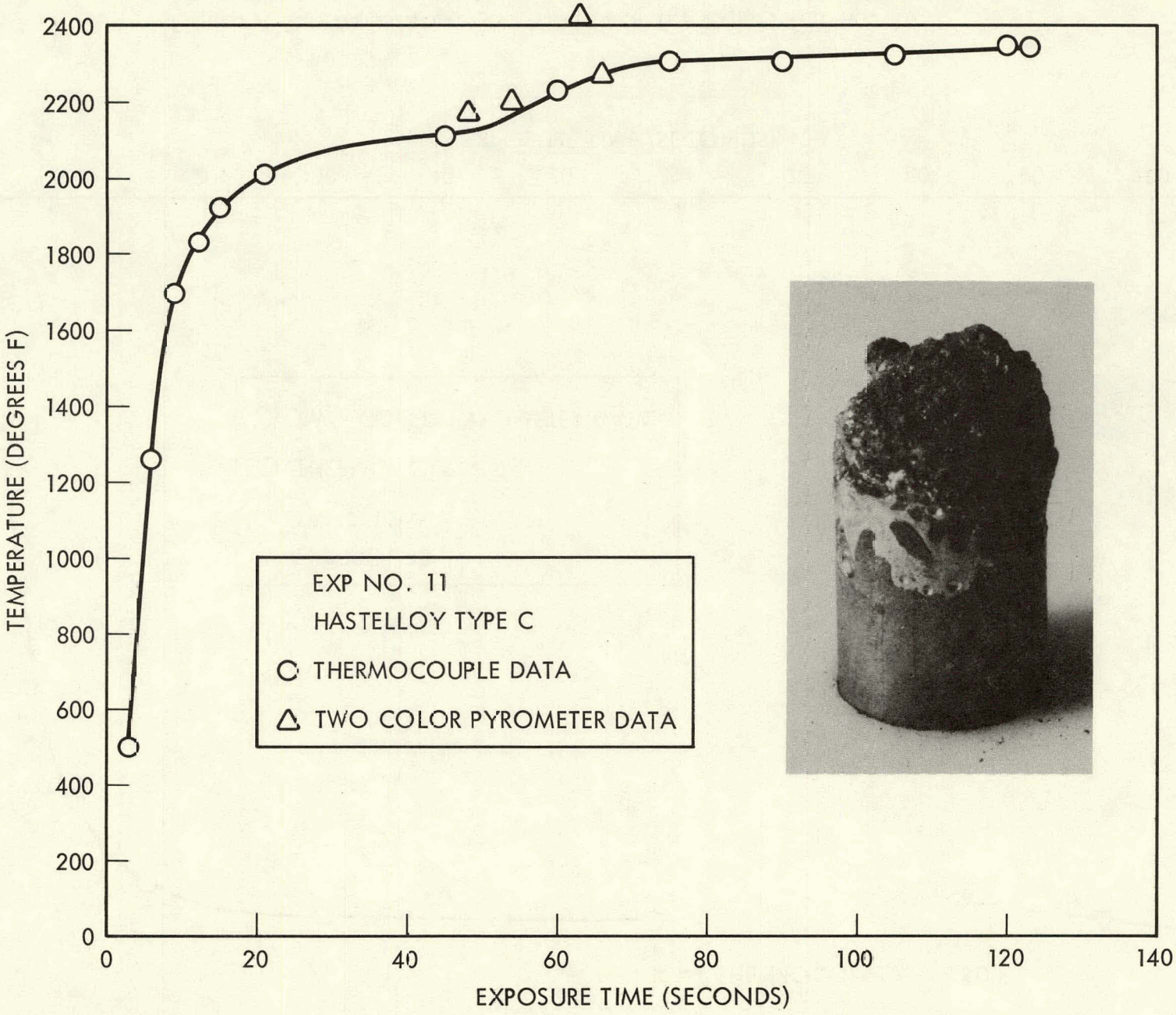

Figure A-5. Temperature vs. Time Data for Experiment No. 11

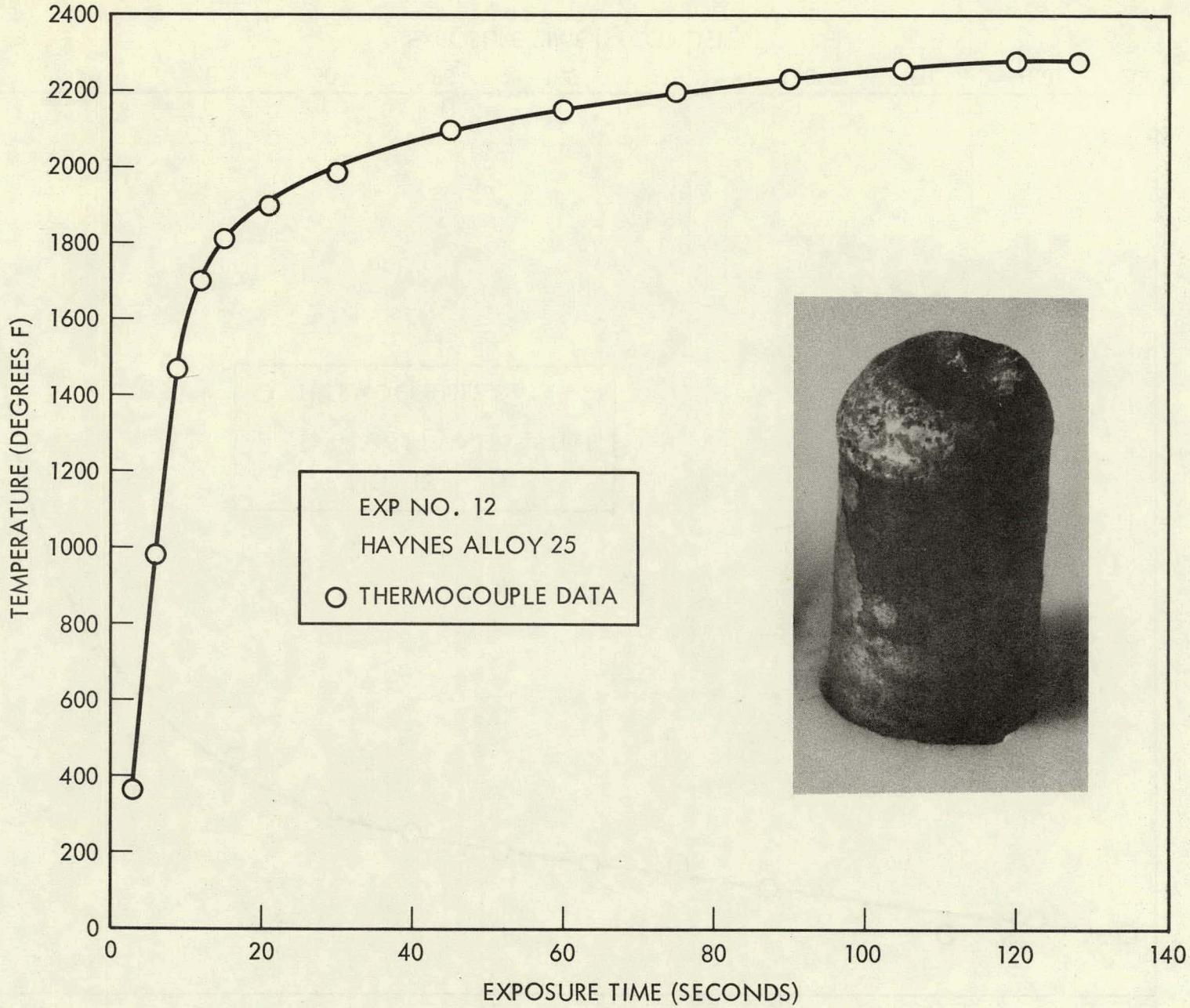

Figure A-6. Temperature vs. Time Data for Experiment No. 12

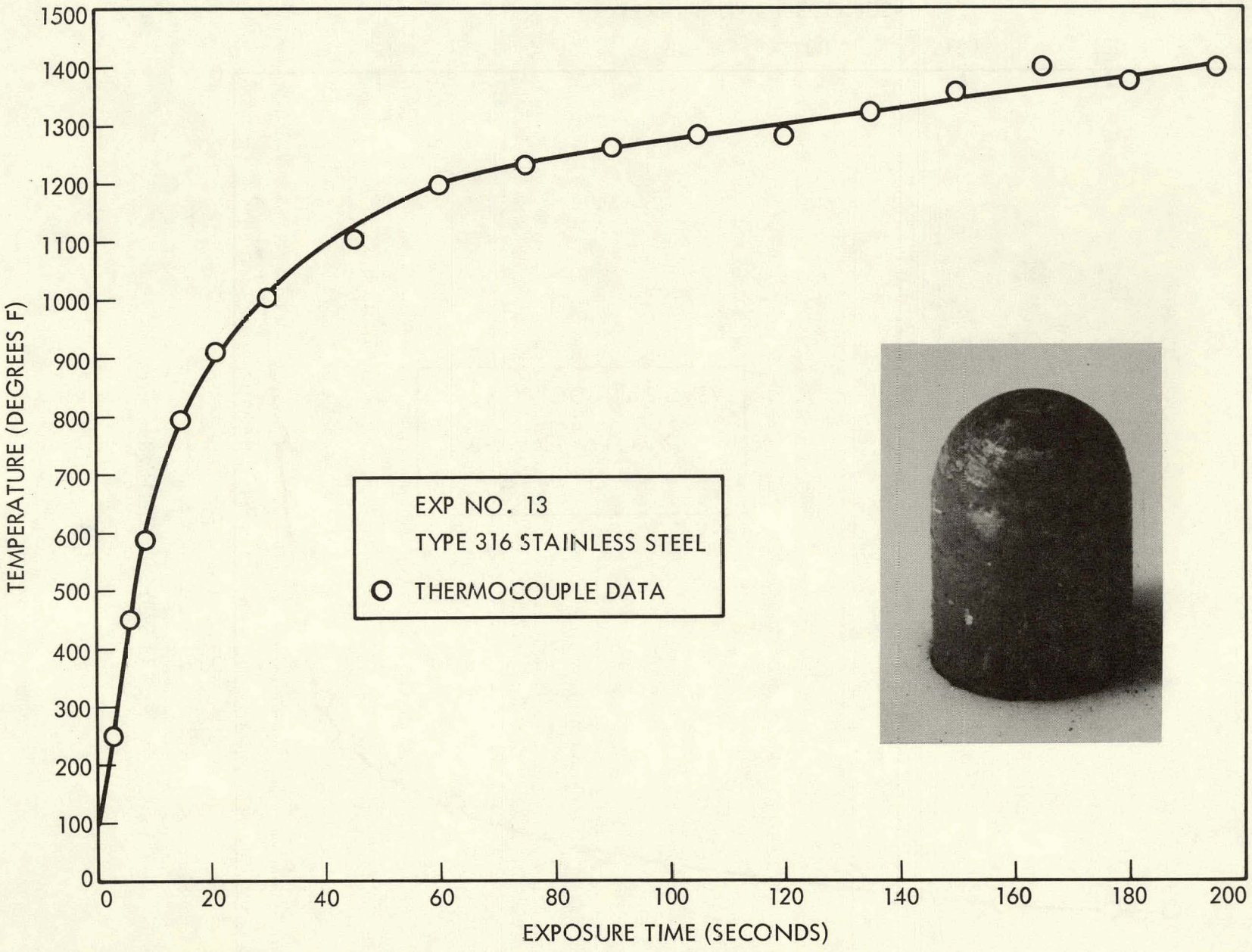

Figure A-7. Temperature vs. Time Data for Experiment No. 13

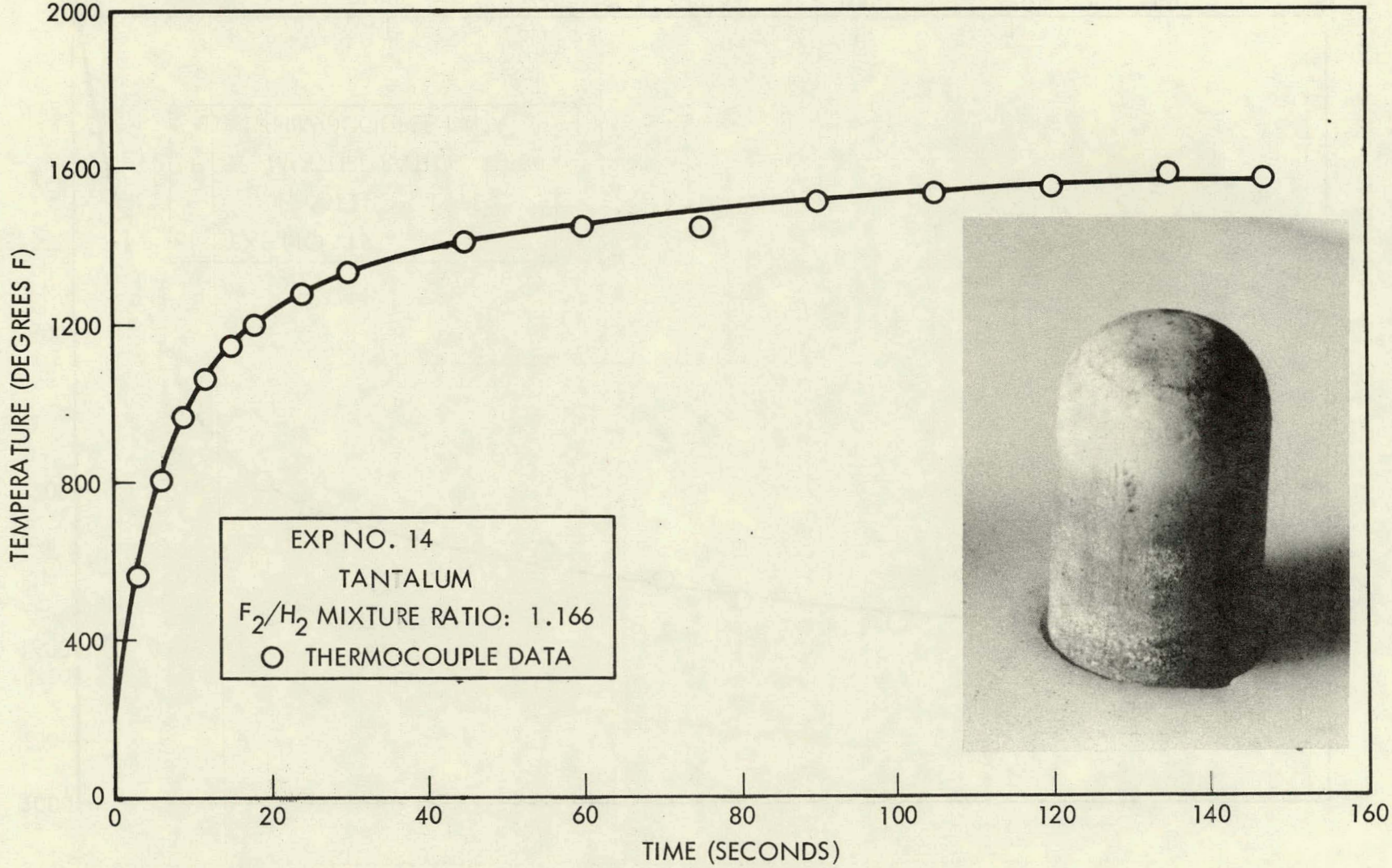

Figure A-8. Temperature vs. Time Data for Experiment No. 14

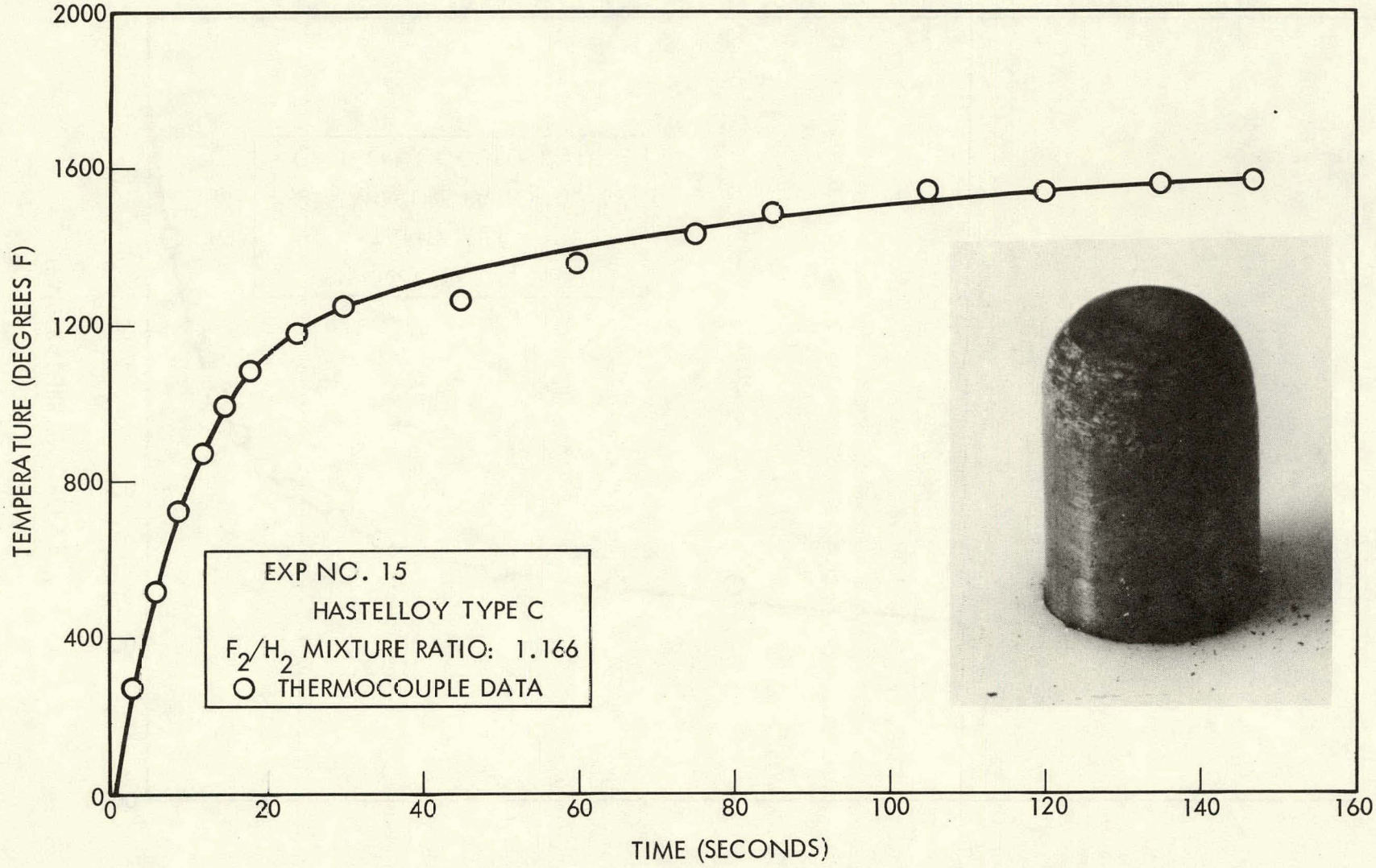

Figure A-9. Temperature vs. Time Data for Experiment No. 15

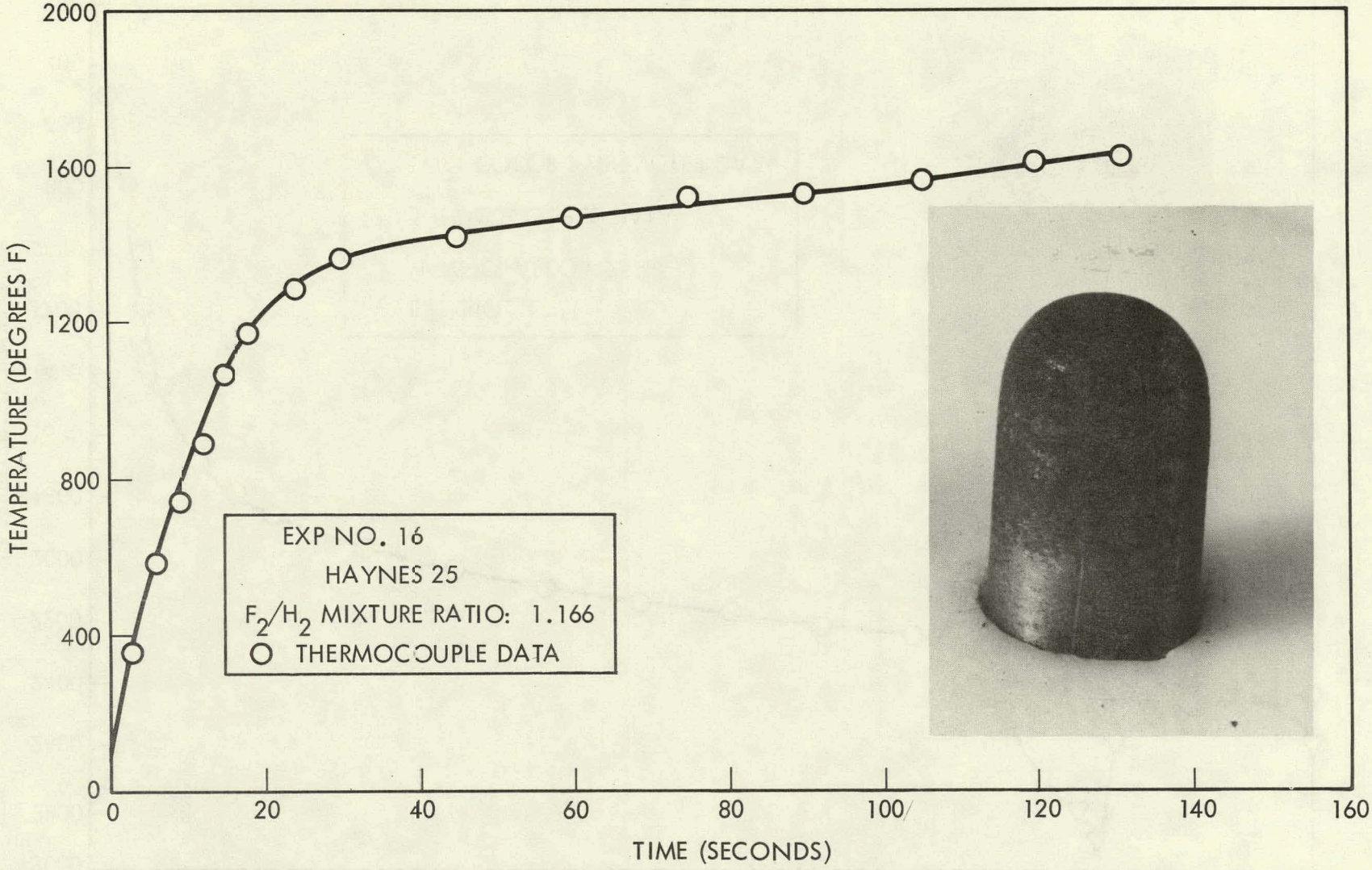

Figure A-10. Temperature vs. Time Data for Experiment No. 16

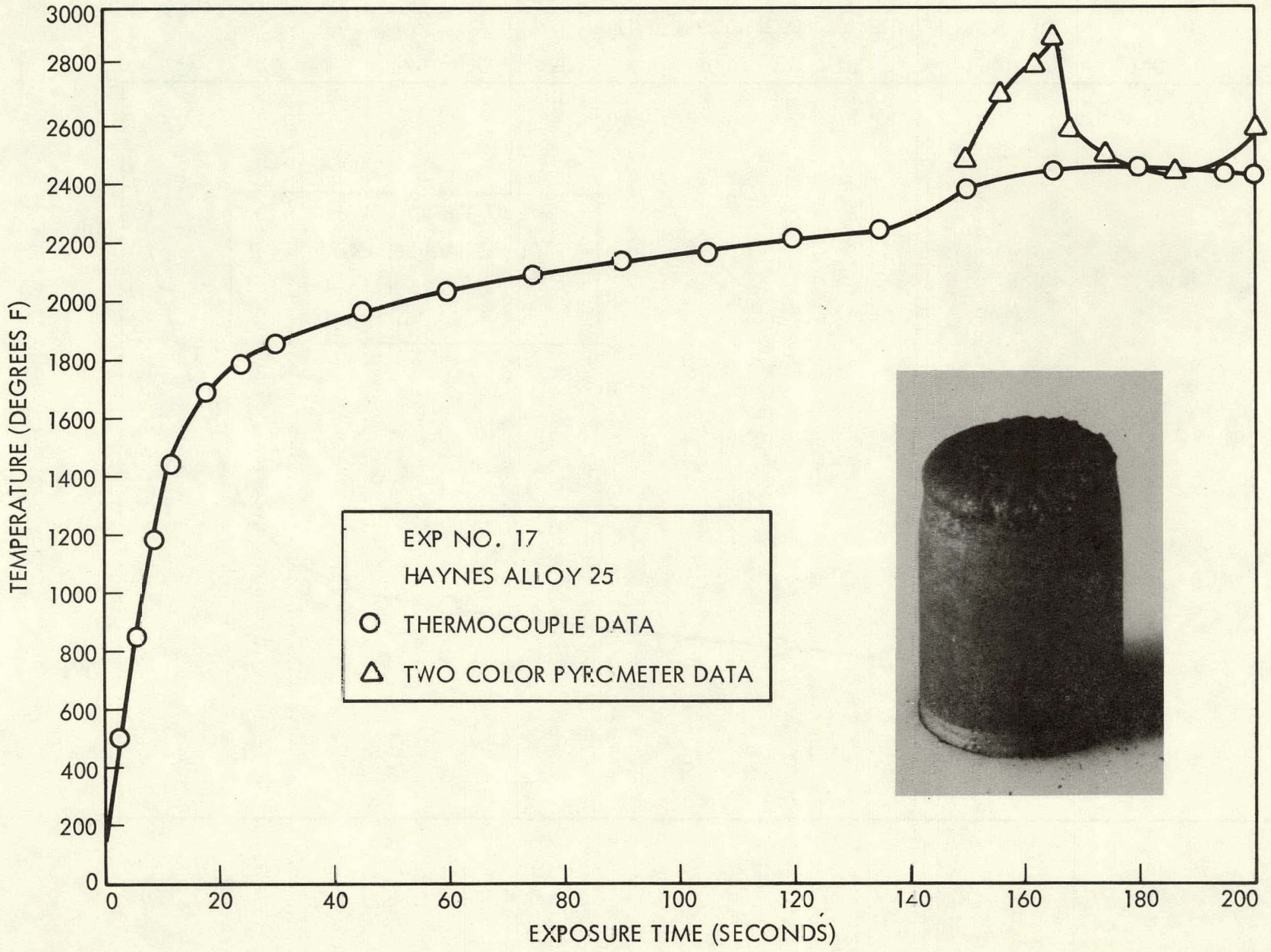

Figure A-11. Temperature vs. Time Data for Experiment No. 17

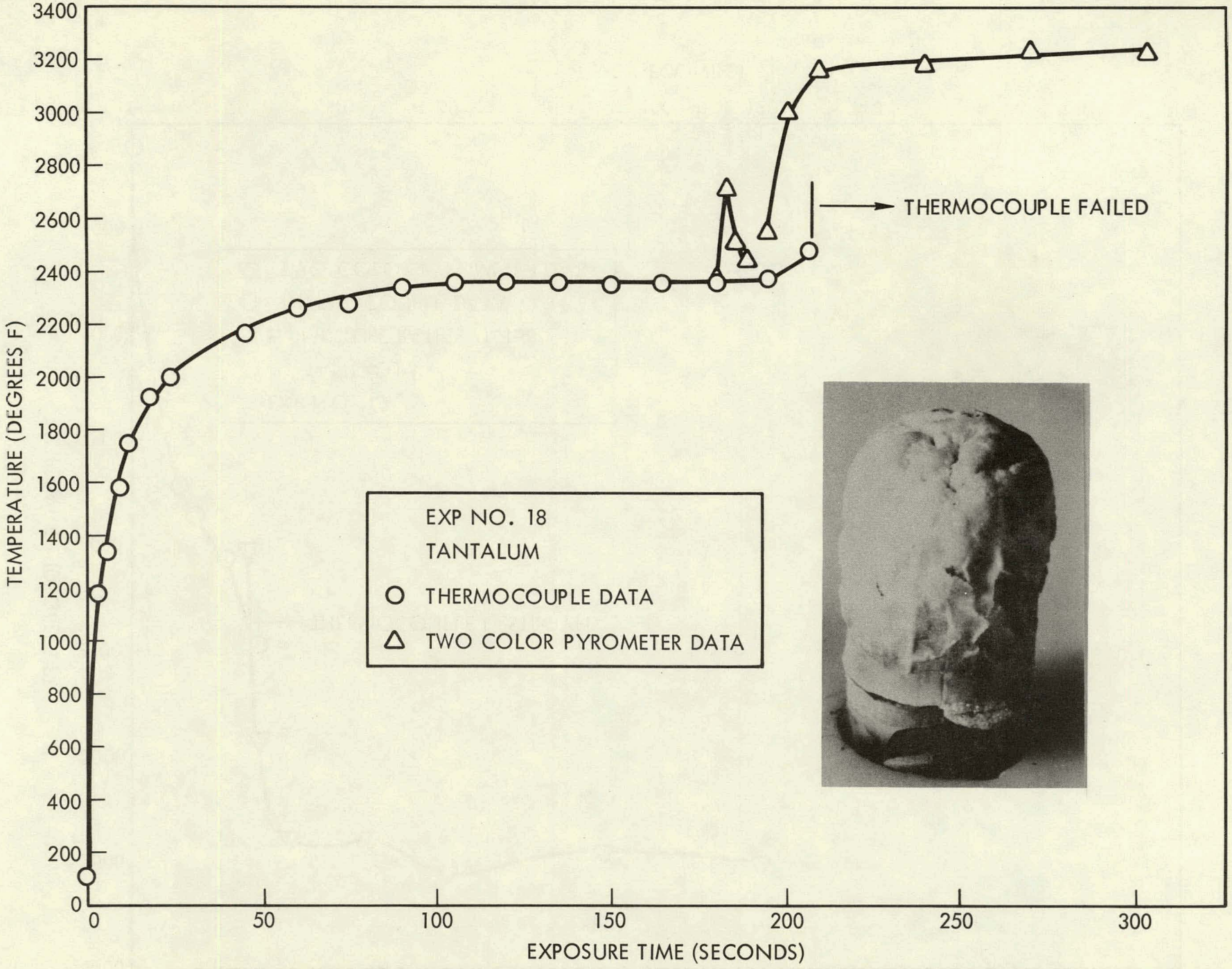

Figure A-12. Temperature vs. Time Data for Experiment No. 18

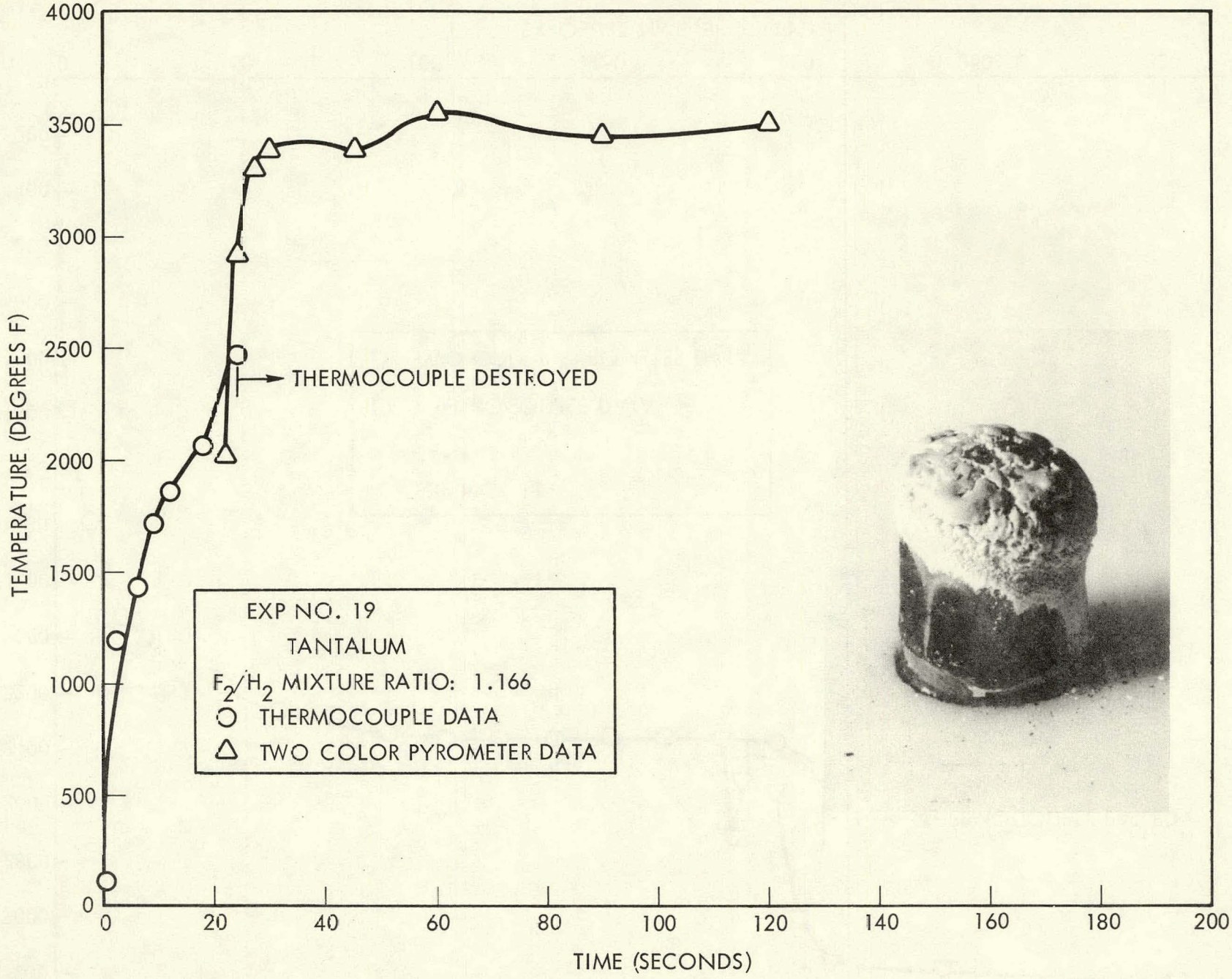

Figure A-13. Temperature vs. Time Data for Experiment No. 19

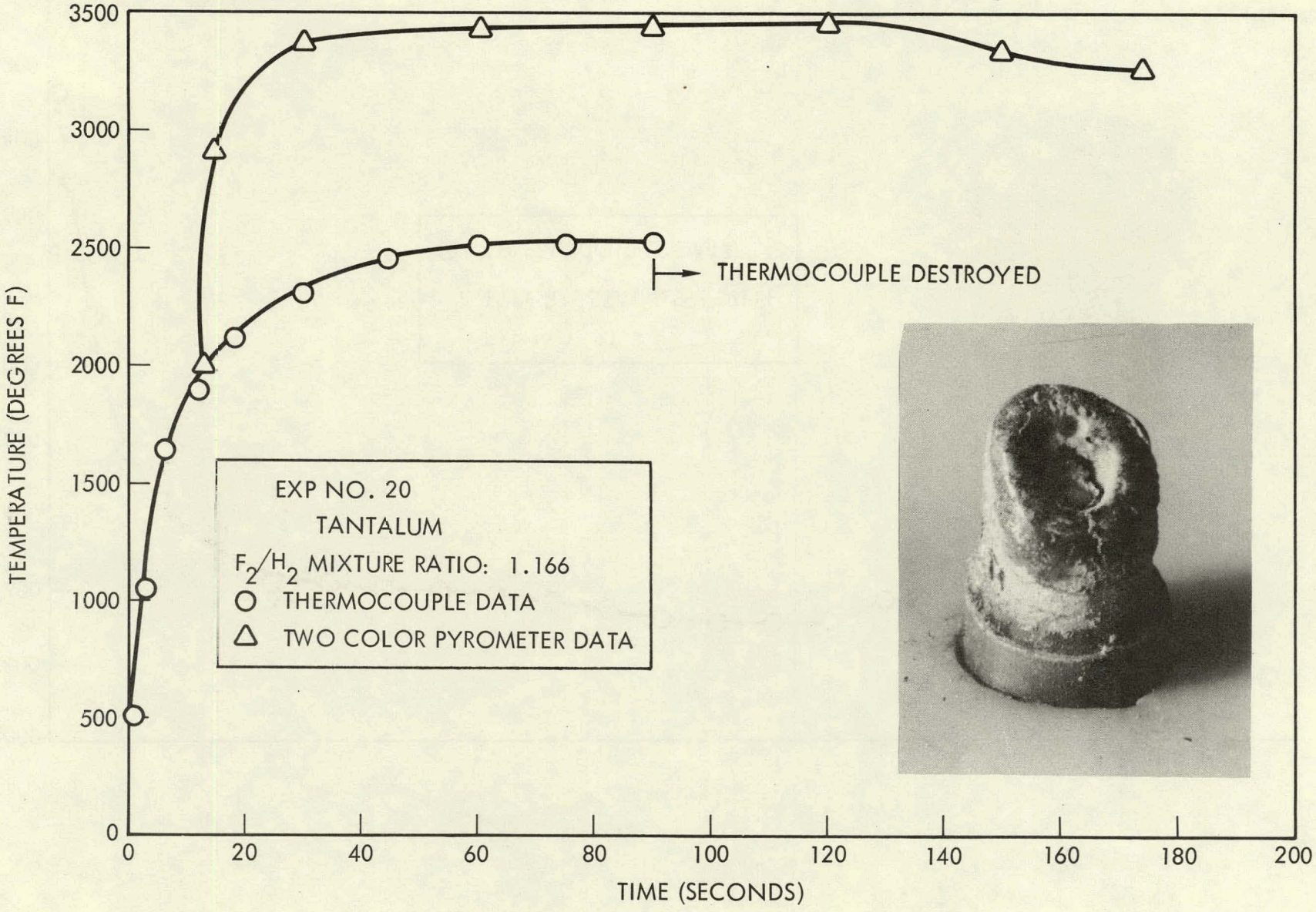

Figure A-14. Temperature vs. Time Data for Experiment No. 20

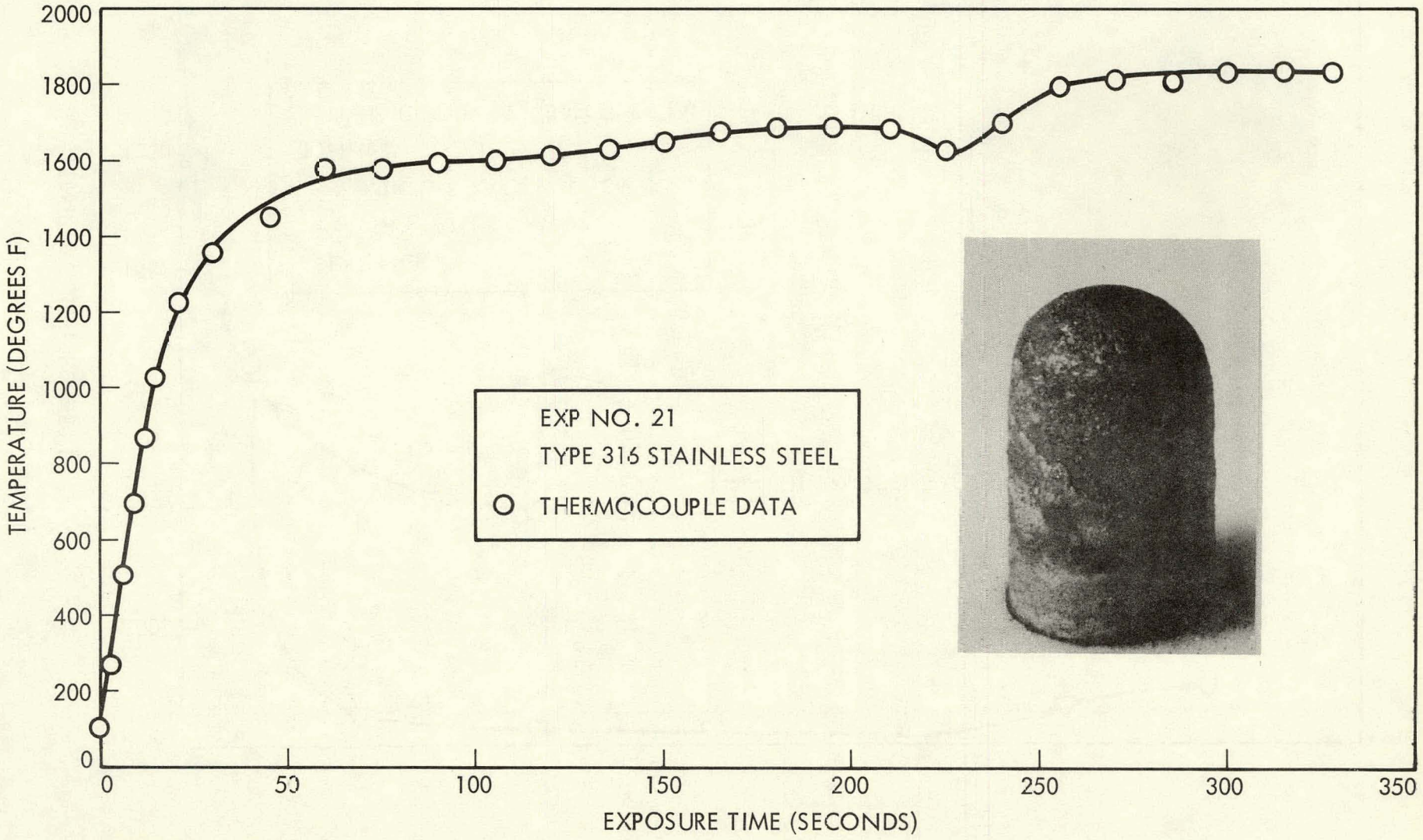

Figure A-15. Temperature vs. Time Data for Experiment No. 21

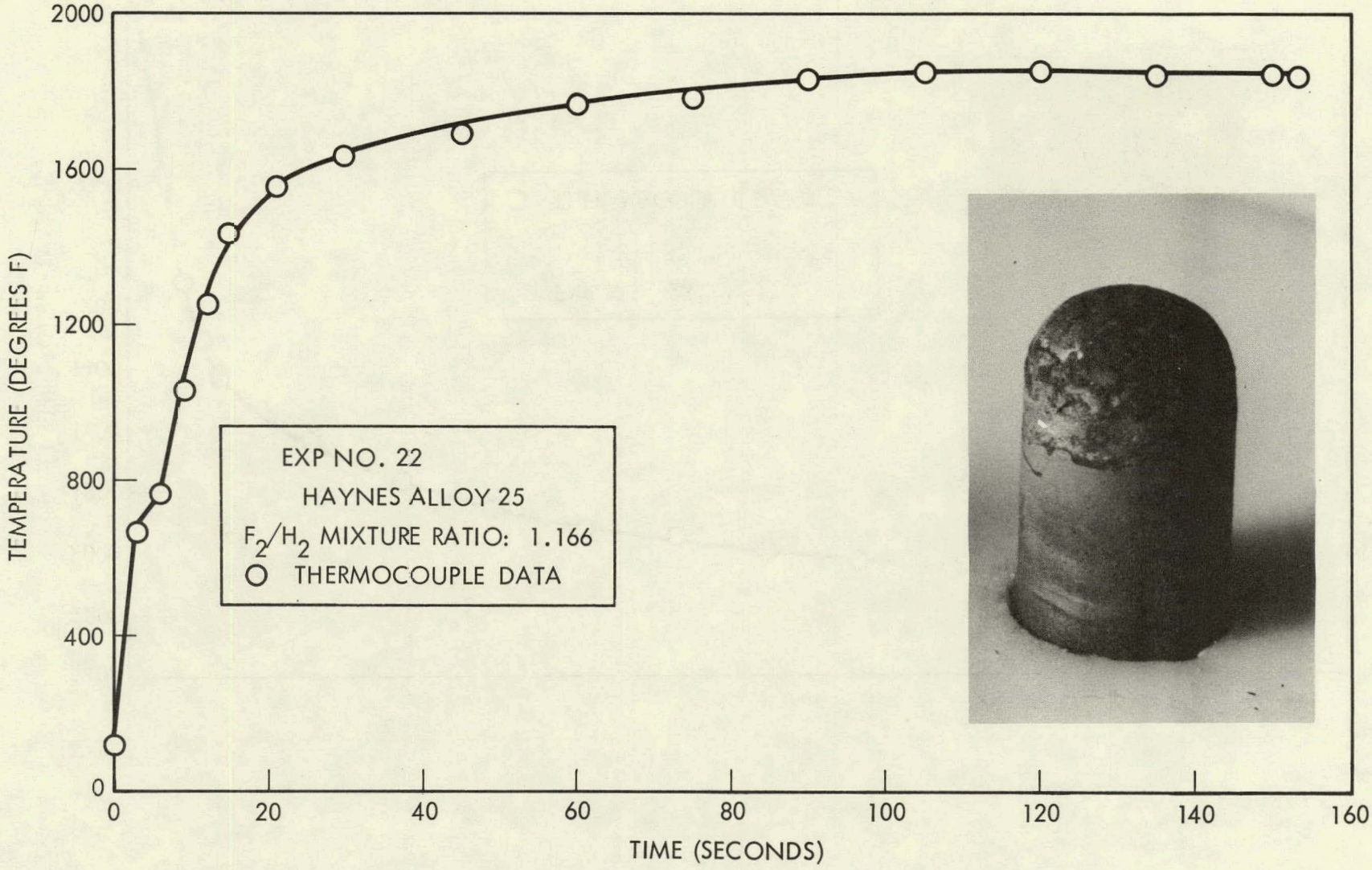

Figure A-16. Temperature vs. Time Data for Experiment No. 22

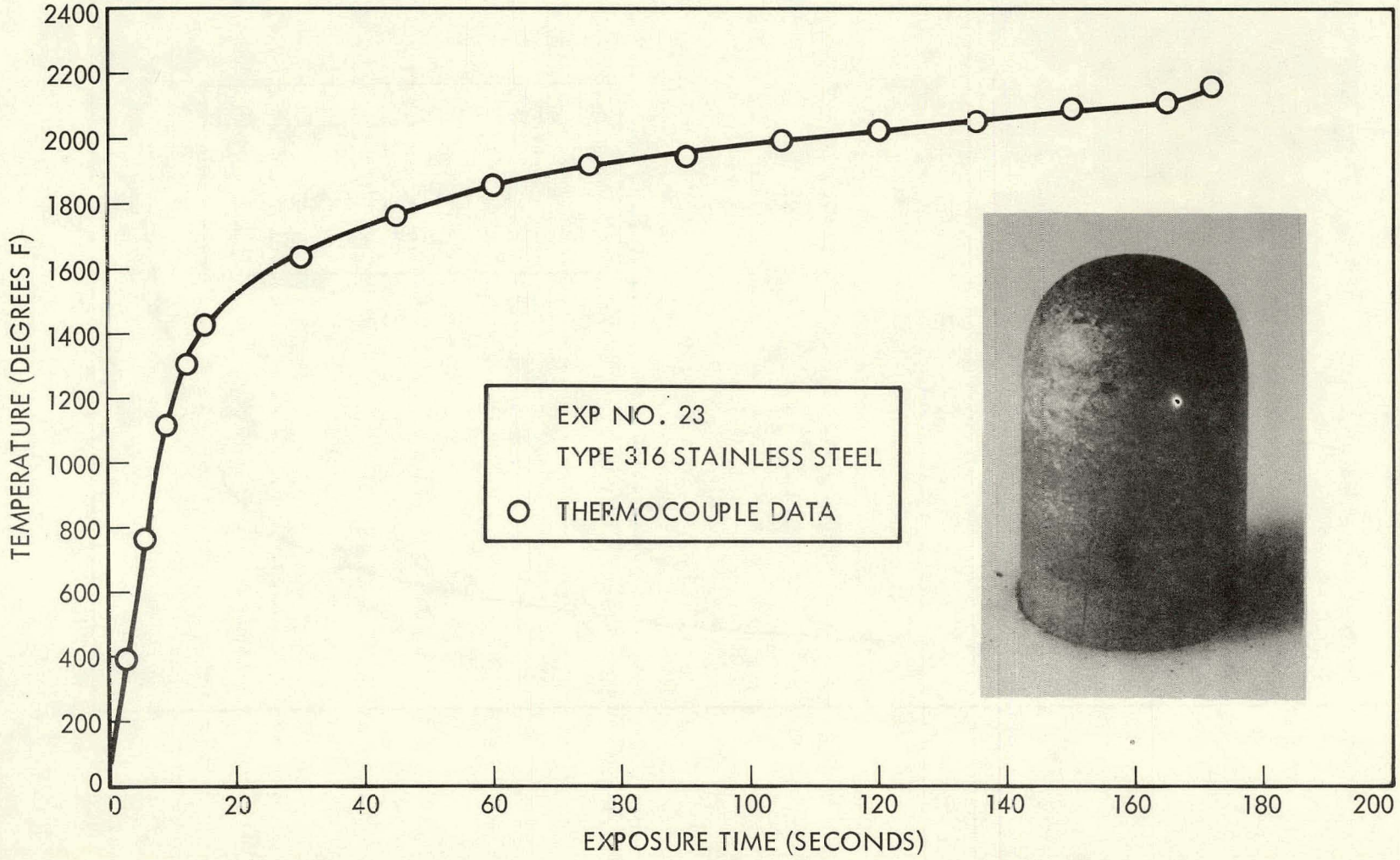

Figure A-17. Temperature vs. Time Data for Experiment No. 23

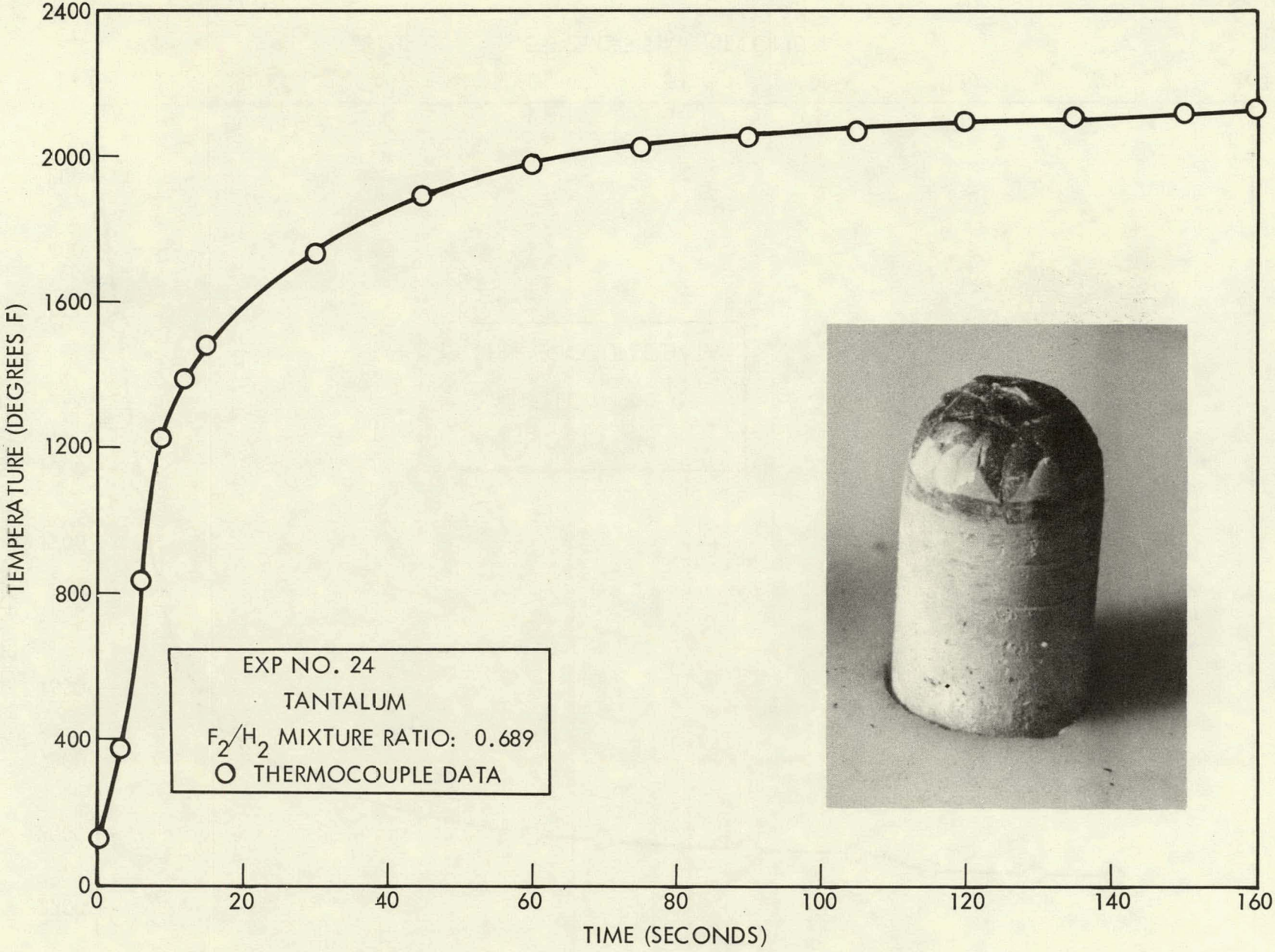

Figure A-18. Temperature vs. Time Data for Experiment No. 24

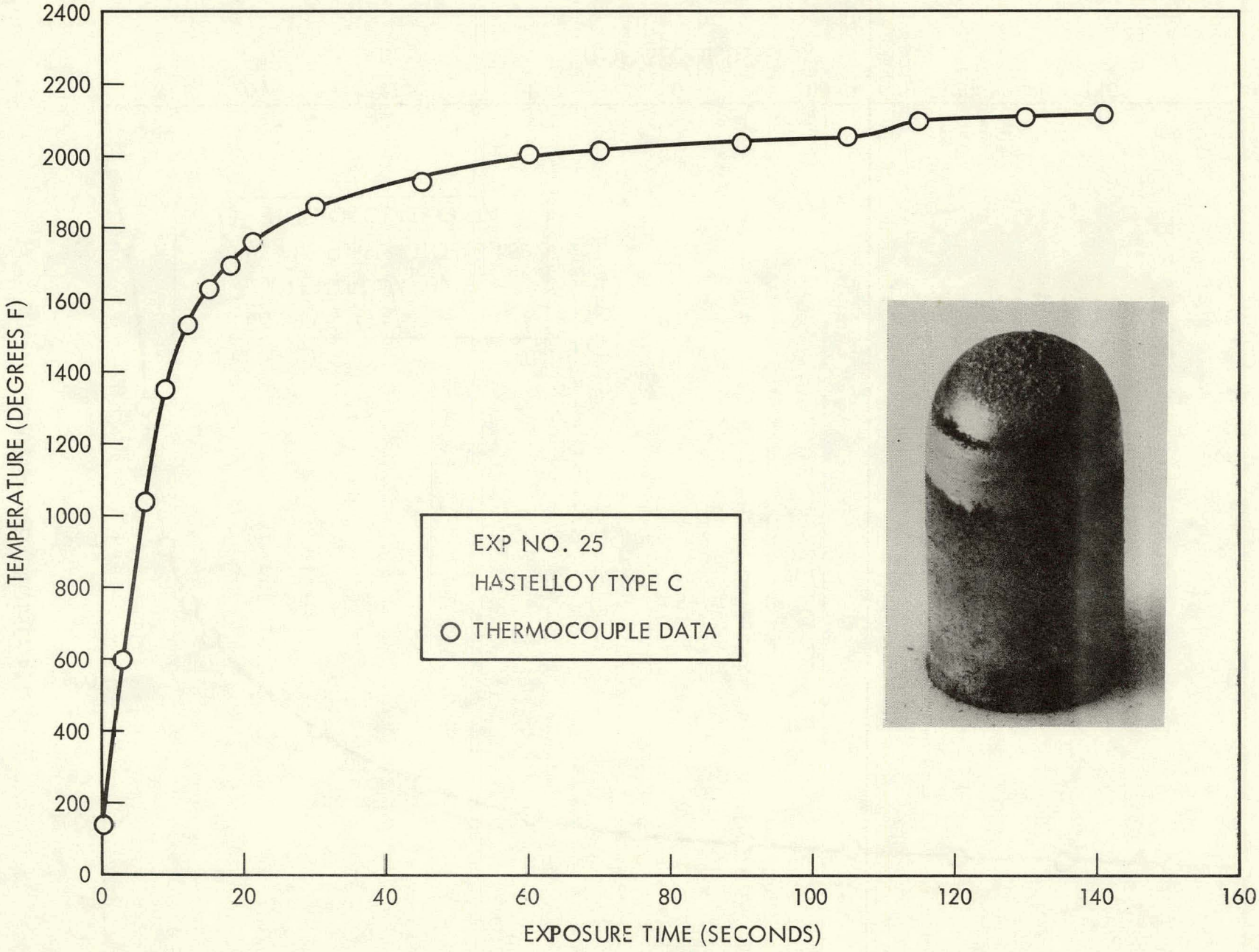

Figure A-19. Temperature vs. Time Data for Experiment No. 25

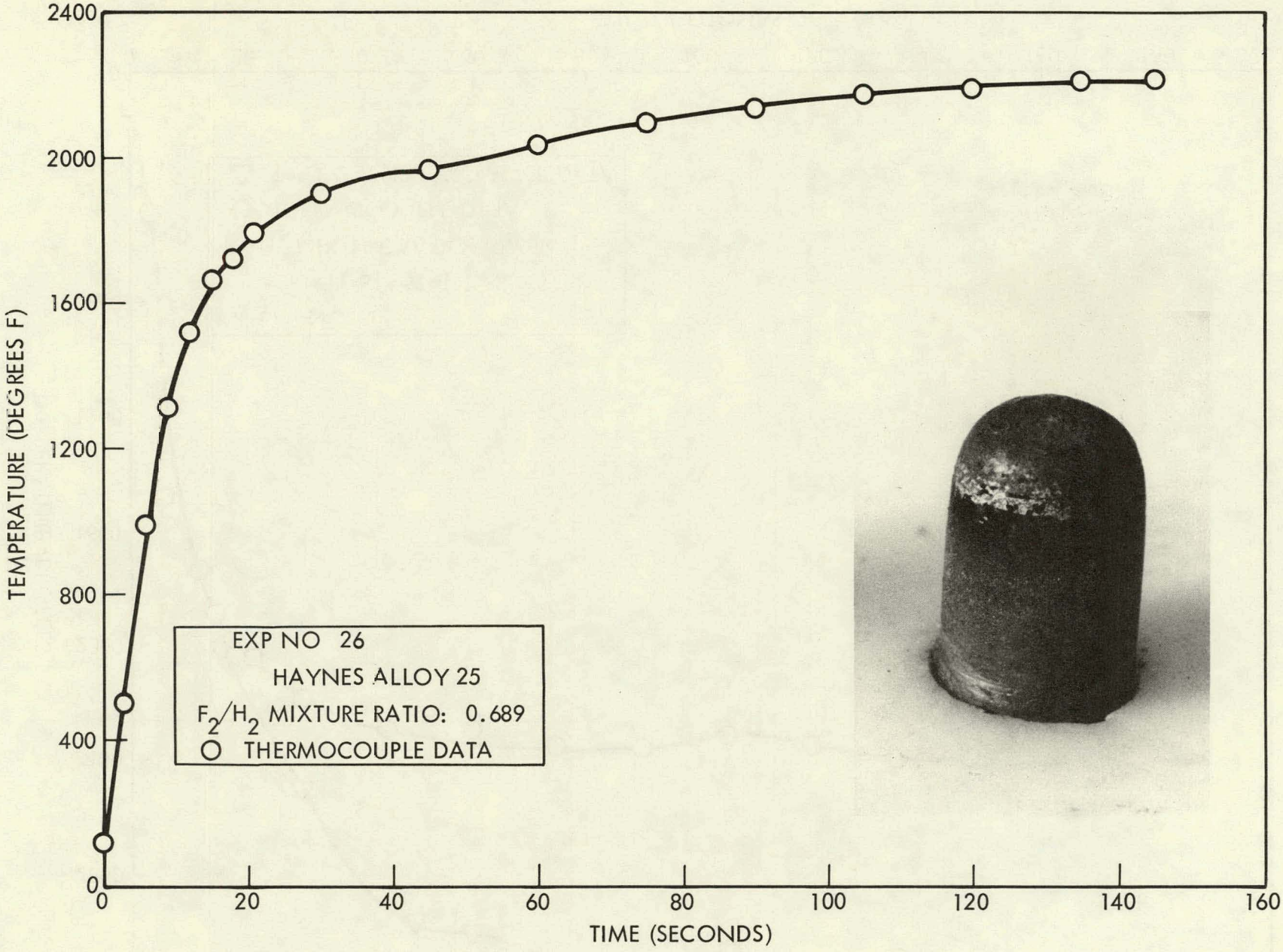

Figure A-20. Temperature vs. Time Data for Experiment No. 26

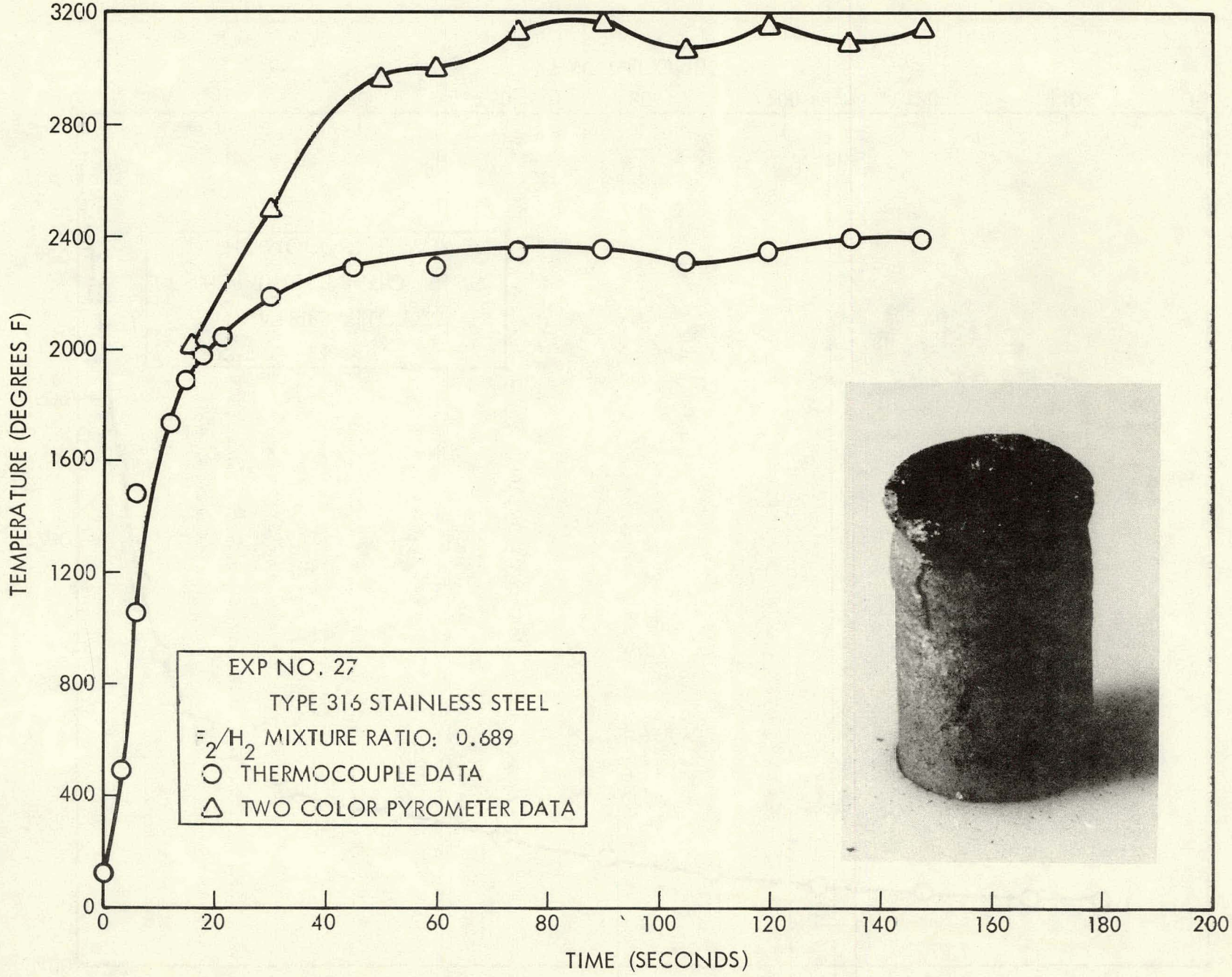

Figure A-21. Temperature vs. Time Data for Experiment No. 27

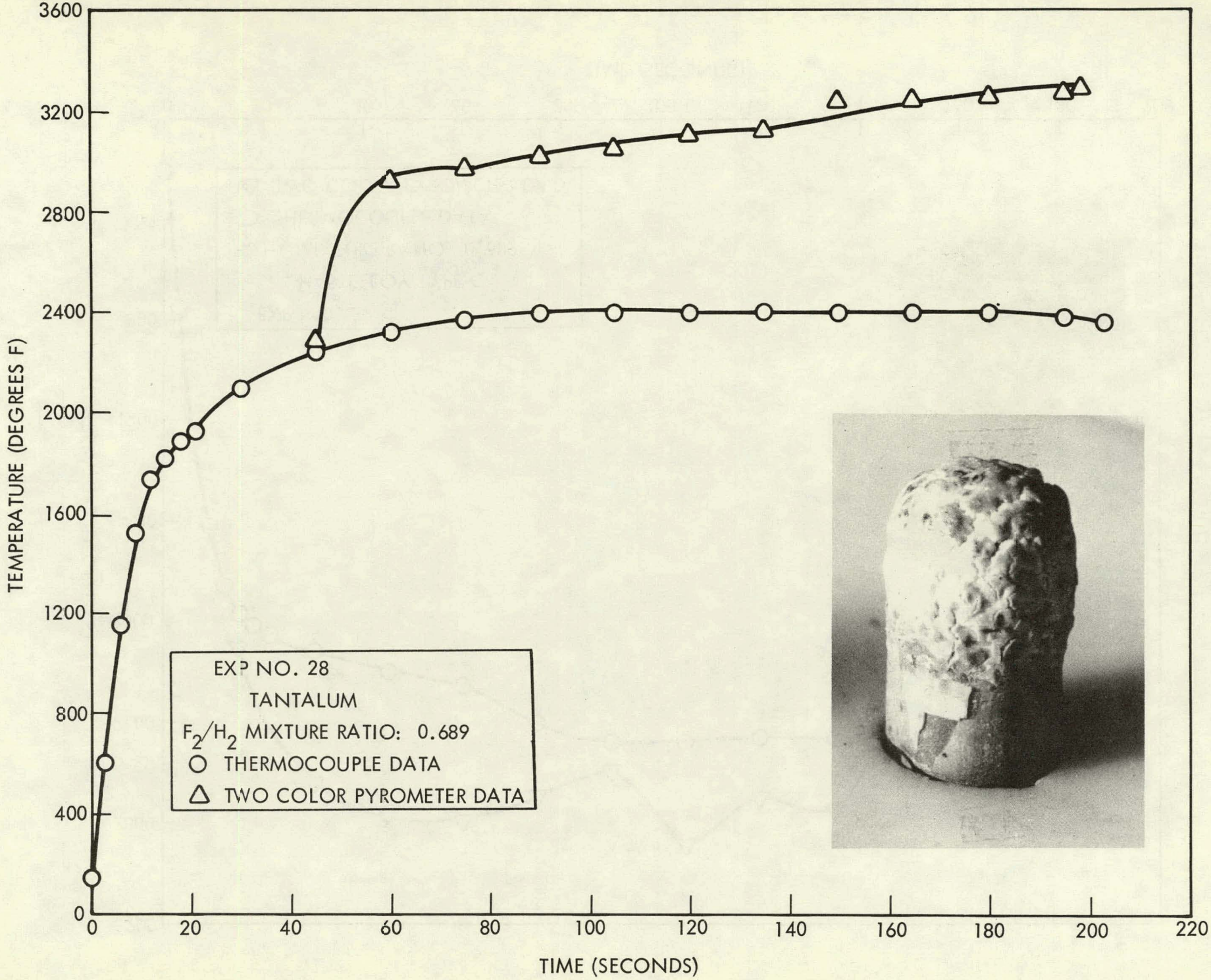

Figure A-22. Temperature vs. Time Data for Experiment No. 28

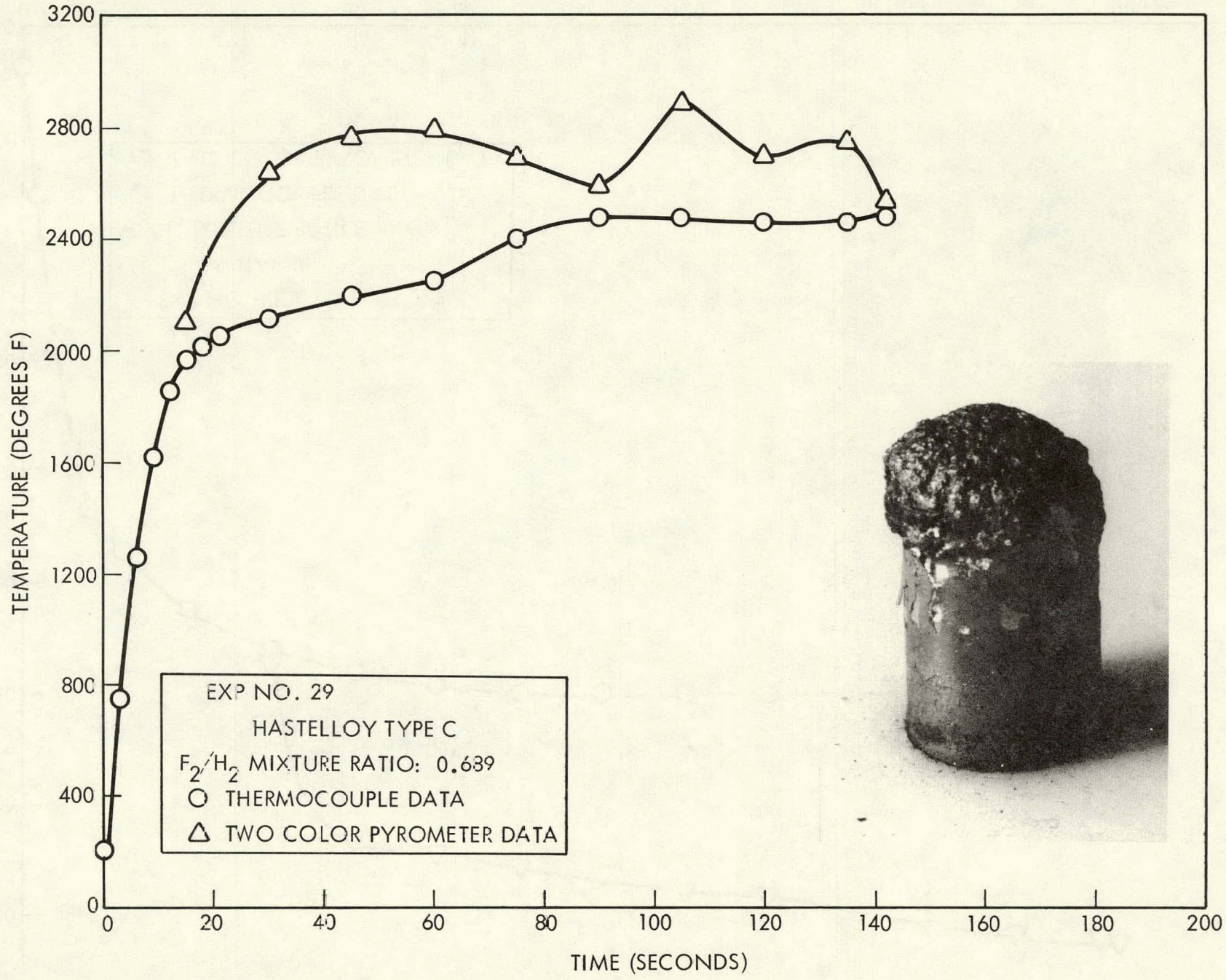

Figure A-23. Temperature vs. Time Data for Experiment No. 29

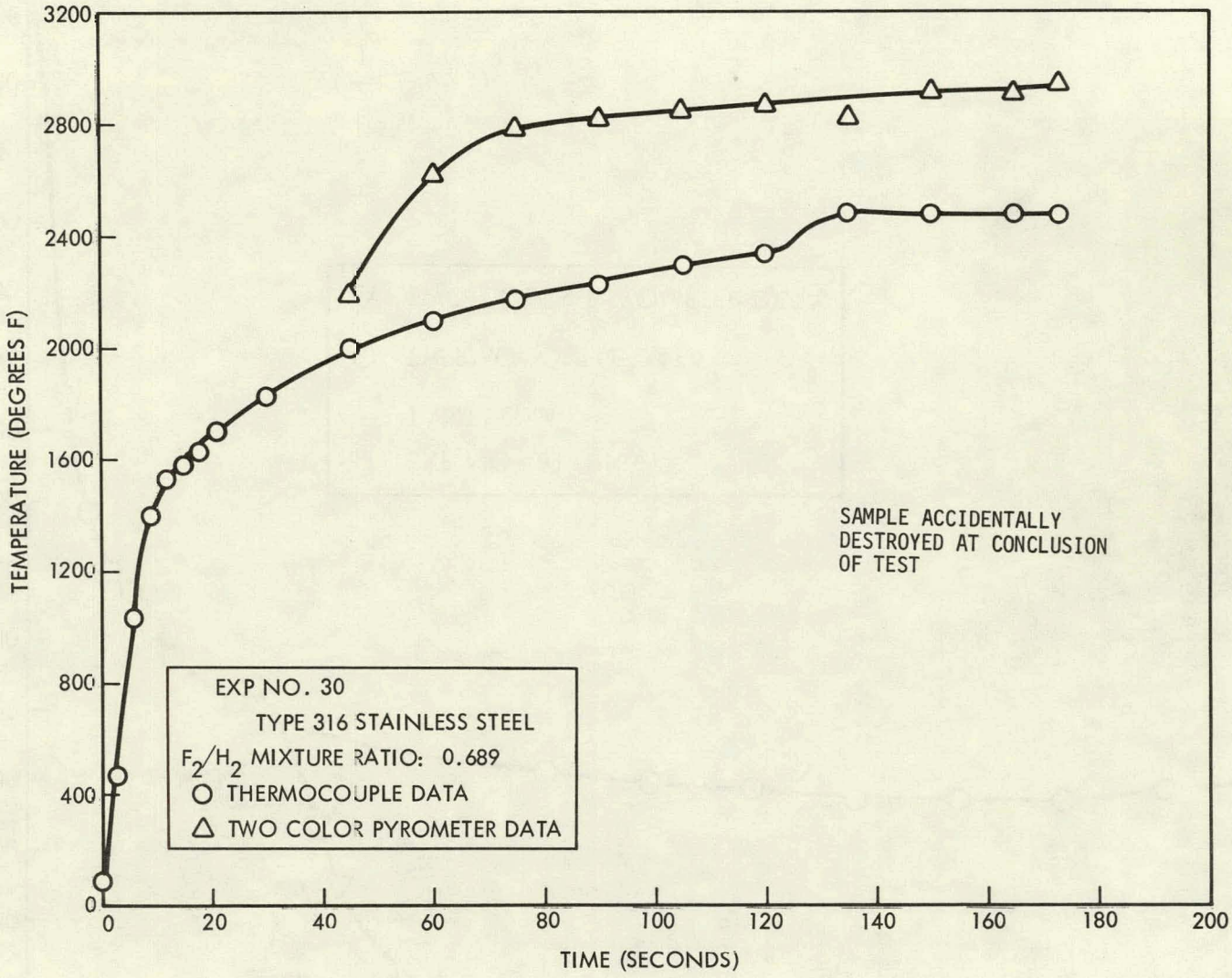

Figure A-24. Temperature vs. Time Data for Experiment No. 30

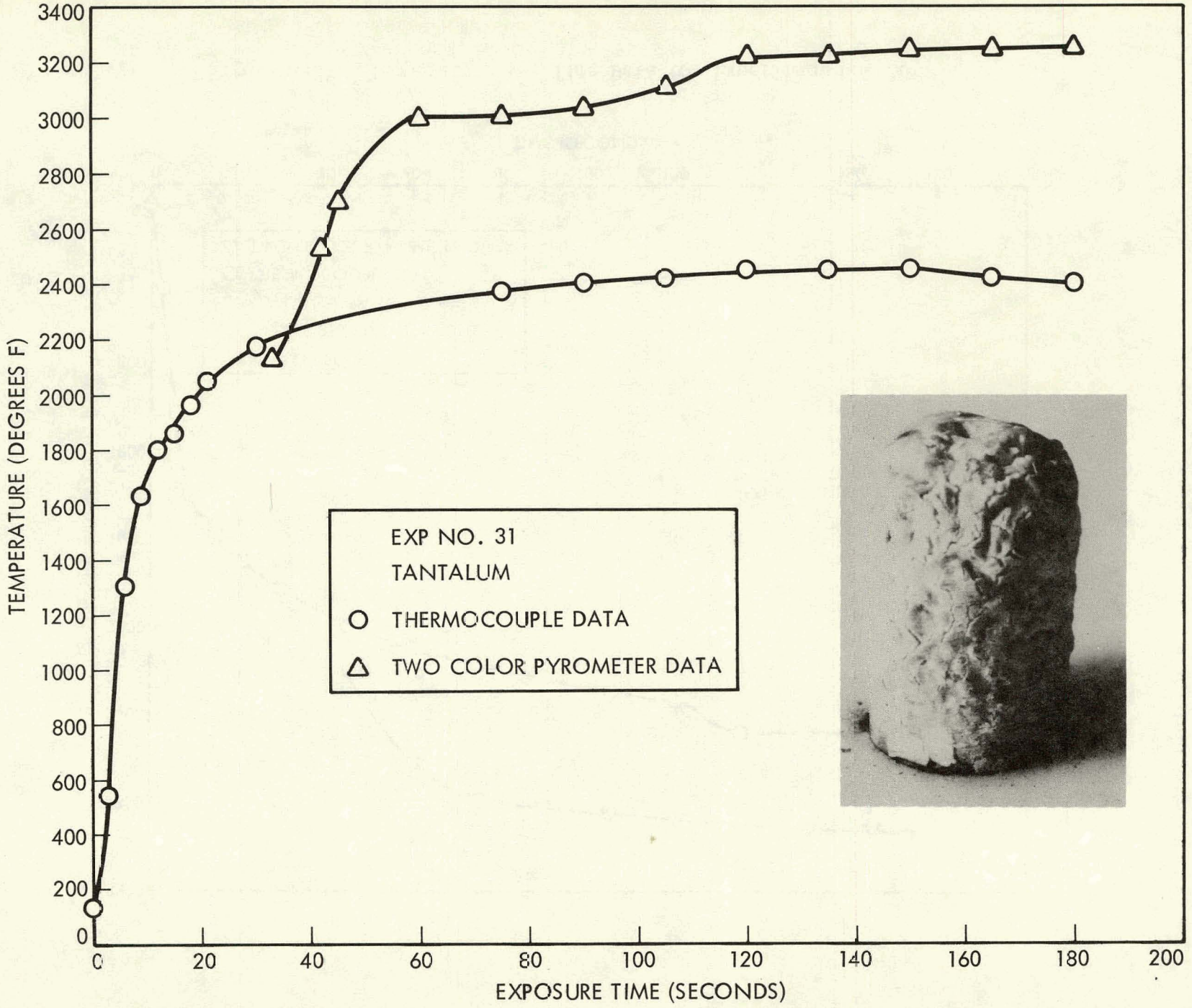

Figure A-25. Temperature vs. Time Data for Experiment No. 31

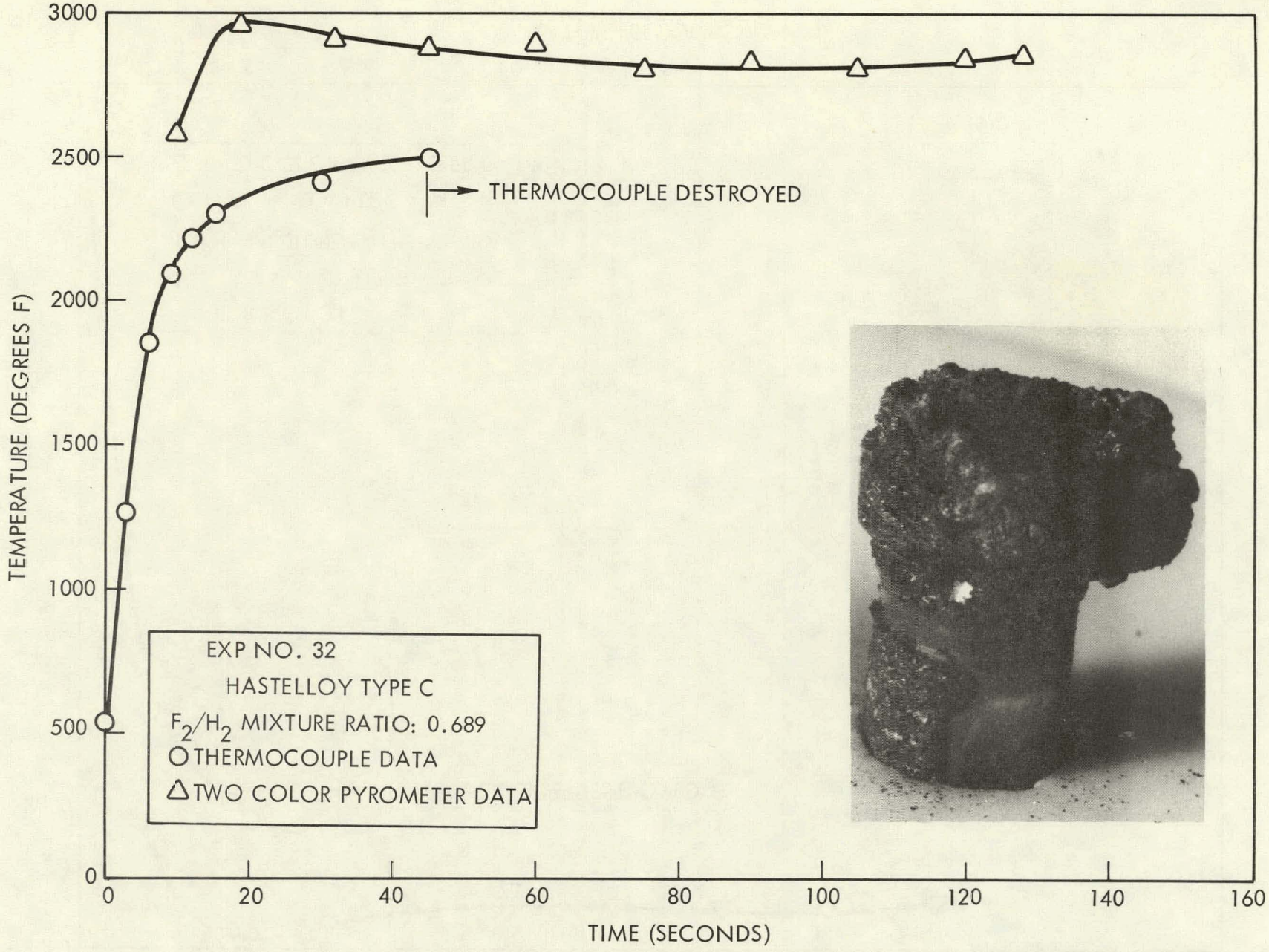

Figure A-26. Temperature vs. Time Data for Experiment No. 32

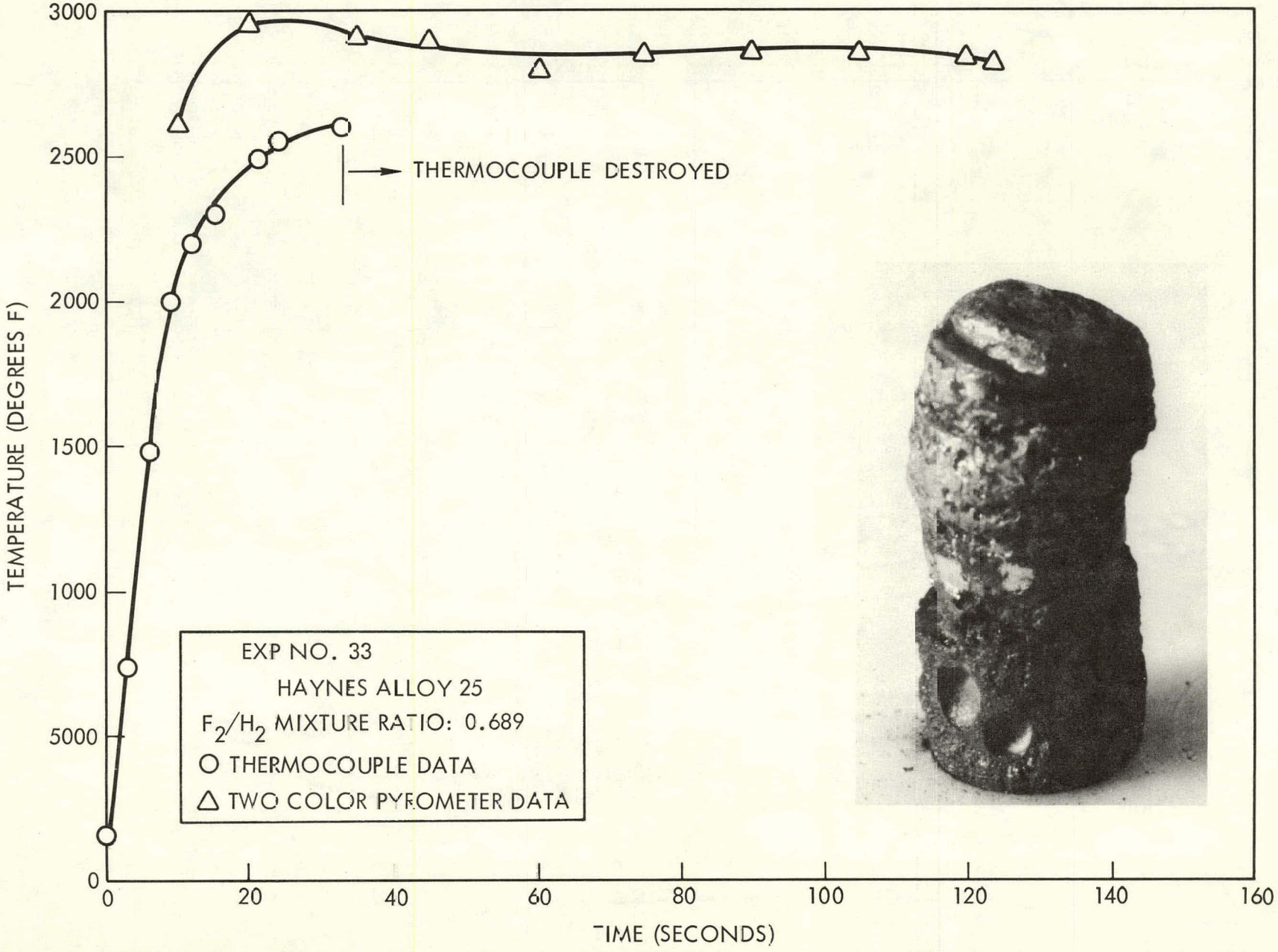

Figure A-27. Temperature vs. Time Data for Experiment No. 33

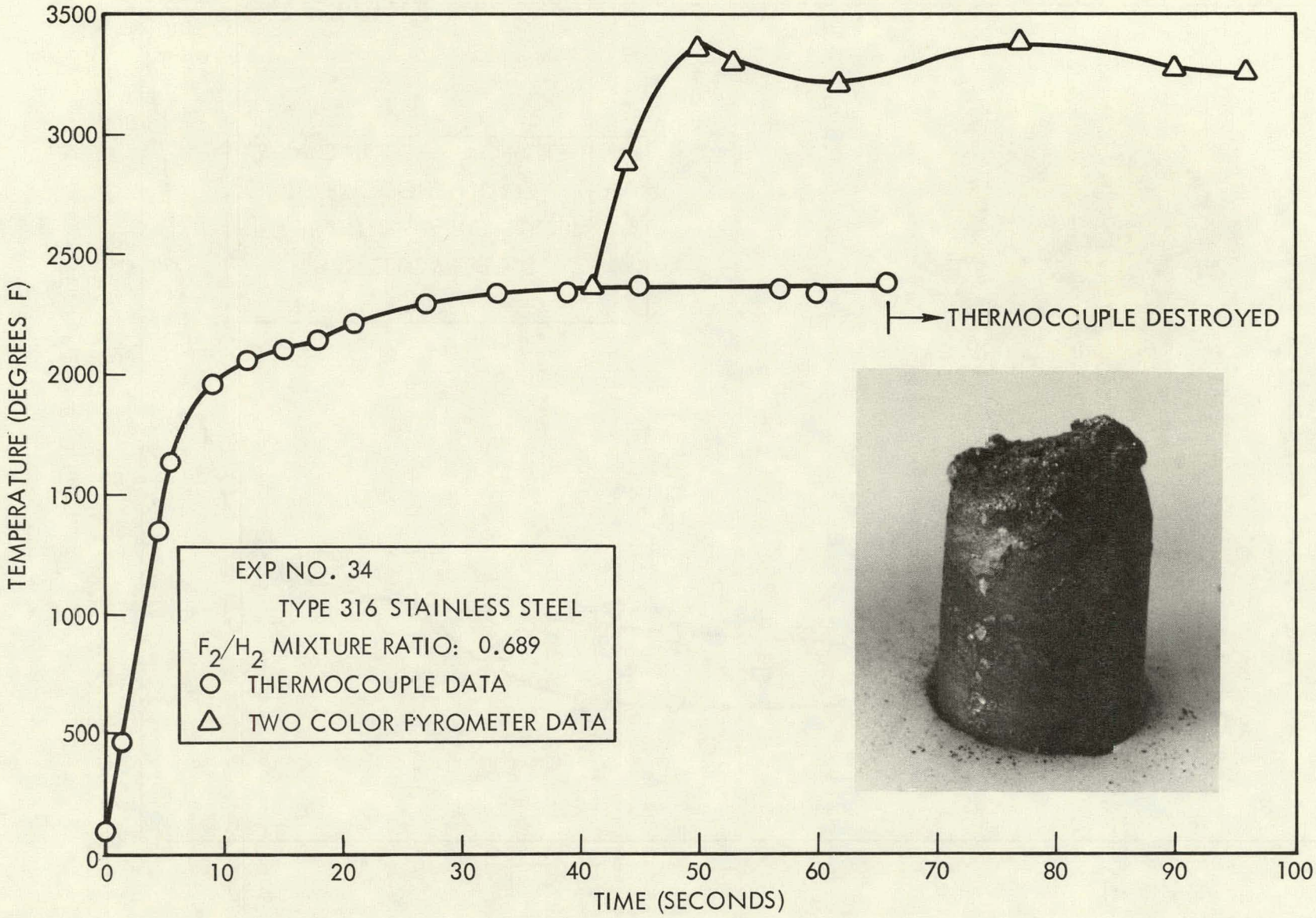

Figure A-28. Temperature vs. Time Data for Experiment No. 34

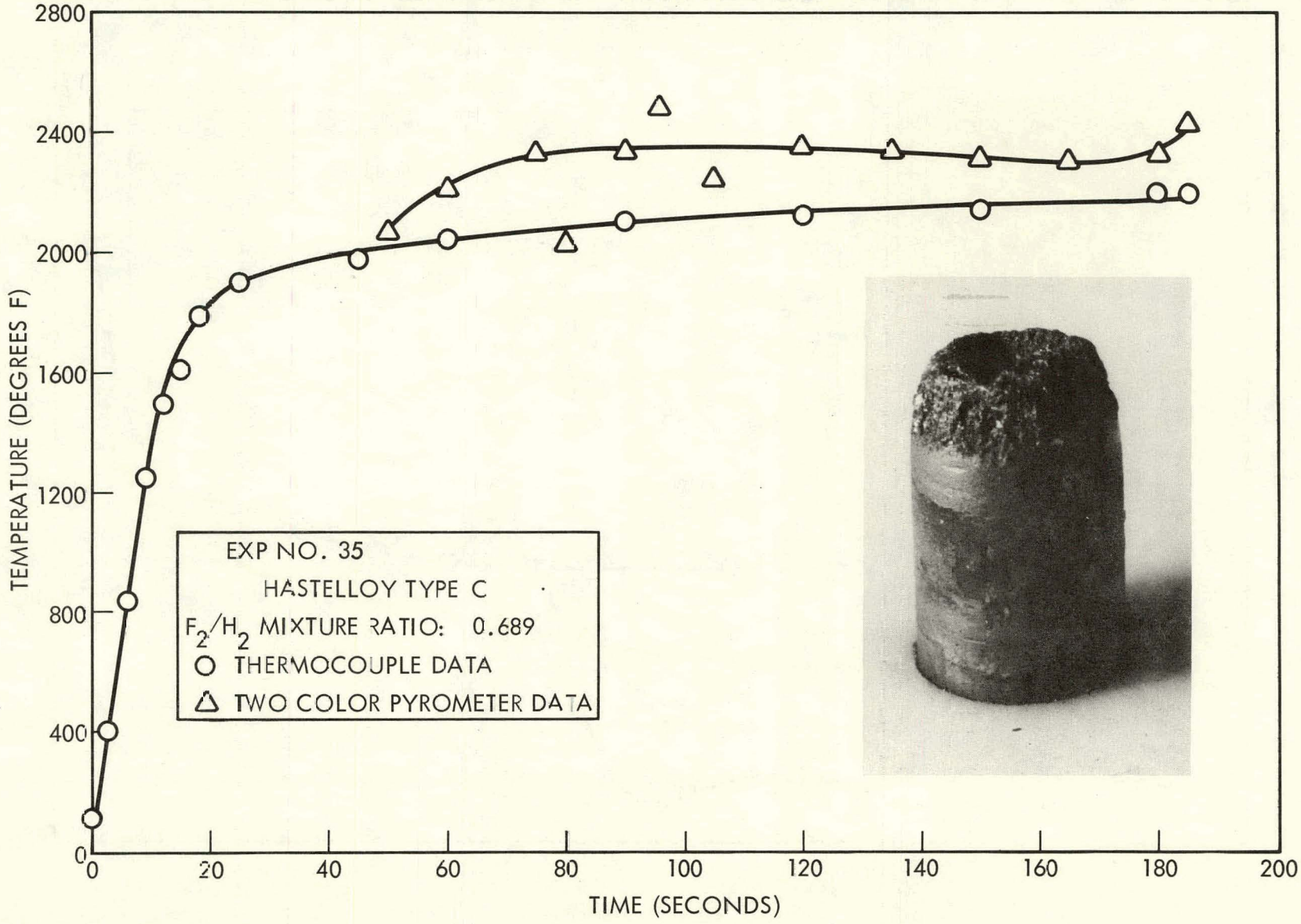

Figure A-29. Temperature vs. Time Data for Experiment No. 35

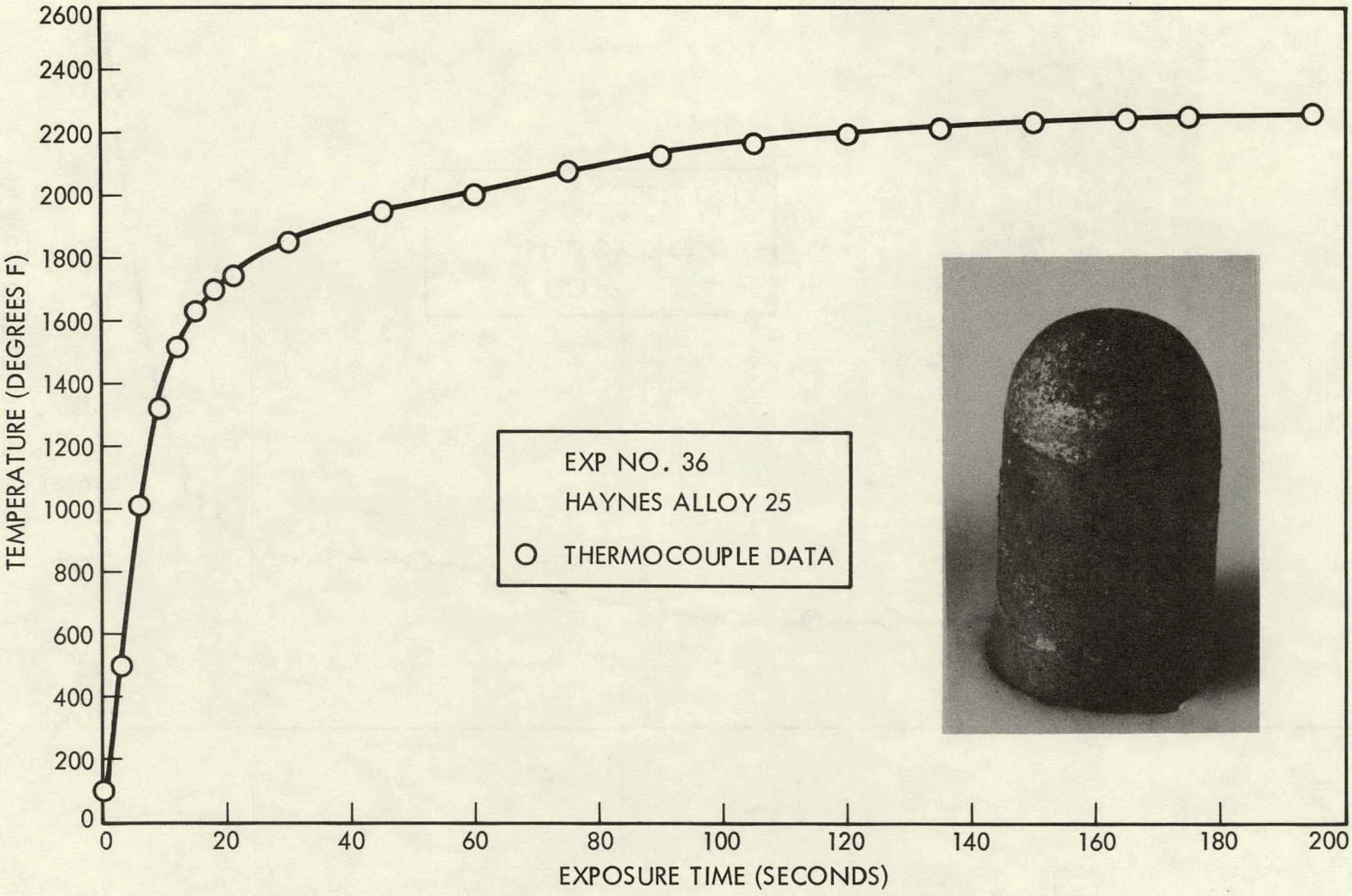

Figure A-30. Temperature vs. Time Data for Experiment No. 36

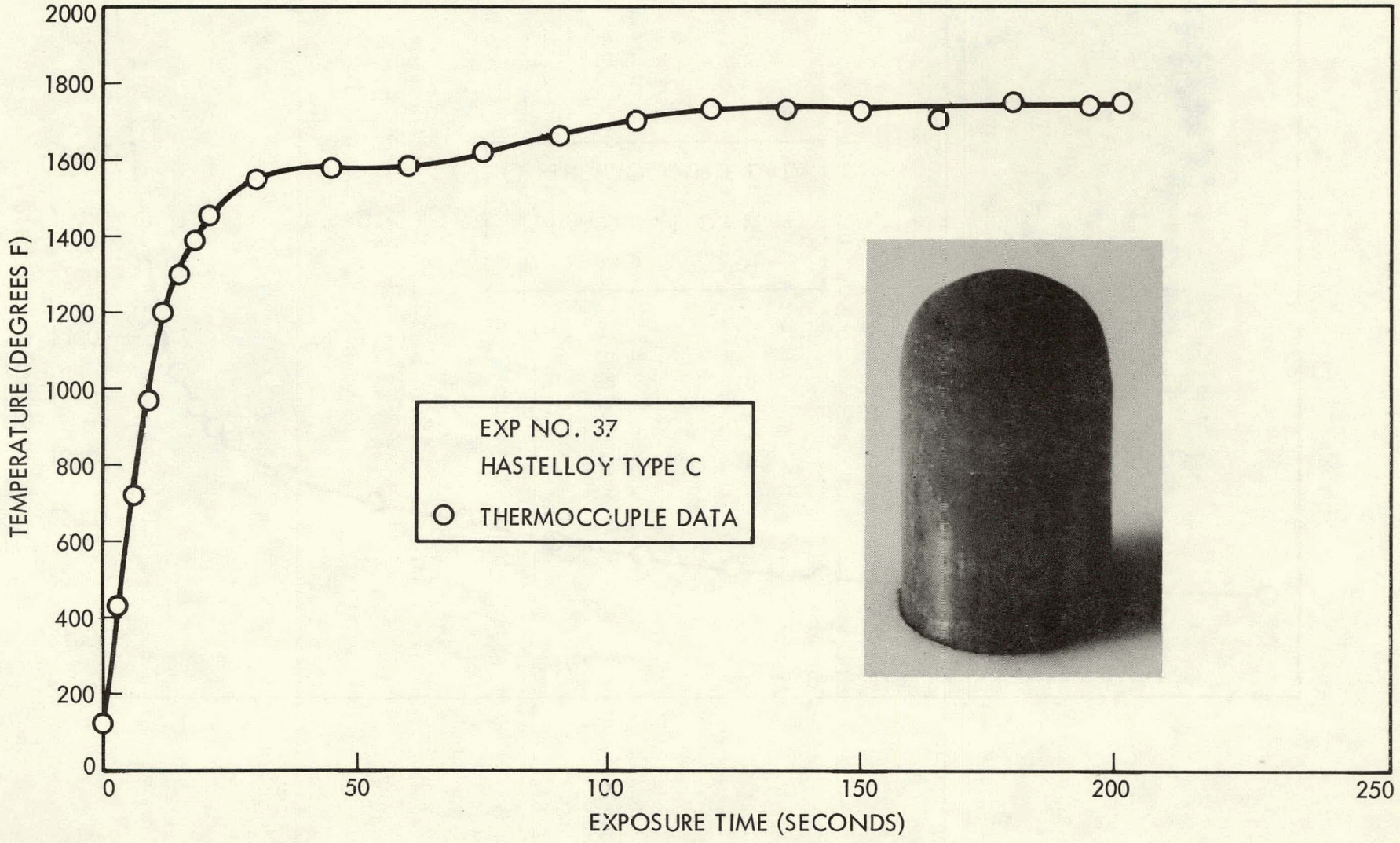

Figure A-31. Temperature vs. Time Data for Experiment No. 37

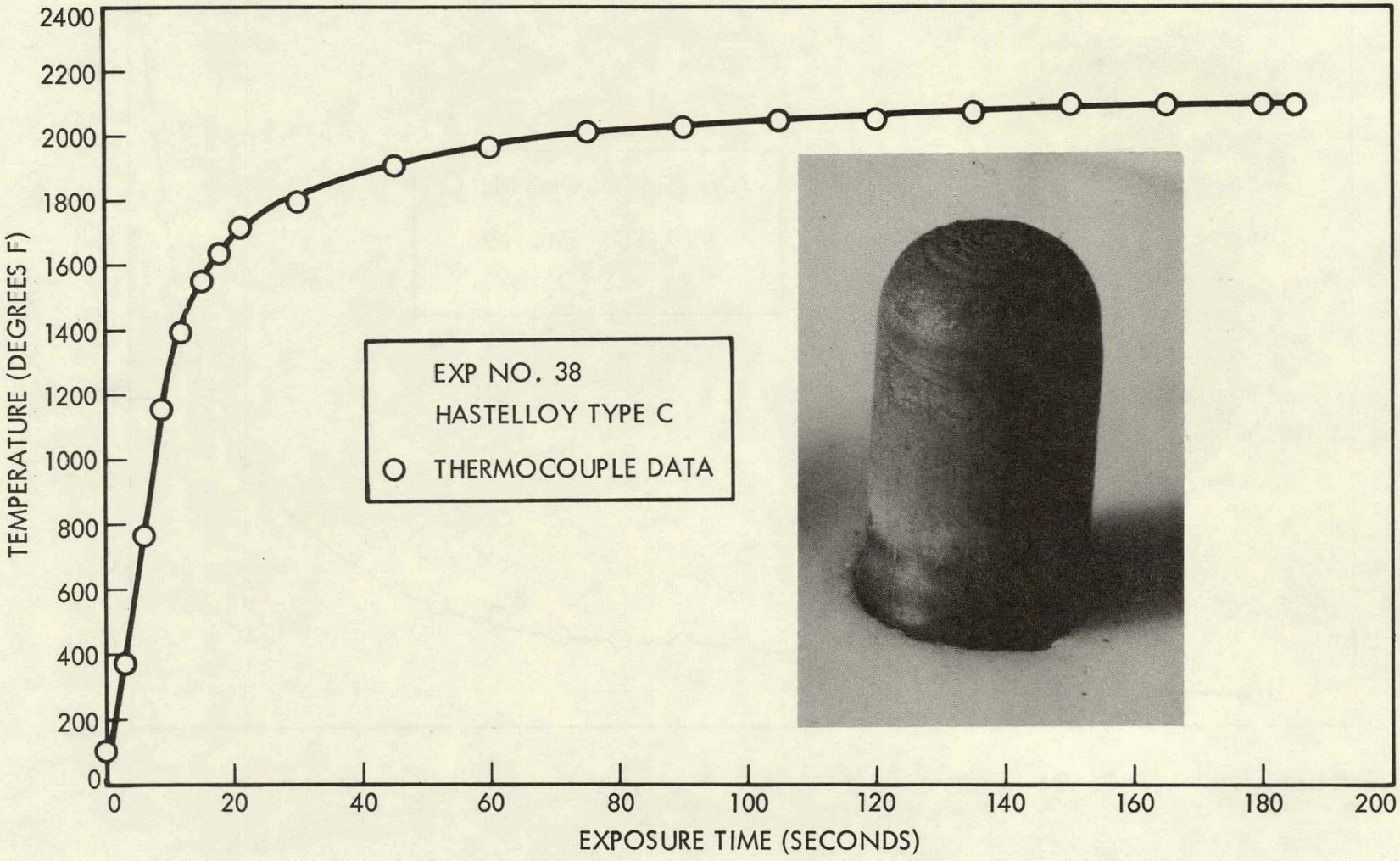

Figure A-32. Temperature vs. Time Data for Experiment No. 38

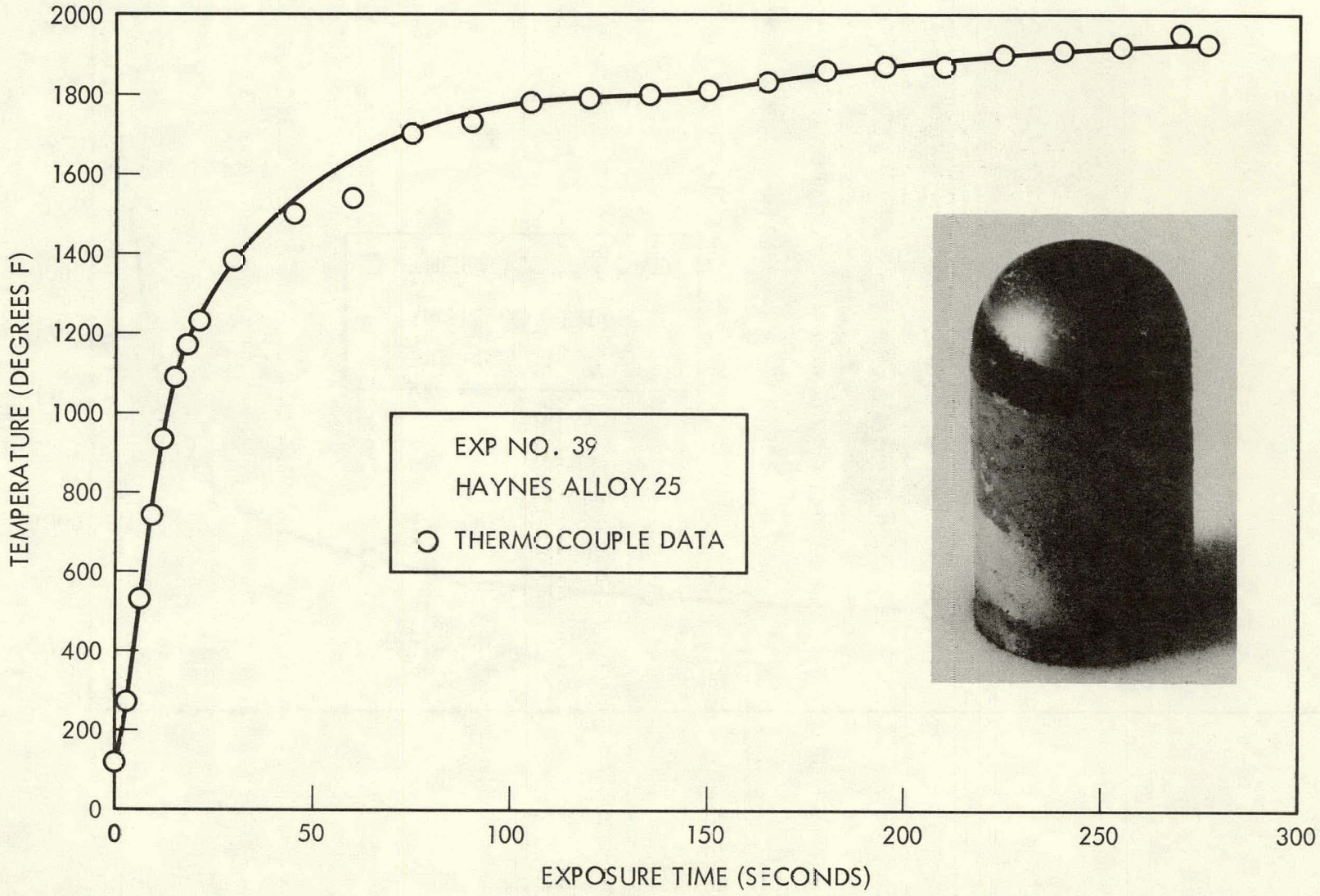

Figure A-33. Temperature vs. Time Data for Experiment No. 39

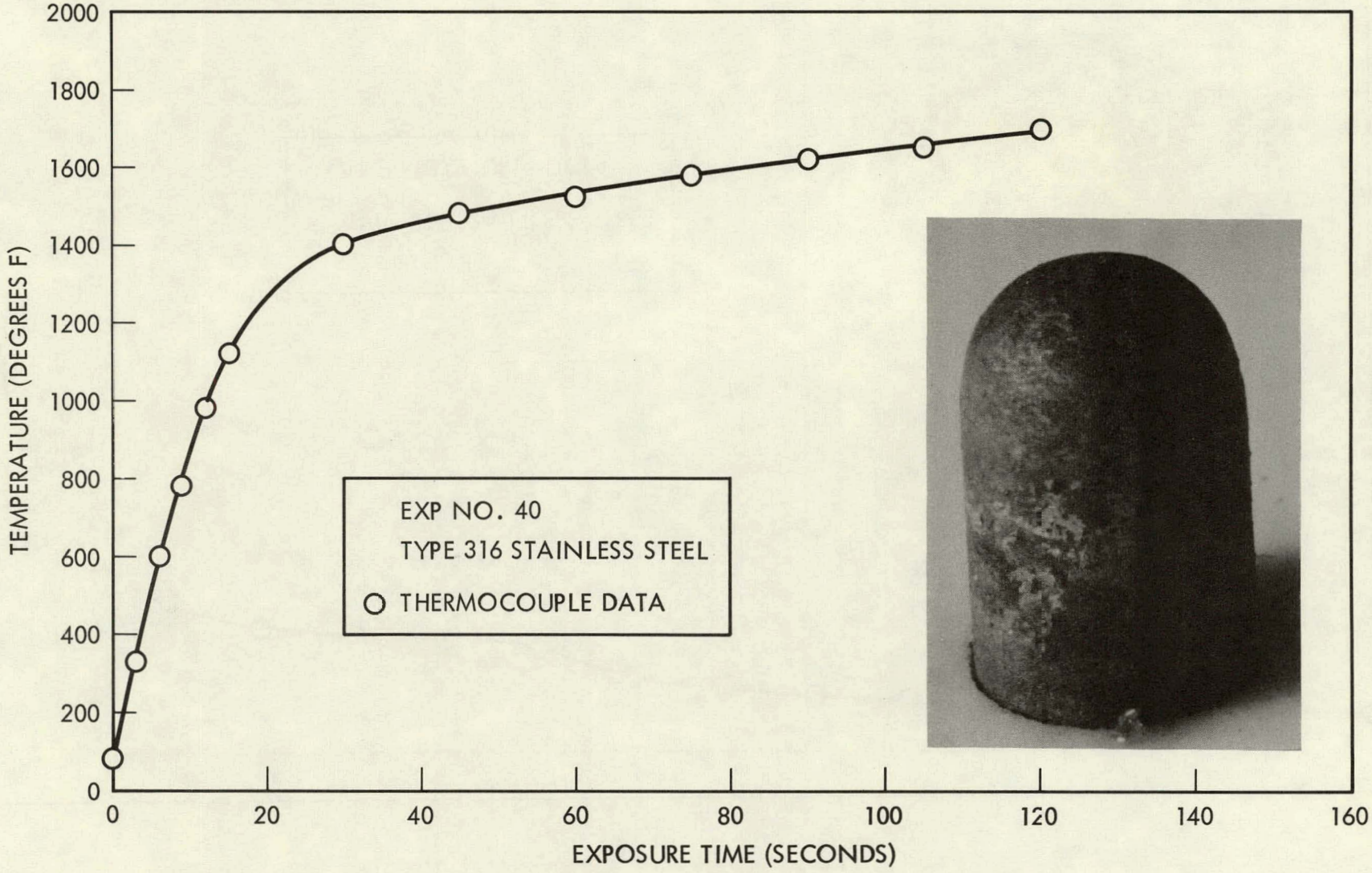

Figure A-34. Temperature vs. Time Data for Experiment No. 40

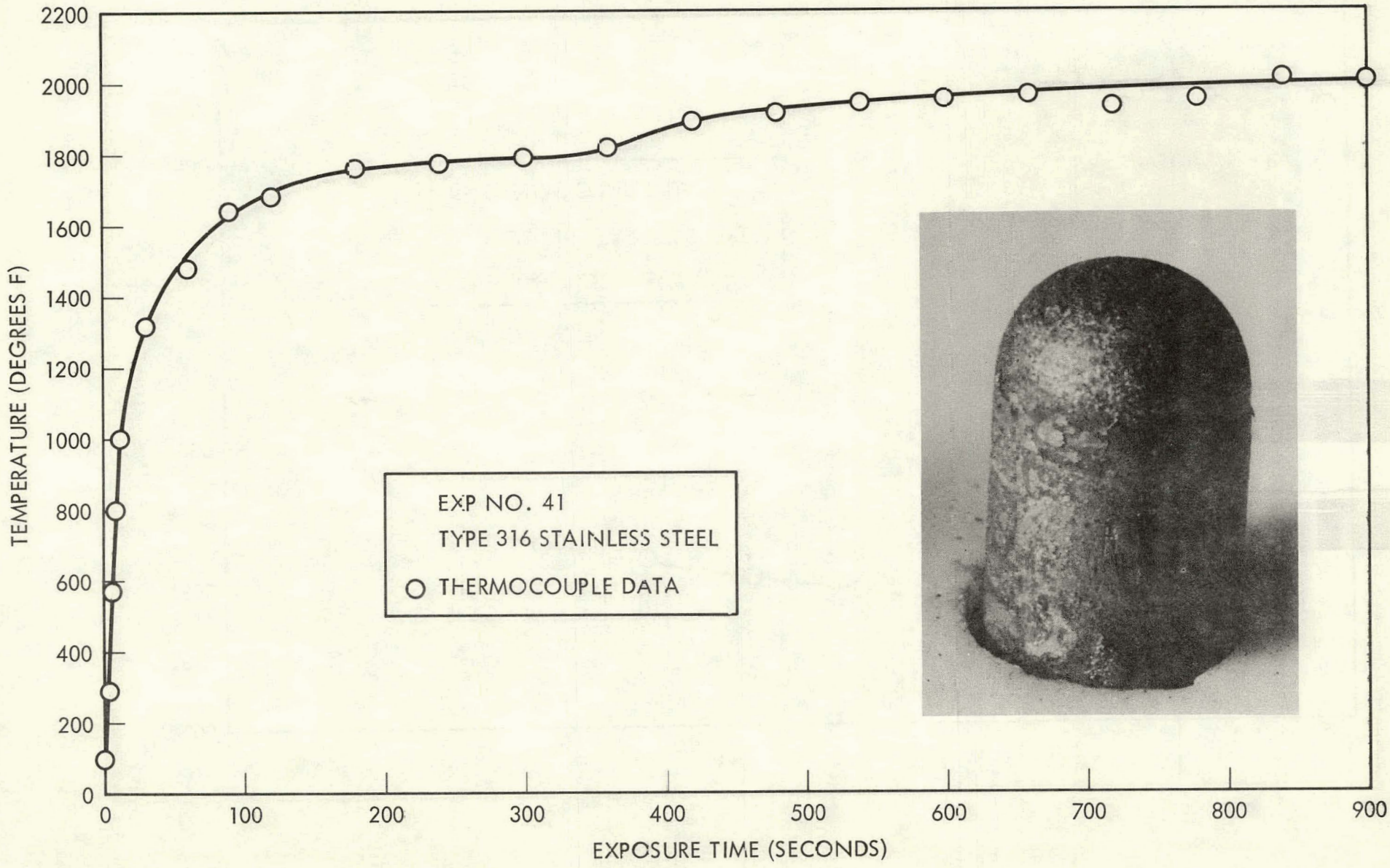

Figure A-35. Temperature vs. Time Data for Experiment No. 41

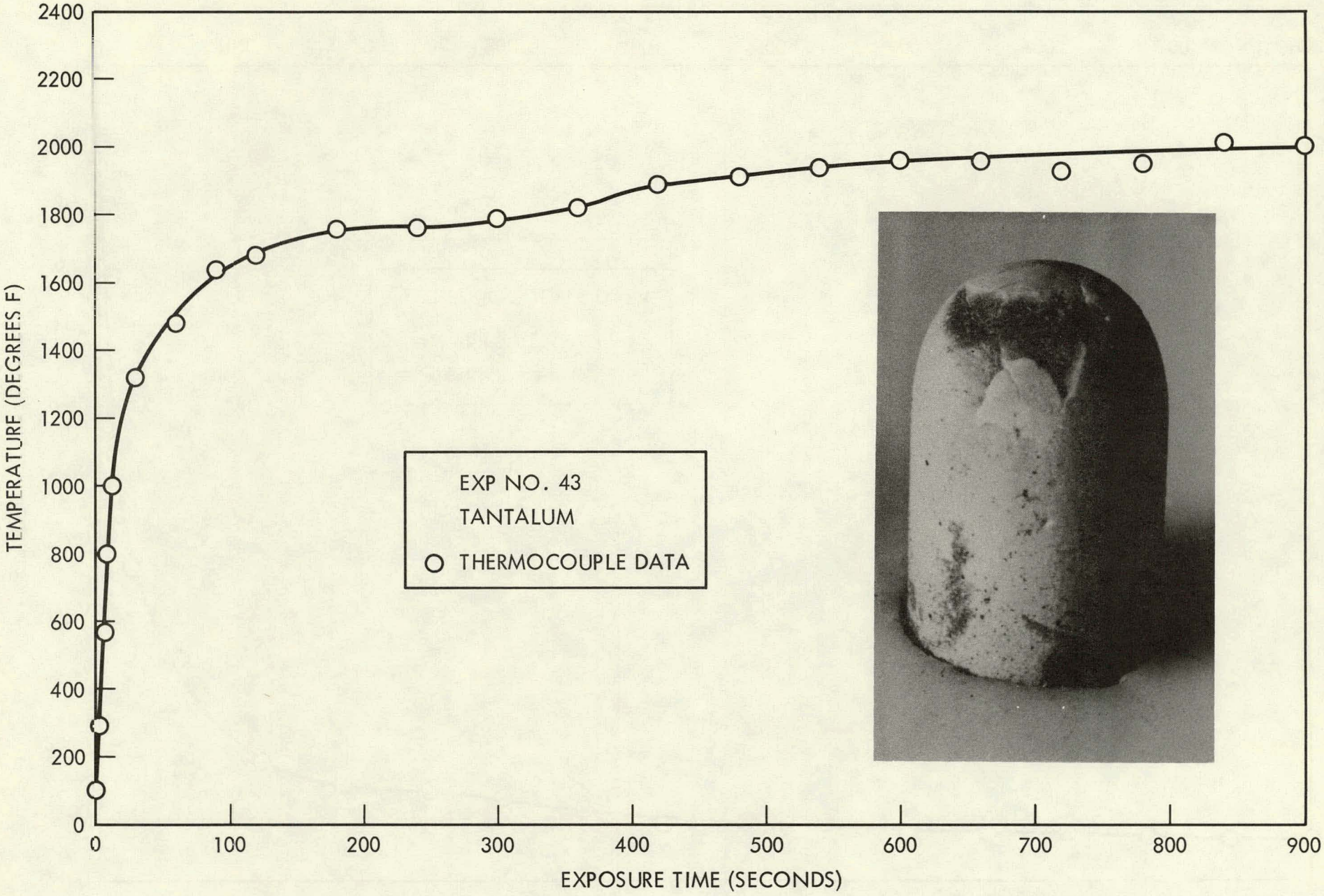

Figure A-36. Temperature vs. Time Data for Experiment No. 43

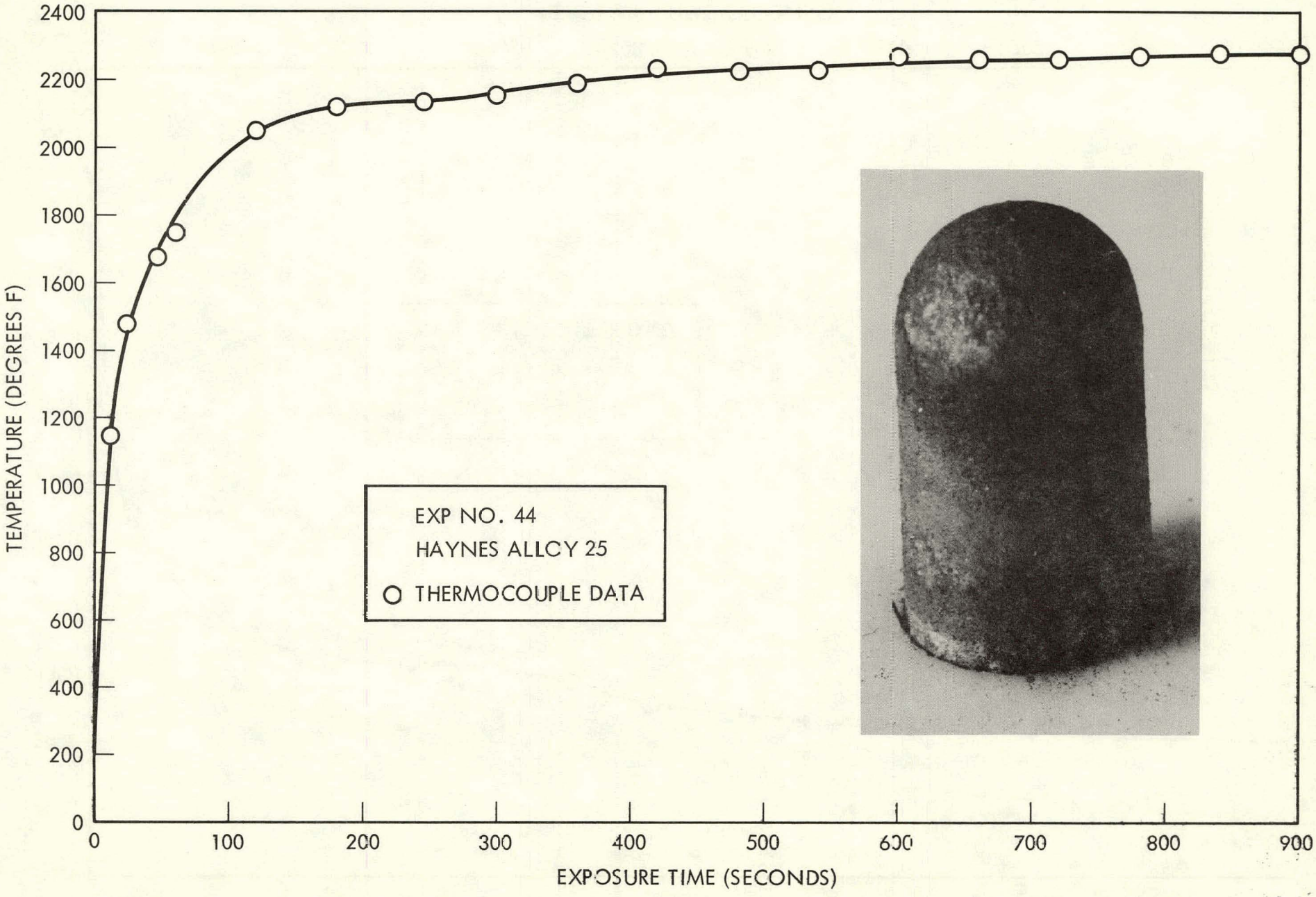

Figure A-37. Temperature vs. Time Data for Experiment No. 44

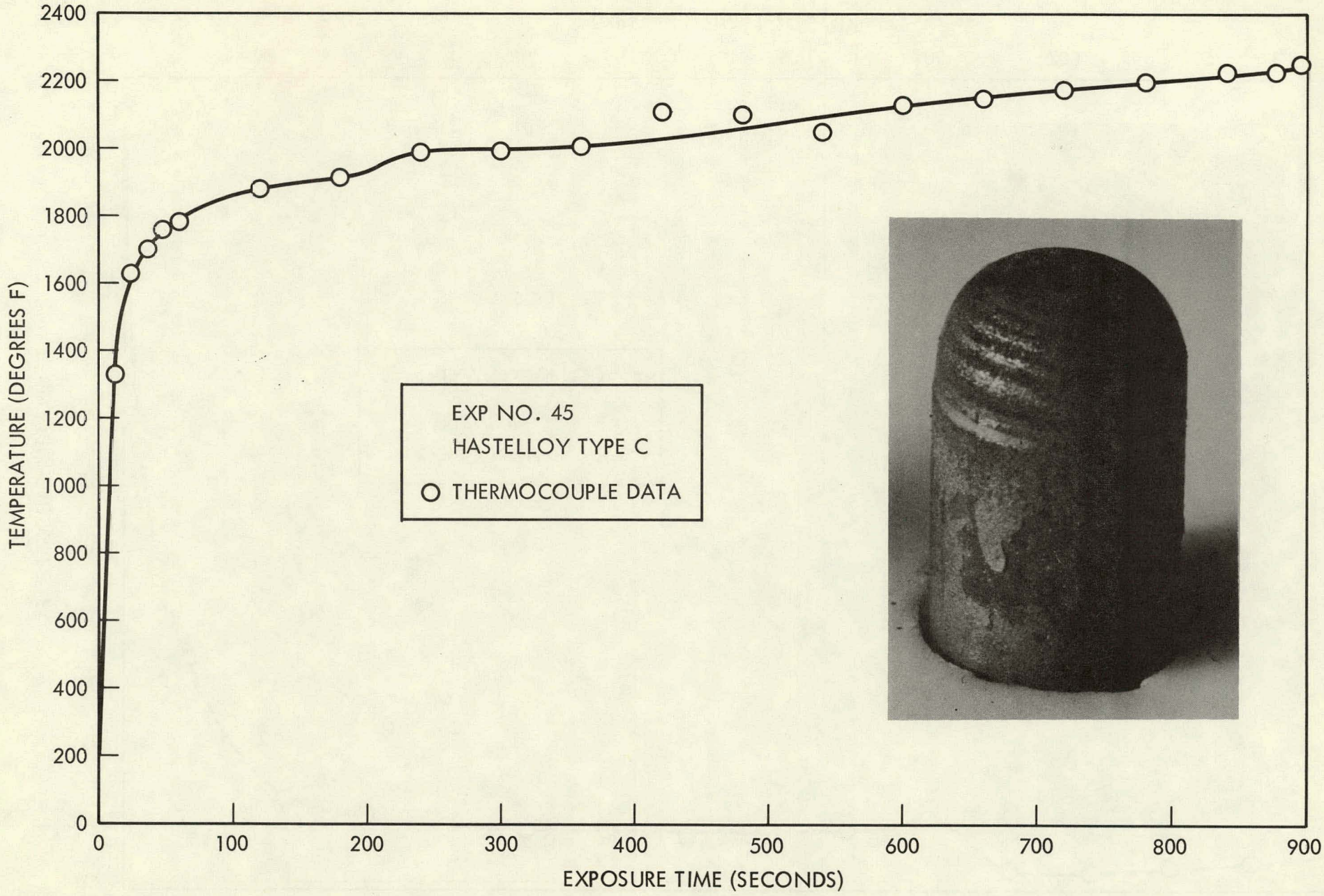

Figure A-38. Temperature vs. Time Data for Experiment No. 45

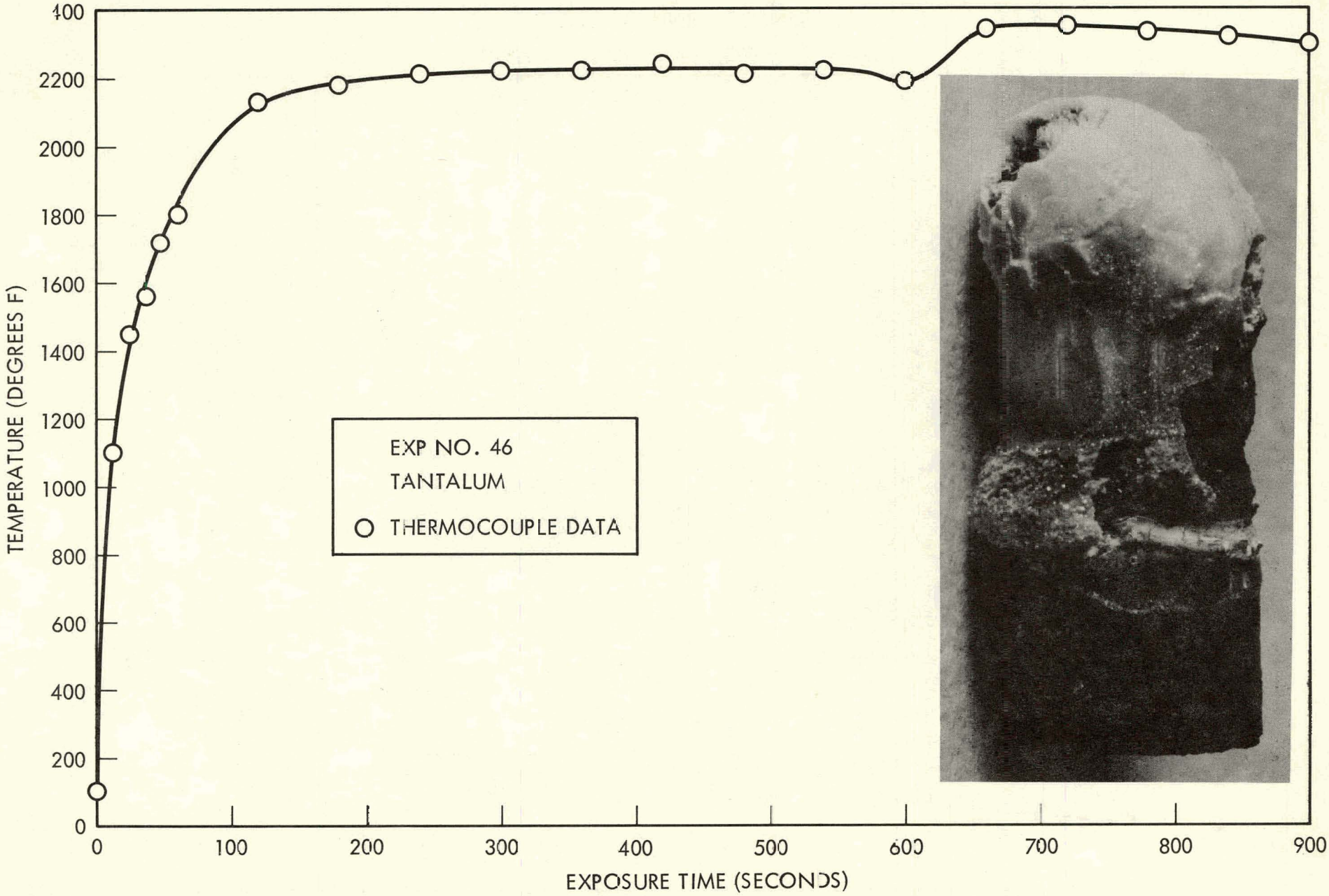

Figure A-39. Temperature vs. Time Data for Experiment No. 46

DISTRIBUTION:

U.S. Atomic Energy Commission
Division of Space Nuclear Systems
Space Electric Power Office
Washington, D.C. 20545
Attn: G. P. Dix, (1)
Chief, Safety Branch
Attn: R. S. Decker, Jr., (1)
Chief, Safety Branch
Attn: R. T. Carpenter, (1)
Chief, Isotope Power Systems Branch
Attn: J. A. Powers (1)
Chief, Isotope & Materials Br.
Attn: C. Johnson (1)
Chief, Reactor Power Systems Br.

U.S. Atomic Energy Commission
Space Nuclear Propulsion Office
Albuquerque Extension
Albuquerque Operations Office
P.O. Box 5400
Albuquerque, New Mexico 87115
Attn: H. P. Smith

U.S. Atomic Energy Commission
Division of Isotope Development
Washington, D.C. 20545

U. S. Public Health Service
National Center for Radiological Health
1901 Chapman Avenue
Rockville, Maryland 20852
Attn: Nuclear Facilities Section

U.S. Atomic Energy Commission
Division of Biology and Medicine
Washington, D.C. 20545
Attn: J. Z. Holland, (1)
Chief, Fallout Studies Branch
Attn: H. D. Bruner, (1)
Asst. Director Medical and Health Research

U. S. Atomic Energy Commission (3)
Division of Technical Information
Headquarters Library G-017
Washington, D.C. 20545

U.S. Atomic Energy Commission
Albuquerque Operations Office
P.O. Box 5400
Albuquerque, New Mexico 87115
Attn: S. A. Upson, (1)
Director, Research and Classification Division
Attn: V. C. Vespe, (1)
Director, Operational Safety Division

U.S. Atomic Energy Commission
Canoga Park Area Office
P.O. Box 591
Canoga Park, California
Attn: D. E. Reardon

U.S. Atomic Energy Commission
Chicago Operations Office
9800 South Cass Avenue
Argonne, Illinois 60439
Attn: Chief, Office Services Branch

U.S. Atomic Energy Commission
Oak Ridge Operations Office
Mail and Document Accountability Section
P.O. Box E
Oak Ridge, Tennessee 37831
Attn: Director, Research and Development Division

Aerojet-General Corporation
REON Division
P.O. Box 15847
Sacramento, California 95813
Attn: D. F. Vanica, Dept. 7400

Headquarters
Air Force Systems Command (SCIZN)
Washington, D.C. 20331
Attn: Nuclear Safety Branch

Air Force Weapons Laboratory
Kirtland Air Force Base,
New Mexico 87117
Attn: Major K. D. McAllister (WLAS)

DISTRIBUTION: (cont)

Air University Library
Maxwell Air Force Base,
Alabama 36112
Attn: Elizabeth C. Pittman

Atomics International
P.O. Box 309
Canoga Park, California 91304
Attn: R. L. Detterman (2)

Battelle Memorial Institute
505 King Avenue
Columbus, Ohio 43201
Attn: J. E. Davis,
Projects Administrator

Battelle Memorial Institute
Pacific Northwest Laboratory
P.O. Box 999
Richland, Washington 99352
Attn: E. A. Coppinger (1)
Attn: Dr. Roy Thompson (1)
Attn: M. T. Walling (1)

The Boeing Company
Aerospace Group
P.O. Box 3707
Seattle, Washington 98124
Attn: T. L. Smith, Mail Stop 23/82

Brookhaven National Laboratory
Technical Information Division
Upton, Long Island, New York 11973
Attn: Research Library

Director, Defense Atomic Support Agency
P.O. Box 2610
Washington, D.C. 20301
Attn: Document Library Branch

Donald W. Douglas Laboratories
P.O. Box 310
Richland, Washington 99352
Attn: S. P. Gydesen

Douglas Aircraft Company, Inc.
Missile and Space Systems Division
3000 Ocean Park Boulevard
Santa Monica, California
Attn: Sig Gronich
Advanced Space Technology

E. I. Du Pont De Nemours and Company
Savannah River Laboratory
Aiken, South Carolina 29802
Attn: W. B. Scott,
Document Division

E. I. Du Pont De Nemours and Company
Explosives Department
Atomic Energy Division
Wilmington, Delaware 19898
Attn: Document Custodian
For: J. W. Croach

General Atomic Division
General Dynamics Corporation
P.O. Box 608
San Diego, California 92112
Attn: Library

General Electric Company
Nuclear Materials and Propulsion Operation
P.O. Box 15132
Cincinnati, Ohio 45215
Attn: J. W. Stephenson
For: W. Briskin

General Electric Company
Valley Forge Space Technology Center
P.O. Box 8555
Philadelphia, Pennsylvania 19101
Attn: S. M. Scala, Room M9539
Space Sciences Laboratory (1)
Attn: T. F. Widmer
Advanced Nuclear Systems Operation (1)

DISTRIBUTION: (cont)

Hittman Associates, Inc.
P.O. Box 2685
4715 East Wabash Avenue
Baltimore, Maryland 21215

Deputy I. G. for Inspection and Safety,
USAF, Kirtland Air Force Base,
New Mexico 87117
Attn: Col. D. C. Jameson (AFINSR)

Institute for Defense Analyses
400 Army Navy Drive
Arlington, Virginia 22200
Attn: Richard Briceland

Lockheed Missiles and Space Company
P.O. Box 504
Sunnyvale, California
Attn: H. H. Greenfield (1)
Manager, Nuclear Power
Development
Attn: R. F. Hausman (Dept 30/63) (1)
Cryogenic and Nuclear Stage
Programs
Attn: Harold F. Plank (1)

Los Alamos Scientific Laboratory
P.O. Box 1663
Los Alamos, New Mexico 87544
Attn: Dr. L. D. P. King (1)
Attn: Dr. Wright Langham (1)
Attn: C. F. Metz, CMB 1 (1)
Attn: F. W. Schonfeld, CMF 5 (1)

Lovelace Foundation for Medical
Education and Research
5200 Gibson Blvd, SE
Albuquerque, New Mexico 87108
Attn: Roger McClellan

Martin-Marietta Corporation
Martin Company
Nuclear Programs
Middle River, Maryland 21203
Attn: D. Anderson

Minnesota Mining and Manufacturing Co.
2501 Hudson Road, Maplewood
St. Paul, Minnesota 55119
Attn: J. P. Ryan, TCAAP 675
Nuclear Products Department

Monsanto Research Corporation
Mound Laboratory
P.O. Box 32
Miamisburg, Ohio 45342
Attn: G. R. Grove

Administrator
National Aeronautics and Space
Administration
Washington, D.C. 20545
Attn: T. B. Kerr (RNS)

National Aeronautics and Space
Administration
Ames Research Center
Moffet Field, California 94035
Attn: Glenn Goodwin

National Aeronautics and Space
Administration
Goddard Space Flight Center
Glenn Dale Road
Greenbelt, Maryland 20771
Attn: A. W. Fihelly
Nimbus Project

National Aeronautics and Space
Administration
Lewis Research Center
21000 Brookpark Road
Cleveland, Ohio 44135
Attn: Library

USAEC
Director of Regulation
Washington, D. C. 20545
Attn: C. K. Beck, Deputy Director (1)
Attn: F. D. Anderson, Regulation (1)

DISTRIBUTION: (cont)

National Aeronautics and Space Administration
Manned Spacecraft Center
Houston, Texas 77058
Attn: Technical Information Dissemination Branch (Code BM6)

National Aeronautics and Space Administration
Scientific and Technical Information Facility
P.O. Box 33
College Park, Maryland 20740
Attn: SAK/DL

Naval Facilities Engineering Command
Department of the Navy, Code 042
Washington, D. C. 20390
Attn: Graham Hagey (2)

Nuclear Materials and Equipment Co.
Apollo, Pennsylvania 15613

NUS Corporation
Environmental Safeguards Division
Suite 1100
1730 M Street, NW
Washington, D.C. 20036
Attn: M. S. Goldman, Vice President

Phillips Petroleum Company
NRTS Technical Library
P.O. Box 2067
Idaho Falls, Idaho 83401

Radio Corporation of America
Astro Electronics Division
P.O. Box 800
Princeton, New Jersey 08540
Attn: S. H. Winkler, Ldr. Adv. Power

Director, USAF Project Rand
Via Air Force Liaison Office
The Rand Corporation
1700 Main Street
Santa Monica, California 90406
Attn: Library

Space Nuclear Propulsion Office
Lewis Research Center
21000 Brookpark Road
Cleveland, Ohio 44135
Attn: L. Nichols

TRW Systems (10)
P.O. Box 287
Redondo Beach, California 90278
Attn: Dr. Donald Jortner

U. S. Naval Radiological Defense Lab.
Commanding Officer and Director
San Francisco, California 94135
Attn: P. E. Zigman

Union Carbide Corporation
Nuclear Division
P.O. Box X
Oak Ridge, Tennessee 37831
Attn: R. A. Robinson (1)
Isotope Development Center
Attn: B. R. Fish (1)
Health Physics Division

Union Carbide Research Institute
P.O. Box 278
Tarrytown, New York 10591
Attn: Joseph Agresta
Space Sciences Group

DISTRIBUTION: (cont)

University of California
Lawrence Radiation Laboratory
P.O. Box 808
Livermore, California 94551
Attn: Dr. James Hadley (1)
Chief, R Division
Attn: Technical Information Div (1)

Westinghouse Electric Company
Astronuclear Laboratory
P.O. Box 10864
Pittsburgh, Pennsylvania 15236
Attn: Joanne M. Bridges
Supervisor, Flight Safety
Analysis Group

U. S. Atomic Energy Commission
Division of Technical Information
Extension (56)
P.O. Box 62
Oak Ridge, Tennessee 37831

Clearinghouse for Federal Scientific
and Technical Information (25)
5285 Port Royal Road
Springfield, Virginia 22151

Princeton University
Princeton, New Jersey
Attn: J. G. Hansel (10)

J. R. Banister, 5120
J. D. Shreve, 5234
D. B. Shuster, 5600
H. E. Viney, 7250
L. E. Lamkin, 7300
G. A. Fowler, 9000
J. H. Scott, 9200
A. Y. Pope, 9300
Attn: V. E. Blake, Jr., 9310
H. E. Hansen, 9311
S. L. Jeffers, 9312
S. McAlees, 9314
R. J. Everett, 9315
J. D. Appel, 9319
J. D. Appel, 9319 (ANSIC) (2)
R. C. Maydew, 9320
A. J. Clark, 9330
J. W. McKiernan, 9331
R. P. Stromberg, 9333
B. F. Hefley, 8232
B. R. Allen, 3421
C. H. Sproul, 3428-2 (10)
L. S. Nelson, 5234 (10)
E. Brinegar, 9319
R. S. Gillespie, 3413,
Attn: M. S. Goldstein